Caractérisation et connectivité des habitats écologiques essentiels des stades adulte et juvénile du bar européen

Chloé Dambrine

DOCTORAT SCIENCES BRETAGNE DE LA MER LOIRE ET DU LITTORAL

UBO Université de Bretagne Occidentale

THESE DE DOCTORAT DE

L'UNIVERSITE
DE BRETAGNE OCCIDENTALE

ECOLE DOCTORALE N° 598
Sciences de la Mer et du littoral
Spécialité : *Ecologie Marine*

Par
Chloé DAMBRINE

Caractérisation et connectivité des Habitats Ecologiques Essentiels des stades adulte et juvénile du bar européen

Thèse présentée et soutenue à Plouzané, le 04 Décembre 2020
Unité de recherche : IFREMER, Sciences et Technologies Halieutiques

Rapporteurs avant soutenance :

Patrick LAMBERT
Ingénieur de Recherche, INRAE, France

Marie-Laure BEGOUT
Chercheure, Ifremer, France

Composition du Jury :

Président du jury
Fred JEAN
Professeur des Universités,
Université de Bretagne Occidentale, France

Patrick LAMBERT
Ingénieur de Recherche, INRAE, France

Marie-Laure BEGOUT
Chercheure, Ifremer, France

Geneviève LACROIX
Directrice de recherche, RBINS, Belgique

Nicolas BEZ
Directeur de recherche, IRD, France

Directrice de thèse
Hélène de PONTUAL
Chercheure, Ifremer, France

Invités

Co-encadrants scientifiques
Mathieu WOILLEZ
Chercheur, Ifremer, France

Martin HURET
Chercheur, Ifremer, France

À mon grand-père Henri

« Ne vous découragez pas, c’est souvent la dernière clef du trousseau qui ouvre la porte. »

Paulo Coelho

Remerciements

Voici venu la tâche compliquée des remerciements, le moment où il ne faut oublier personne et surtout, celui où il faut réussir à lâcher son « bébé », porté depuis trois longues années...

Tout d'abord, je tiens à remercier mes trois encadrants, sans qui, ce travail n'aurait pas vu le jour. Je sais que je n'ai pas toujours été facile avec vous, alors, un grand merci de m'avoir supportée de bout en bout et d'avoir été présents à tous les moments clefs. C'est dur de revenir sur ces années, qui ont été chargées, pour tous, de nombreux événements plus ou moins appréciables… Je dirais alors simplement, merci Hélène pour ton écoute et ton soutien dans les moments de doutes, merci Mathieu de m'avoir portée quand j'en avais besoin et de m'avoir fait évoluer scientifiquement par nos discussions, et merci Martin pour ton expertise technique et pour ta fâcheuse habitude à détourner les questions et en amener d'autres.

Je tiens également à remercier les membres de mon jury de thèse. Merci, aux docteurs Nicolas Bez, Geneviève Lacroix et Fred Jean pour l'examen de ce travail. Merci au docteur Marie-Laure Bégout pour le temps passé à évaluer mon manuscrit. Et un merci plus particulier au docteur Patrick Lambert, sans qui, je dois bien l'avouer, je n'aurais pas commencé cette thèse… Je suis ravie que tu puisses voir l'accomplissement en tant que rapporteur, j'espère que tu ne seras pas trop déçu en tout cas, merci d'avoir pris le temps de me lire et de m'évaluer.

Ensuite, je souhaite remercier toute l'équipe du Laboratoire de Biologie et d'Halieutique dans lequel j'ai pu m'épanouir tant scientifiquement qu'humainement. J'ai passé trois belles années dans votre équipe et j'ai fait de jolies rencontres. Merci à mes nombreux co-bureaux pour ces jolis moments et pour votre soutien. Ghassen, je ne t'oublie pas, tu as cru en moi dès le début et je t'en remercie. Cyria, j'ai vraiment apprécié travailler avec toi, merci pour ta gentillesse et ton sourire. Juan, même si ça a fini de manière compliquée, merci pour m'avoir fait pratiquer l'anglais au quotidien et pour ton aide sur R. Emilie, merci de m'avoir permis de me décharger émotionnellement et d'être la personne adorable que tu es. Pablo, même si on n'a pas pu partager le bureau très longtemps (foutu Covid), merci pour ton attitude positive, et ton recul pour m'aider à surmonter cette fin de thèse. Merci aux petits nouveaux du SIH : Charlène, Jonathan et Thomas, je ne vous connais pas encore très bien, mais j'ai apprécié partager ces moments de pause et de repas en votre compagnie. Merci aussi à tous les techniciens,

principalement pour nos repas animés à la cantine et l'entretien du mythe que les gens de LBH parlent fort. Un merci spécial à toi Le Baron pour ta bonne humeur, tes blagues et ta cuisine. Un merci aussi à toi, Soso, entre autre pour nos fous rires et pour m'avoir si souvent nourrie à base de « boules coco ». Merci aussi à toi Jérôme, tu es vraiment une jolie personne même si je déteste que tu m'effrayes si souvent à base de bruits de chat enragé ! Un merci également particulier à toi, mon Domi, pour ta gentillesse et aussi pour ta fâcheuse tendance à râler, il en faut des personnes comme ça. Merci de m'avoir accueillie si souvent chez toi comme si j'étais chez moi et de m'avoir fait goûter des choses aussi bonnes, j'espère pouvoir vite embarquer sur ton bateau ! Merci aussi à toi Cindy, j'ai été ravie de travailler avec une personne aussi dynamique et souriante, ne change rien et félicitations pour ce poste que tu mérites. Merci aussi à toi Christophe, tu sais tellement bien écouter, tu es un super encadrant, n'en doute pas. Une mention spéciale pour toi, Clara, la reine de la taquinerie et des pauses, on ne s'ennuie pas avec toi, ni au boulot, ni à la maison… Merci de m'avoir supportée et soutenue durant cette fin de thèse mais j'attends toujours mes brownies ! Merci aussi à toi, François, pour ta poisse légendaire, toutes ces sorties sur Brest et ces nombreux moments à discuter tous les deux, tu as fait défiler mes premiers mois de thèse et m'as permis de vraiment apprécier la vie à Brest. Je te souhaite une très belle vie en Nouvelle Calédonie et j'espère que tu t'y épanouis comme tu le souhaitais, à très vite ! Et puis, on dit toujours : « le meilleur pour la fin », alors, pour finir en beauté, merci à toi Aurore, je n'aurais pas assez de place ici, mais merci pour tout ce que tu as pu faire pour moi durant ces trois années, tu as toujours été là pour moi, tu as toujours su bien me conseiller et m'aiguiller, je ne serais pas la personne que je suis aujourd'hui sans toi. Je ne m'épancherai pas plus ici, tu vois de quoi je parle, mille fois merci, je suis tellement heureuse de t'avoir rencontrée, toi ainsi que ta petite famille, je peux maintenant dire que j'ai un petit frère, et ça n'a pas de prix !

Je souhaite aussi remercier les personnes avec qui j'ai eu la chance d'embarquer à bord du Thalassa pour vivre deux campagnes extraordinaires dans le golfe de Gascogne. Merci à tout l'équipage et un grand merci à vous, Anne et Laetitia, pour tous ces moments complices que l'on a pu partager et surtout pour tous ces fous rires. Merci aussi à toi, JH, j'ai beaucoup aimé nos moments à nous charrier mutuellement. Merci Mathieu pour avoir géré le son en hydro tous les soirs et pour ta sympathie, bon postdoc à Seattle. Merci à toi JB pour tous ces moments à discuter, ton aide pour les manips au milieu de la nuit et bien entendu, pour nos nombreuses parties de ping-pong, je n'oublierai jamais ta fameuse « bola de fuego ». Je ne peux pas parler de tennis de table sans te remercier toi aussi, Pierre, pour ces moments sportifs et pour ton

apparente sagesse qui dissimule une folie fort agréable. Merci aussi à toi Mathilde, malgré ton mal de mer, tu as toujours été d'excellente compagnie à bord. Je suis super contente d'avoir fait ta connaissance et sache que je suis toujours ravie de te revoir autour d'un verre ou repas à terre. Et puis, merci à tous ces animaux marins qui ont eu la gentillesse de venir nous frôler et à ces nombreux couchers de soleil qui font que je n'oublierai jamais ces moments magiques…

Merci également à mes amis doctorants brestois pour tous ces moments partagés et également pour avoir su m'apaiser et me montrer le chemin à prendre. Merci Elyne pour m'avoir intégrée au LEMAR et aussi dans ta famille, vous êtes tous géniaux. Merci Céline et Fabien d'avoir fait partie de ma vie quelques mois ici, votre fraîcheur me manque beaucoup. Merci Will pour ton humour et pour toutes ces soirées à se déhancher sur des rythmes endiablés, je ne sais pas si je retrouverai quelqu'un avec qui danser aussi bien ! Merci Gaetan pour ta culture générale et pour cette escapade à l'île de Sein (même si la maison de ta grand-mère était très probablement hantée !). Merci Lucien d'avoir toujours fait partie des folles nuits brestoises et de m'avoir proposée ton aide quand j'en avais besoin. Merci Nico pour tes blagues, ta gentillesse, ta disponibilité, nos séances d'escalade et bien entendu, nos rocks (presque) acrobatiques. Merci Jordan pour tes doubles sens, ton soutien moral, tes cours de sport tortionnaires, ta gentillesse et tes bons repas. Merci Houda pour tes retards (que je sais désormais dompter), nos nombreuses discussions (autour d'un sujet récurrent, il faut bien l'avouer !), nos séances de nage et notre rituel du lundi soir. Merci Natalia pour tous ces moments passés ensemble, je ne pourrais pas tous les citer ici, mais sache que j'ai adoré chacun d'eux. Par contre, j'attends toujours que tu m'emmènes chez le coiffeur en fin de thèse… Merci pour ton écoute, ta gentillesse, ton accent (mais de quoi je parle ?), ta souplesse et aussi de m'avoir donnée l'illusion que j'étais douée sur R et que mon intervention te sauvait la vie !

La vie à Brest n'aurait pas été la même non plus sans vous, alors, merci Béné, Sophie et Jules. Béné, on s'est rencontrées à la voile à un moment particulier de ta vie. Je suis heureuse d'avoir pu être là pour te voir évoluer et devenir la jolie femme que tu es aujourd'hui. Merci pour tous ces moments passés ensemble à rire (très, trop fort), nager, manger, danser, chanter... Merci aussi à toi Sophie, pour nos repas, nos soirées et ce samedi à explorer Brest à la recherche d'une invitation pour un mariage où trouver Sherlock Holmes. Je te souhaite une très belle vie avec ton magnifique (mais un peu trop speed) Rio. Et merci à toi Jules, pour ces nombreux repas à la cantine (ce n'était vraiment pas des postillons !) et ces soirées à Brest, il est si facile de te charrier mais j'avoue que je ne m'en lasse pas, continue de porter fièrement ton pull Gryffondor, quoi que je dise !

Merci aussi à mes amies plus lointaines mais non moins essentielles. Merci Julia pour tes temps de réponse inégalés et pour ta gentillesse. Merci Chloé, pour m'écouter, me conseiller et me charrier. Merci Pauline d'être là depuis si longtemps et d'apporter le soutien dont j'ai besoin. Merci Fiona pour tes messages à rallonge, ton écoute, ta bonne humeur et pour toutes nos excursions en Bretagne ou en Normandie, avec ou sans crème solaire !

Pour finir, un immense merci à ma famille qui me soutient depuis toujours dans mes choix et me supporte malgré mon caractère. Merci Mamie de t'intéresser à ce que je fais et de me donner l'impression que c'est extraordinaire. Merci Papy, tu n'es plus là pour le voir, mais ça y est, j'ai enfin terminé mes études ! Je te dédie mon travail et ne doute pas que tu aurais été fier de moi. Merci Maman, je sais que je ne suis pas toujours délicate mais j'apprécie tout ce que tu as toujours fait pour moi et n'oublie pas que je te dois beaucoup. Merci Papa, tu n'aimes pas trop les démonstrations, mais sache que tu m'apportes beaucoup et que tu me portes chaque jour. Merci Florus, mon dino, ma confidente de toujours, mon Pierre Richard, ma partenaire de voyage et bien plus encore, tu me fais grandir et devenir meilleure au quotidien. Je ne sais pas ce que l'avenir me réserve, mais je sais que vous serez toujours derrière moi et c'est plus que réconfortant, alors encore une fois, merci !

Table des matières

INTRODUCTION

PRÉAMBULE

Les poissons sont ectothermes, les conditions biotiques et abiotiques qu'ils vont rencontrer tout au long de leur cycle de vie vont donc conditionner leur développement individuel ainsi que le renouvellement de leur population. Chez certaines espèces, des besoins environnementaux différents sont nécessaires à chaque stade de développement. Ces poissons vont alors coloniser divers habitats (Harden-Jones, 1968) afin d'optimiser leur succès reproducteur et donc leur survie (Gross, 1996).

Ces habitats sont alors adaptés pour assurer les différentes fonctions physiologiques (e.g. alimentation, croissance, reproduction) mais peuvent être plus ou moins éloignés géographiquement. Le bouclage du cycle de vie tient alors dans le maintien de la connectivité entre ces différents habitats (e.g. Tétard *et al.*, 2016).

Bien comprendre quels habitats sont fréquentés par une espèce et comment ils sont reliés entre eux permet donc une meilleure gestion et protection de celle-ci. D'autant plus que les écosystèmes marins font face à de nombreuses pressions d'origine anthropique : pêche, nombreux rejets dans la mer (e.g. plastiques, polluants et nutriments d'origine agricole et industrielle), réchauffement climatique, dégradation et destruction directe de certains habitats, notamment côtiers ou encore déplacement d'espèces à l'échelle planétaire pouvant être « invasives ».

Dans le cas du bar européen (*Dicentrarchus labrax*), il a été mis en évidence un manque de connaissances sur les habitats fréquentés par l'espèce en Atlantique nord-est pouvant altérer sa gestion (ICES, 2012). Des campagnes de marquages de bars adultes ont révélé qu'ils pouvaient effectuer des migrations de plusieurs centaines de kilomètres entre leurs habitats estivaux, où ils se nourrissent, et leurs habitats hivernaux, où ils se reproduisent (Pawson *et al*., 2007 ; de Pontual *et al*., 2019). Par ailleurs, le processus de dispersion larvaire du bar est encore mal connu alors que celui-ci est considéré comme le plus impactant sur la connectivité des espèces marines (Cowen & Sponaugle, 2009).

De plus, la gestion européenne du bar s'appuie sur deux stocks distincts (i.e. le stock Nord et le stock golfe de Gascogne) alors qu'aucune barrière physique n'empêche cette espèce migratrice de se déplacer entre les deux. Les recherches récentes n'ont pas encore pu déterminer si chaque stock correspondait à une seule population, pourtant, les mesures de gestions sont très

différentes entre les deux zones. En effet, pour le stock « nord », ces dernières années ont révélé une biomasse reproductrice faible pouvant être liée à une surpêche et à une série de mauvais recrutements (ICES, 2012). Cela a entrainé la modification des mesures de gestion de l'espèce (e.g. augmentation de la taille limite de capture, interdiction de la pêche sur frayères) mais uniquement pour ce stock. Il convient donc de mieux appréhender le processus de recrutement de l'espèce pour comprendre sa diminution récente, mais également d'améliorer la compréhension de la structuration de ses populations pour éventuellement uniformiser les mesures de gestion.

Cette thèse se propose d'explorer, par une caractérisation des zones de reproduction puis la modélisation de la dispersion larvaire, la connectivité entre les zones de reproduction et de nourriceries du bar européen, le long des côtes françaises, en vue de mieux comprendre quels habitats sont fréquentés par l'espèce pour se reproduire, ainsi que d'évaluer quels facteurs environnementaux régulent leur connectivité avec les zones de nourriceries des juvéniles. La question de la connectivité entre les deux stocks évalués annuellement a également été abordée.

1. Cycle de vie et habitats des poissons

Le cycle de vie des poissons

Le cycle de vie des poissons, schématisé en Figure 1, peut être divisé en différents stades de développement, chaque stade étant rattaché à un habitat particulier (Harden Jones, 1968). Les changements de stade sont associés à des changements des besoins physiologiques et donc des préférenda environnementaux, nécessitant parfois des migrations actives (juvéniles/adultes) ou passives (dispersion larvaire).

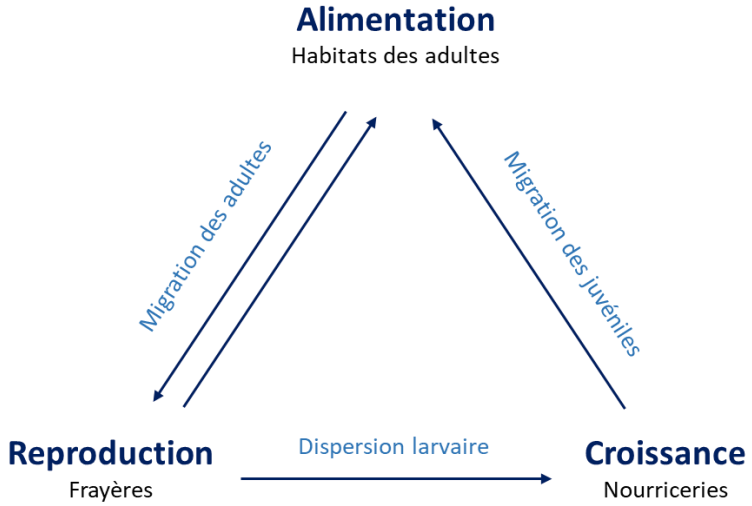

Figure 1. Cycle de vie des poissons et migrations associées. Les adultes partent se reproduire à un moment précis dans des lieux qui vont favoriser la dispersion larvaire jusqu'à des nourriceries propices au développement des juvéniles. Les adultes peuvent migrer plusieurs fois au cours de leur cycle de vie pour se reproduire (cf double flèche pour la migration des adultes). Triangle adapté de Harden Jones (1968).

Les adultes, autrement dit les individus matures, se trouvent sur des zones d'alimentation pendant le cycle saisonnier pour assurer leur croissance, même si celle-ci est ralentie suite à la première reproduction (Enberg *et al.*, 2008), et constituer des réserves énergétiques pour la maturation des gamètes et la future reproduction. Les habitats associés à ce stade de développement sont donc des zones riches en ressources trophiques avec des conditions physico-chimiques adaptées à l'espèce (Compaire *et al.*, 2016).

À la première maturité sexuelle, ils migrent pour se reproduire, et ce, une fois par an (espèce itéropare ; par opposition à une espèce sémelpare qui ne se reproduit qu'une fois au cours de son cycle de vie). Si la reproduction participe au maintien de l'espèce, elle présente néanmoins

un coût énergétique et physiologique important pour les adultes (Callow, 1985). La reproduction se passe généralement sur des zones de forte concentration d'individus appelées frayères (Domeier, 2012). Ces zones présentent des caractéristiques physico-chimiques propres à l'espèce : si celle-ci dépose ses œufs, alors le substrat sera important (Lelièvre *et al.*, 2014), alors que si elle émet ses œufs directement dans la colonne d'eau, l'environnement favorisera, ou non, la dispersion des œufs et des larves vers des zones de croissance adaptées (Harden Jones, 1968).

Le développement embryonnaire et la vie larvaire sont généralement associés à une phase de vie pélagique où embryons et larves dérivent passivement avec les courants (Sassa *et al.*, 2008 ; Asch & Checkley Jr., 2013). Cette phase est l'une des plus sensibles du cycle de vie (Juanes, 2007) car les œufs et les larves sont soumis à la prédation, au manque de nourriture ou encore aux mauvaises conditions hydrodynamiques (Houde & Hoyt, 1987). Cela génère des variations interannuelles importantes de survie (Houde, 2008). Le taux de survie a été estimé par Le Pape & Bonhommeau (2015) à un juvénile pour 1000 œufs émis pour la plupart des espèces marines.

Une fois arrivés sur les zones de croissance, bien souvent côtières, que l'on appelle nourriceries, les juvéniles vont y grandir. Ces zones doivent donc fournir des ressources trophiques en quantité et de qualité (Islam et Tanaka, 2005) mais également servir d'abris pour limiter la prédation. Le Pape & Bonhommeau (2015) ont estimé un taux de survie d'un adulte pour 100 larves arrivées sur nourricerie pour la plupart des poissons marins.

Des habitats écologiques essentiels à la niche ontogénique

Le choix des habitats colonisés par les poissons est souvent issu d'un compromis en vue d'optimiser leur « fitness », c'est-à-dire, leur contribution relative aux générations futures. Cette recherche de compromis vient de la nécessité, pour les poissons, à chaque stade de leur cycle de vie, de remplir trois exigences fondamentales (Lévêque, 1995) : (i) se protéger des contraintes du milieu, des prédateurs voire des compétiteurs afin d'assurer leur survie, (ii) se nourrir pour assurer la croissance et la maturation, et (iii) se reproduire, une fois que cela est possible, pour assurer le renouvellement de l'espèce.

Les Habitats Ecologiques Essentiels (HEE) sont alors définis comme les habitats qui sont le siège d'au moins une phase du cycle de vie des poissons. Ils ont été définis dans le Magnuson-Stevens Fishery Act (2007) comme « les eaux et substrats nécessaires aux poissons pour la

ponte, la reproduction, l'alimentation et la croissance jusqu'à maturité ». Chacun de ces habitats est défini par son environnement physique, chimique et biologique et est fréquenté par l'espèce en vue d'optimiser ses traits vitaux (e.g. comportement reproducteur, spécialisations alimentaires) qui ont été sélectionnés au cours de l'évolution.

C'est donc premièrement l'héritage phylogénétique qui détermine les besoins en terme d'habitats d'une espèce. Malgré tout, la plasticité d'une espèce, liée à la variabilité de son génome, permet une certaine adaptation, nécessaire à sa survie, en réponse à des modifications naturelles ou anthropiques, de son environnement.

En terme de gestion, il convient de caractériser tous les HEE d'une espèce puisque de leur qualité dépend le bouclage du cycle de vie et donc l'état de la population (Beck *et al.*, 2001 ; Vasconcelos *et al.*, 2013). Intervient alors le concept de « niche ontogénique » (Lowe-McConnell, 1985) qui regroupe l'ensemble des HEE dont l'espèce a besoin au cours de son développement.

Les frayères et nourriceries, parce qu'elles regroupent un grand nombre d'individus dans un espace restreint (Dahlgren *et al.*, 2006; Domeier, 2012) et sont le lieu de processus qui participent activement au renouvellement de la population (Figure 1), nécessitent une attention particulière. En effet, le maintien du potentiel reproductif d'une population passe par une contrainte voire une restriction des pressions anthropiques sur les frayères pendant la période de reproduction (Hoegh-Guldberg, 2010) et le bon recrutement, par le maintien des surfaces et la conservation de la qualité des zones de ponte, de dérive larvaire et de nourricerie (Corrales *et al.*, 2015 ; Rochette *et al.*, 2010 ; Peterson, 2003).

La connectivité entre habitats

La connectivité se définit par les mouvements d'organismes au sein d'un environnement (Crooks & Sanjayan, 2006). Puisque le cycle de vie des poissons est spatialisé (Figure 1), on peut alors parler de « connectivité entre habitats ». En effet, le lien entre les HEE d'une espèce est maintenu par des migrations actives et passives (Figure 1), plus ou moins longues, d'individus.

La migration a été définie par Northcote (1978) comme le « déplacement entre deux habitats d'une grande partie de la population et ce, de manière régulière durant la vie d'un individu ». Ce processus, pourtant coûteux en énergie, est issu de l'évolution et a été préféré lorsque les

bénéfices pour la survie des jeunes étaient supérieurs au coûts de déplacement (Jonsson & Jonsson, 1993 ; Dahlgren & Eggleston, 2000).

Chez les poissons, la migration est parfois liée à la reproduction, avec des individus qui vont migrer en vue de rechercher des zones favorables à la ponte puis au bon développement des juvéniles. Cette trajectoire ontogénique est appelée modèle indirect (Balon, 1990). Dans des cas extrêmes (e.g. saumon, anguille), les adultes peuvent parcourir des milliers de kilomètres pour aller se reproduire. On comprend alors que les pressions subies durant ce trajet sont nombreuses et que, pour maintenir la population, il convient d'assurer le maintien de la connectivité entre ces deux HEE (e.g. Tétard *et al.*, 2016).

Fruit de l'évolution, cette connectivité entre HEE peut être modifiée lors de variations de l'environnement via la sélection naturelle de génotypes adaptés. Néanmoins, les pressions anthropiques telles que la pêche ou la destruction d'habitats ont des impacts à une échelle de temps faible qui ne permet que peu d'adaptation. Décrire les HEE d'une espèce ainsi que leur connectivité permet donc une meilleure gestion/protection de l'espèce puisque cela permet de caractériser les facteurs expliquant sa répartition spatiale et temporelle et de mieux comprendre comment se structurent ses populations.

2. Lien entre les notions de population, métapopulation et stock

Métapopulation et connectivité des sous-populations

Une définition de la notion d'espèce est : « population ou ensemble de populations dont les individus peuvent effectivement, ou potentiellement, se reproduire entre eux et engendrer une descendance viable et féconde, dans des conditions naturelles » (Ernst Mayr, 1942). La définition écologique d'une population serait donc « groupe d'individus se reproduisant entre eux et coexistant dans l'espace et dans le temps ».

Une population peut être isolée, souvent géographiquement, des autres (c'est le cas de la population de gauche en Figure 2). Elle peut, au contraire, se composer d'un assemblage de populations locales, appelées « sous-populations », également plus ou moins isolées géographiquement, mais interconnectées par des échanges, plus ou moins importants d'individus. C'est le cas de la population de droite en Figure 2, qu'on appelle alors « métapopulation » (Hanski, 1999).

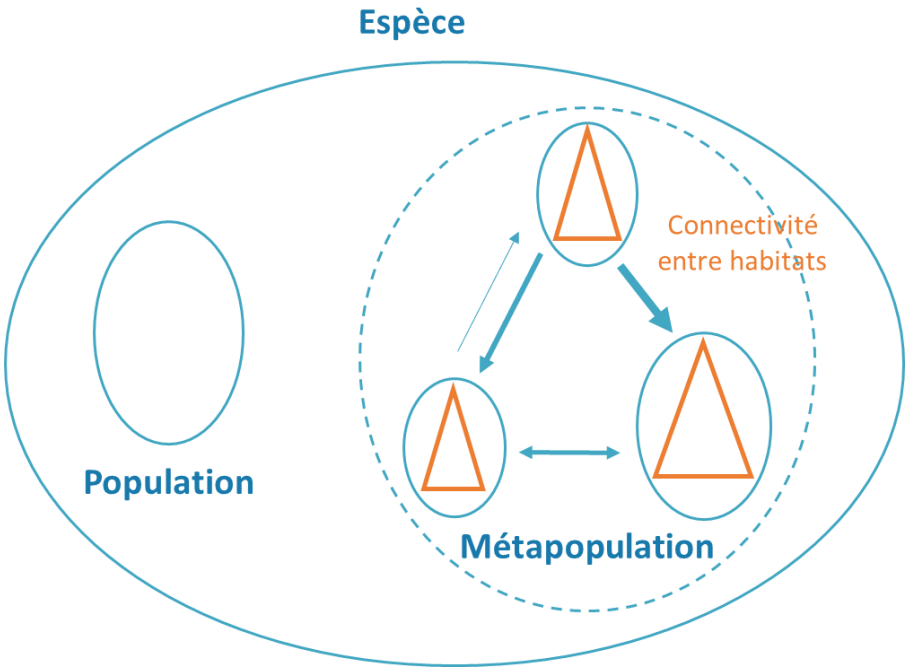

Figure 2. Simplification de l'organisation biologique d'une espèce en population et métapopulation. Les flèches représentent les échanges d'individus, plus ou moins importants, entre les sous-populations (i.e. ronds bleus) de la métapopulation. La connectivité entre habitats (i.e. triangles oranges) doit être maintenue pour que les sous-populations subsistent et que la structuration des populations de l'espèce reste inchangée.

Cette notion de métapopulation, composée de sous-populations reliées par des échanges plus ou moins forts, rejoint alors la notion de connectivité.

La connectivité peut être mesurée à différentes échelles spatio-temporelles (Cowen *et al.*, 2007). À l'échelle écologique, on parle de connectivité démographique. Elle illustre les échanges directs d'individus entre sous-populations pouvant entraîner des impacts mesurables sur leur dynamique (Sale *et al.*, 2010). À l'échelle évolutive, ces échanges peuvent aboutir à des transferts de gènes, on parle alors de connectivité génétique (Cowen *et al.*, 2007 ; Cowen & Sponaugle, 2009). Cette homogénéité génétique implique des échanges assez faibles entre deux sous-populations (i.e. un individu par génération en moyenne ; Hedgecock *et al.*, 2007).

Chez les poissons, les échanges sont assurés par le déplacement actif ou la dispersion des individus au cours de leur cycle de vie (Figure 1). Ainsi, la connectivité entre habitats et la connectivité démographique sont intimement liées. Cependant, les mouvements des poissons, non directement observables, rendent difficile la caractérisation de la structure des populations

en milieu aquatique (Grimm *et al*., 2003). Pourtant, leur connaissance est essentielle si l'on veut gérer les ressources marines à la bonne échelle.

Le stock comme unité de gestion

Des organismes intergouvernementaux sont en charge de l'évaluation des ressources exploitées. En Europe, dans l'Atlantique nord-est, c'est le Conseil International pour l'Exploration de la Mer (CIEM/ICES) qui rend annuellement des avis pour la gestion des ressources et des écosystèmes marins. La production de ces avis est confiée à des groupes d'experts qui évaluent l'état des populations marines.

L'unité de gestion utilisée est le « stock ». D'un point de vue halieutique, cette unité de gestion représente la partie exploitable d'une population. Un stock ne représente donc que les individus d'une population ayant une taille suffisante pour être capturés par la pêche.

Il existe d'autres définitions du stock, et une définition plus biologique serait : « groupe intraspécifique d'individus s'accouplant au hasard selon une intégrité temporelle et spatiale » (Ihssen *et al*., 1981). Cette définition se rapproche ainsi de la notion de population (Figure 2).

De fait, il est considéré dans les modèles actuels que les stocks sont, comme les populations, totalement isolés et homogènes. En pratique, un stock peut présenter des échanges plus ou moins importants avec les stocks voisins et peut comporter des sous-ensembles. Il reste important que les échanges au sein d'un même stock soient forts et en tout cas, que les échanges que ce stock entretient avec d'autres stocks restent faibles. En effet, la définition du stock reste une hypothèse forte lors de l'évaluation des ressources (Kutkuhn, 1981) et il est nécessaire de prendre en compte les notions de connectivité qui peuvent exister entre stocks pour les gérer à la bonne échelle (Petitgas *et al.*, 2013 ; Frisk *et al.*, 2014).

Finalement, la pertinence de cette unité de gestion dépend de la connaissance du cycle de vie d'une espèce et de la dynamique spatio-temporelle associée. Il convient de prendre ces informations en compte lors de la définition d'un stock pour que son évaluation et les mesures de gestion qui en découlent soient adéquates (Carson *et al.*, 2011 ; Frisk *et al.*, 2014).

3. **L'étude de la connectivité liée à la phase de vie pélagique**

Méthodes d'évaluation des connectivités

À l'origine, la plupart des stocks ont été définis, par manque de connaissances, à partir de considérations politiques plutôt que biologiques (Bosley *et al.*, 2019). L'inadéquation entre stock, dans la pratique halieutique, et population(s) sous-jacente(s) a pu entraîner la surexploitation (Cadrin & Secor, 2009 ; Ying *et al.*, 2011) voire l'effondrement (Hilborn *et al.*, 2003 ; Neat *et al.*, 2014) de certains stocks. Le cas extrême serait alors la disparition de certaines sous-populations et donc l'érosion de la diversité génétique qui nuirait gravement à l'espèce, par exemple en réduisant les possibilités d'adaptation à des changements de l'environnement. De fait, des méthodes permettant d'évaluer la structure des populations et leurs connectivités ont été développées afin de vérifier l'adéquation entre stock et population. Cadrin *et al.* (2013) synthétisent ces méthodes permettant d'étudier les connectivités entre (sous-)populations et entre habitats et les relient au stade de vie des individus.

Dans le cas des adultes, les méthodes s'appuient, entre autres, sur des marqueurs artificiels (marques conventionnelles ou électroniques) ou naturels (otolithes, écailles, tissus etc.) permettant de reconstituer, *a posteriori*, les environnements rencontrés par un individu durant son cycle de vie. Ces analyses nécessitent l'analyse génétique de tissus biologiques, l'étude de la microchimie des pièces calcifiées et de la matrice des mouvements apparents, ou encore la reconstruction de trajectoires par un modèle de géolocalisation.

Pour les jeunes stades, l'étude de la dérive des œufs et des larves est complexe (Levin, 2006) car elle est conditionnée par de nombreux facteurs interdépendants : hydrodynamisme, conditions environnementales et/ou comportement larvaire. Pour synthétiser l'impact simultané de ces facteurs sur ce processus, des modèles simulant la survie et la croissance des individus soumis à des conditions environnementales et hydrodynamiques très variables (Houde, 2008) ont été développés. Ceci en vue (i) d'identifier les nourriceries potentielles d'une population, (ii) d'évaluer leur importance ainsi que celle des facteurs à l'origine de la variabilité spatio-temporelle de recrutement ou encore, (iii) d'étudier les relations dynamiques entre frayères et nourriceries (e.g. Rochette *et al.*, 2012 ; Lacroix *et al.*, 2013).

Les modèles de dérive larvaire

Les modèles de dérive larvaire reposent bien souvent sur un couplage entre un modèle individus-centré (IBM) et un modèle hydrodynamique.

Les IBMs sont des modèles mathématiques simulant la dynamique d'une population comme une propriété émergente des comportements de chaque individu la composant (Grimm & Railsback, 2005). Ils permettent de suivre et de conserver les trajectoires de vie (e.g. température et nourriture rencontrées) de chaque individu simulé et une dimension spatiale peut leur être ajoutée en les couplant à des modèles qui reconstruisent les habitats fréquentés par les individus. En recherche halieutique pour l'étude des stades précoces pélagiques, la dimension spatiale est assurée par un couplage avec un modèle hydrodynamique qui reconstruit les courants et les conditions physiques et abiotiques auxquelles sont soumis les poissons.

Ces couplages ont déjà été largement utilisés pour étudier les durées de dérive (Bonhommeau *et al*., 2009), le comportement de migration verticale (Fox *et al*., 2006 ; Sentchev & Korotenko, 2007), les noyaux de dispersion (e.g. Koutsikopoulos *et al*., 1991 ; Ellien *et al*., 2000 ; Huret *et al.*, 2010) ou encore la connectivité au sein d'une population (e.g. Savina *et al*., 2009 ; Rochette *et al*., 2012 ; Lacroix *et al.*, 2013).

De l'intérêt des modèles de bioénergétique

La connectivité induite par les jeunes stades peut être étudiée de manière purement physique une fois le couplage avec un modèle hydrodynamique effectué. Dans ce cas, la dispersion ne dépend que des courants et de la turbulence. Cette dérive peut durer plusieurs mois et les facteurs de mortalité sont nombreux (Houde & Hoyt, 1987). Prendre en compte la biologie de l'espèce en simulant sa croissance, sa mortalité, son comportement (e.g. nage active, migration verticale…) etc. semble donc essentiel.

La croissance des individus est bien souvent gérée dans le modèle de manière empirique en fonction de la température et reste constante pour un stade de vie donné (e.g. Lacroix *et al*., 2013). Cette approche peut être améliorée en couplant l'IBM à un modèle bioénergétique qui va simuler les flux d'énergies au sein d'un organisme en réponse à la température et la quantité de nourriture disponible. Ainsi, un individu va croître différemment selon les conditions de température et nourriture rencontrées. La mortalité liée à des conditions environnementales défavorables (e.g. manque de nourriture) est également prise en compte grâce au couplage avec ce type de modèle.

Parmi les modèles de bioénergétique, nous avons choisi une théorie qui se veut universelle : la théorie DEB (Dynamic Energy Budget, Kooijman, 2010). Applicable à l'ensemble du vivant, elle permet de prédire la croissance et la survie d'un individu à partir de données environnementales. Cette théorie est attractive car elle comprend un nombre limité d'équations synthétisant les flux d'énergie au sein d'un organisme et dont les paramètres peuvent être calibrés à partir de jeux de données ne nécessitant que peu d'expérimentation, contrairement aux autres modèles bioénergétiques (e.g. Scope For Growth models ; Winberg, 1956). Malgré tout, son inconvénient principal réside dans la difficulté de faire correspondre les paramètres du modèle à des variables physiologiques mesurables.

Dans la théorie DEB, les fonctions physiologiques sont transcrites en un nombre réduit d'équations différentielles. Ainsi, les conditions environnementales rencontrées par un individu sont directement transformées en performances individuelles : croissance, survie, reproduction (Figure 2). Les grands principes d'un modèle DEB, illustrés en Figure 3, sont les suivants :

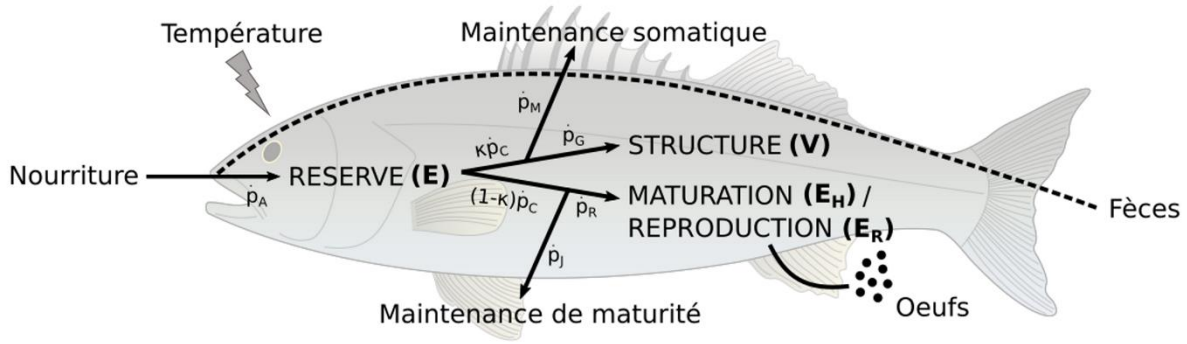

Figure 3. Représentation schématique du modèle DEB standard pour un poisson. Les flèches représentent les flux d'énergie (J/j) au sein de l'organisme, qui sont tous affectés par la température.

Les réserves représentent la quantité de nourriture stockée par l'organisme après ingestion et assimilation ($\dot{p}_A$). Cette énergie est ensuite allouée de manière constante entre la croissance ($\kappa\dot{p}_C$) et la maturation, lorsque les individus ne sont pas matures, ou la reproduction, lorsqu'ils le sont (1- $\kappa\dot{p}_C$). La maturation transcrit les processus de développement de l'organisme qui se complexifie (e.g. formation du tube digestif, prérequis à l'alimentation). C'est d'ailleurs sur cette variable d'état que sont définis les stades de vie d'un individu. Des seuils de maturité sont définis pour chaque stade de vie, le passage d'un seuil donné indiquant que l'individu a obtenu les développements ontogéniques nécessaires pour passer au stade suivant. La maintenance a

toujours la priorité sur les grandes fonctions (i.e. croissance, maturation/reproduction) et lorsqu'elle ne peut plus être assurée, faute de réserves, l'individu meurt.

Finalement, ce cadre est intéressant pour une utilisation dans le cadre d'un modèle de dérive larvaire car il permet d'obtenir des croissances différentielles et de la mortalité en fonction des conditions environnementales rencontrées lors de la dérive.

4. Le bar européen (*Dicentrarchus labrax*) comme cas d'étude

La structure des populations de bar européen

L'aire de répartition du bar européen s'étend du Maroc à la Norvège, en passant par l'Ecosse. Il est également présent dans en mer Méditerranée et en mer Noire (Pickett & Pawson, 1994).

En Europe de l'Ouest, les analyses génétiques ont mis en évidence deux populations distinctes : la population Atlantique et la population Méditerranéenne (Coscia *et al*., 2012; Quere *et al*., 2012 ; Tine *et al*., 2014). Tandis qu'on peut identifier deux sous-populations dans la population Méditerranéenne (Quere *et al*., 2012), la structure génétique de la population Atlantique est plus faible (Souche *et al*., 2015). Une étude récente (Robinet *et al*., 2020) semble remettre en question cette structuration faible en montrant deux zones de rupture : la pointe de Galice et le golfe de Saint Malo.

Pour étudier la structure de cette population Atlantique, des études de marquage conventionnels et électroniques ont été réalisées (Pawson *et al*., 2007 ; de Pontual *et al*., 2019) afin d'étudier la distribution des individus et d'explorer la connectivité entre les potentielles sous-populations de Manche et du Golfe de Gascogne et ainsi aider à la définition des stocks de bar afin d'améliorer sa gestion.

La gestion européenne du bar et l'état de la ressource

Le poids économique du bar européen revient principalement à l'aquaculture. Cette espèce fut même une espèce pionnière en terme d'élevage dès les années 70. En milieu naturel, le bar européen est également très prisé. Il est exploité depuis une cinquantaine d'années par les pêcheurs professionnels et également, depuis plus récemment, par les pêcheurs récréatifs. En raison de sa forte valeur commerciale, la pression de pêche est passée de 2000 tonnes à la fin des années 70, à 9000 t. en 2006, avant de se stabiliser vers 6000 t. en 2013 (ICES, 2012).

Malgré cet engouement, la pêche du bar n'est soumise à aucun quota ou TAC (Total Admissible de Captures). Cette ressource partagée (i.e. exploitée par plusieurs états européens), a longtemps fait l'objet d'un manque de réglementation puisqu'on pensait que c'était une espèce côtière et qu'une réglementation nationale était suffisante.

L'accroissement de la valeur commerciale de l'espèce couplée à une diminution des captures a tout de même amené le CIEM à effectuer la première évaluation du bar en 2012. En l'absence d'information sur la répartition de la (ou des) population(s) de bar le long des côtes européennes, quatre stocks (Figure 3) ont été définis de manière pragmatique et arbitraire (uniquement en fonction de la disponibilité et de la qualité des données, et sans disposer d'élément fiable de nature biologique permettant de démontrer l'existence de sous populations isolées).

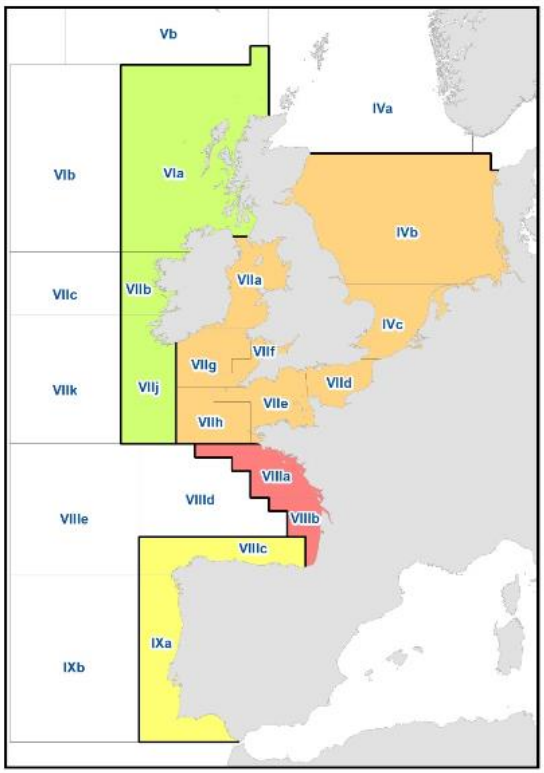

Figure 4. Délimitation des quatre stocks de bar utilisés par le CIEM pour évaluer la ressource. En orange, le "stock Nord", en vert, le "stock ouest de l'Ecosse et l'Irlande", en rouge, le « stock Golfe de Gascogne » et en jaune, le « stock côtes autour de la péninsule Ibérique ». Source : CIEM, WCCSE, 2013.

Lors de cette première évaluation, seul le « stock Nord » (en orange sur la figure 4), a été évalué puisque les informations disponibles n'étaient pas suffisantes pour réaliser l'évaluation

des trois autres stocks. Il a été montré que des années de fort recrutement, entre la fin des années 80 et 2005, ont fait augmenter la biomasse avant que cette tendance ne s'inverse (ICES, 2012). Les hypothèses avancées pour expliquer cette diminution de biomasse reproductive du « stock Nord » sont la surpêche, accompagnée d'une succession d'années à faibles recrutements.

La tendance se poursuivant, la Commission Européenne a décidé de prendre, pour ce stock « nord » des mesures exceptionnelles en 2015 (ICES, 2015) :

- Augmentation de la taille limite de capture de 36 cm à 42 cm
- Interdiction pour les chalutiers pélagiques de cibler le bar durant la période de reproduction
- Une limite de débarquement mensuelle, dépendant du type d'engin, pour les professionnels
- Un nombre limite de bars prélevés, par jour, pour les pêcheurs récréatifs

Les mesures se sont encore durcies en 2016. Durant la première moitié de l'année, le bar a fait l'objet d'une interdiction totale de pêche. Durant la seconde moitié de l'année, la limite d'un bar par sortie pour les pêcheurs récréatifs a été imposée ainsi qu'une limite d'une tonne mensuelle pour les pêcheurs professionnels. De plus, la pêche du bar a été totalement interdite autour de l'Irlande, ne subsiste alors que de la pêche récréative dans cette zone.

Depuis, les mesures se sont un peu assouplies, même si certaines restent applicables. Mais, elles ne concernent que le « stock nord » puisque l'évaluation du « stock golfe de Gascogne » (en rouge sur la figure 4), réalisée depuis 2013, ne montre pas de signes alarmants. Pourtant, pour ce stock, les tendances dans la série de recrutement et de biomasse reproductive suivent la même tendance à la baisse ces dernières années. On peut donc se poser la question d'un facteur commun qui affecterait le recrutement des deux stocks (e.g. un changement dans l'environnement ou la présence d'une unique population). Finalement, puisque ces stocks ont été définis de manière pragmatique et arbitraire et que les mesures de gestion sont désormais très différentes entre les deux stocks, des questions se posent quant à la pertinence de la définition de ces stocks.

Pour répondre à cette question, il convient de mieux comprendre la dynamique spatio-temporelle de l'espèce liée au bouclage de son cycle de vie. Décrire les HEE du bar européen, les processus de migration/dispersion les connectant ainsi que les facteurs environnementaux impliqués pourrait donner des pistes pour comprendre la série de faibles recrutements subie dernièrement par le « stock Nord ».

Le cycle de vie du bar

Les développements zootechniques visant à optimiser la production de bar en aquaculture ont permis d'améliorer considérablement les connaissances sur sa physiologie, sa reproduction et sa croissance en milieu contrôlé (e.g. Alliot *et al.*, 1983 ; Devauchelle & Coves, 1988 a et b ; Blazquez *et al.*, 1998).

Malheureusement, il subsiste encore quelques inconnues sur le bouclage de son cycle de vie en milieu naturel. La Figure 4 résume l'état des connaissances actuelles, que nous développerons ensuite.

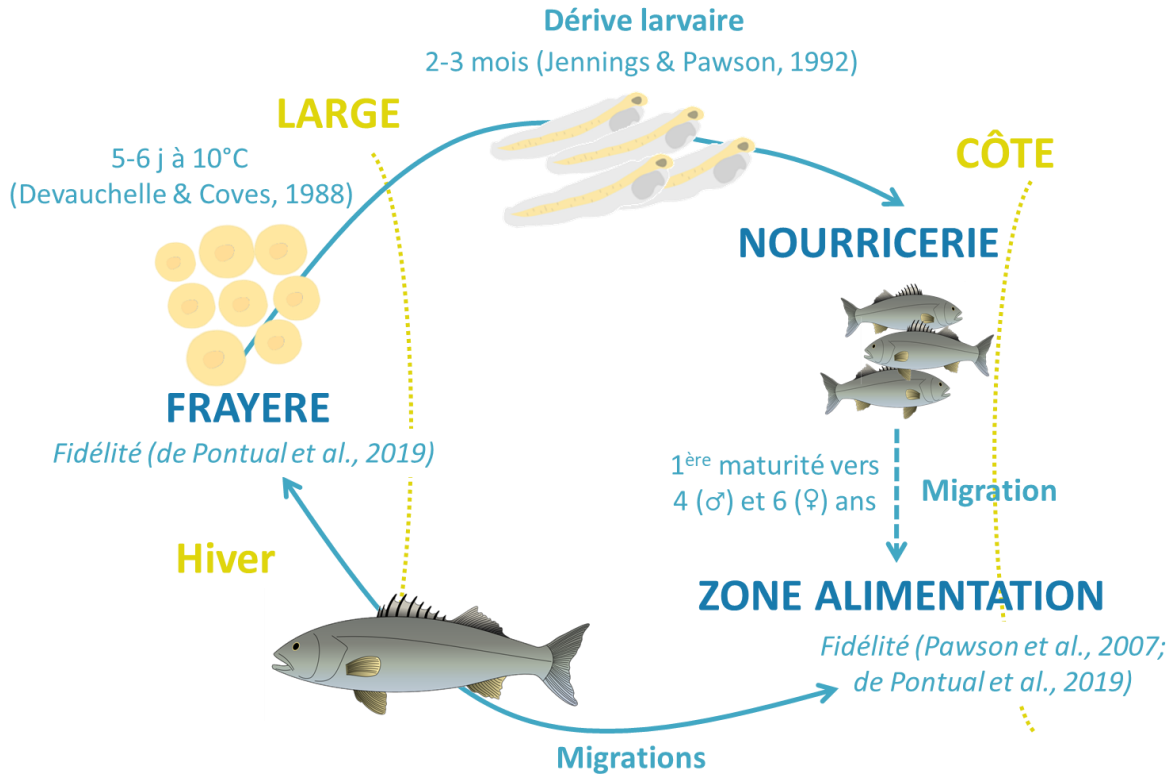

Figure 5. Schématisation du cycle de vie du bar.

Les bars adultes se nourrissent à la côte et sont, pour la plupart, fidèles à ces zones de nourrissage (Pawson *et al.*, 2007 ; de Pontual *et al.*, 2019). En hiver, ils migrent au large pour se reproduire (Pickett & Pawson, 1994 ; Pawson *et al.*, 2007 ; de Pontual *et al.*, 2019), une fidélité à ces zones de reproduction a également été mise en évidence pour certains individus (de Pontual *et al.*, 2019). Les déterminants de cette migration sont encore mal connus, mais la température semble en être un facteur important (Pickett & Pawson, 1994). La période de reproduction a été estimée entre janvier et avril/mai dans le golfe de Gascogne et la Manche (Fristch, 2005). Des gradients dans le début et la fin de saison ont pu être mis en évidence durant

cette période : d'ouest en est en Manche (Thompson & Harrop, 1987) et du sud au nord dans le Golfe de Gascogne et la Manche (Vinagre *et al.*, 2009).

Les œufs de bar sont pondus au large. Ils sont pélagiques et mesurent en moyenne 1.05 mm (Kennedy & Fitzmaurice, 1968). Ils possèdent une flottabilité neutre (Pickett & Pawson, 1994). À 10°C, ils éclosent au bout de 5-6 j (Devauchelle & Coves, 1988b). Les larves se nourrissent ensuite via des réserves nutritives contenues dans leur sac vitellin, durant environ 7 j (Barnabé *et al*., 1976). À la suite de l'ouverture de la bouche, et à l'épuisement des ressources vitellines, la nourriture planctonique est la seule source d'énergie pour les larves, sa limitation peut alors devenir un facteur de mortalité.

Les larves dérivent au gré des courants durant 2 à 3 mois en Manche, les plus petites larves arrivant sur nourricerie mesurant de 15 à 20 mm (Jennings & Pawson, 1992). Le comportement vertical des larves durant la dérive n'est pas connu mais Jennings & Pawson (1992) ont noté que la plupart des larves étaient pêchées à 15 m de profondeur, de jour. Cette donnée pourrait aller dans le sens d'une migration nycthémérale (i.e. entre le jour et la nuit) des larves comme c'est le cas du zooplancton (Forward, 1988), qui se trouve en surface la nuit et légèrement en profondeur la journée. Les larves suivraient ainsi le déplacement de leur source de nourriture et se protégeraient des prédateurs. Les nourriceries sont également mal caractérisées dans notre zone d'étude, toutes les embouchures de cours d'eau pouvant être des habitats potentiels.

Jusqu'à leur première maturation (i.e. vers 5-6 ans), le comportement des juvéniles de bar est incertain. Soit ils restent dans la nourricerie où ils sont arrivés, soit ils se déplacent pour trouver une meilleure nourricerie, soit ils se mélangent progressivement aux adultes en rejoignant leurs habitats d'alimentation estivaux. Dans tous les cas, lorsqu'ils sont devenus adultes, ils vont effectuer la migration de reproduction et ainsi participer, à leur tour, au maintien de la population.

Perspectives d'études

Il est a noté que la plupart des études ayant prodiguées ces informations sur le cycle de vie du bar en milieu naturel se sont concentrées géographiquement sur les zones côtières des pays anglo-saxons (e.g. Kennedy & Fitzmaurice, 1968 ; Dando & Demir, 1985 ; Jennings & Pawson, 1991 et 1992). Plus récemment, des études de marquage (Pawson *et al.*, 2007 ; de Pontual *et al.*, 2019) ont permis de mieux cerner la dynamique spatio-temporelle des adultes et ce, tout le long du littoral français.

La connectivité entre les HEE des adultes a, en effet, été étudiée via des approches de marquage électronique et la reconstruction de trajectoires. De Pontual *et al.* (2019) ont mis en évidence des comportements variés avec des adultes pouvant passer l'été en Manche et migrer, en hiver, dans le Golfe de Gascogne pour se reproduire. La mer d'Iroise étant alors considérée, à l'instar d'autres espèces, comme étant un corridor (Cox *et al.*, 2016). Malgré cela, des comportements de poissons résidents ont également été démontrés et le nombre de poissons marqués et recapturés ne permet pas de discerner quel comportement est le plus répandu, ni de quantifier le taux d'échange entre les deux stocks.

Il semblerait, néanmoins, que les populations de bar soient structurées avec des phénomènes de fidélité des adultes à leurs HEE hivernaux et estivaux (de Pontual *et al.*, 2019). Cela les rend particulièrement sensibles à la pression de pêche lors de leur agrégation pour se reproduire. Ainsi, une surpêche pourrait éventuellement affecter la biomasse reproductive de l'espèce.

Concernant les dernières années de mauvais recrutements (ICES, 2018), ils pourraient également s'expliquer par une altération du succès de dérive des œufs et larves menant à une mauvaise connectivité entre les frayères et les nourriceries principales de l'espèce. Ces habitats, ainsi que leurs liens dynamiques, méritent donc d'être étudiés pour explorer cette hypothèse.

5. Les objectifs de la thèse et l'organisation du manuscrit

De nombreuses inconnues demeurent sur les HEE du bar européen. Le projet BarFray, financé par le Fond Européen pour les Affaires Maritimes et la Pêche (FEAMP), dans lequel s'inscrit cette thèse, se propose de les caractériser ainsi que d'étudier leur fonctionnement afin de donner des pistes pour améliorer sa gestion (e.g. définition des stocks, mesures de gestion spatialisées, etc.).

Une action du projet s'intéresse plus particulièrement à la caractérisation des frayères du large, à la compréhension de leur fonctionnement ainsi qu'à leur connectivité avec les nourriceries côtières. Le but étant d'identifier des zones de frayère-nourricerie qui participent le plus au maintien de la population et sur lesquelles il faudrait éventuellement axer les mesures de gestion.

La Figure 5 schématise les questions de la thèse et l'organisation de ce manuscrit. La première question a été de caractériser les frayères du large et d'expliquer leurs variations intra- et interannuelles (Chapitre 1). Ensuite, pour simuler la connectivité entre frayères et nourriceries, un modèle de dérive larvaire a été mis en place. Le choix a été fait d'y inclure un

modèle bioénergétique pour simuler la croissance et la mortalité des individus (Chapitre 2). Enfin, l'analyse des patrons de dispersion a pu répondre à la question de la connectivité entre frayères et nourriceries, ainsi qu'aboutir à l'identification de « couples » frayère-nourricerie participant le plus au maintien de la population. Le lien entre les deux stocks évalués annuellement par l'ICES a également été abordé grâce à cet outil pour tenter de mieux comprendre la structuration de l'espèce en Atlantique nord-est (Chapitre 3).

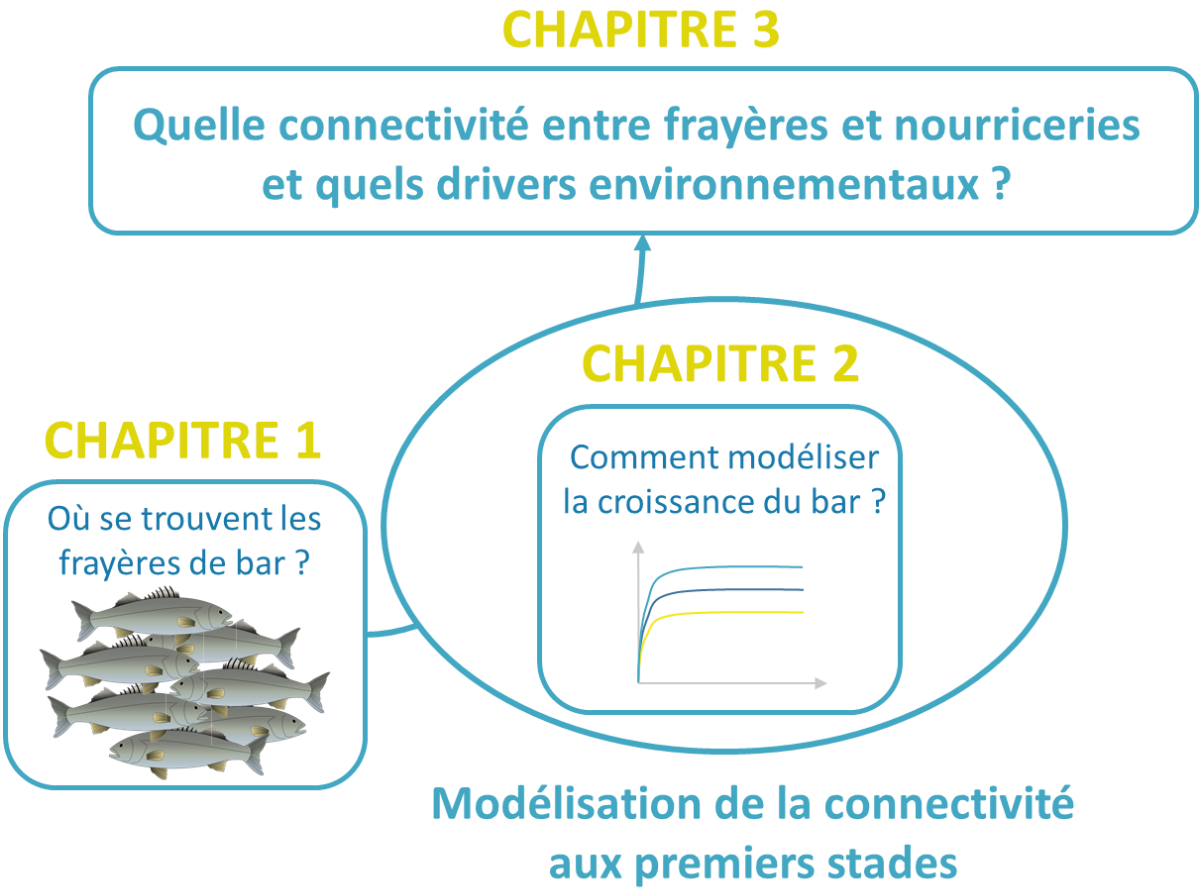

Figure 6. Schématisation des grandes questions de la thèse et leur organisation dans ce manuscrit.

Le premier chapitre s'intéresse à la localisation des frayères du large du bar de l'Atlantique nord-est. En l'absence de campagne scientifique dédiée, cette analyse s'appuie sur des données de pêche, l'enjeu étant de caractériser des zones d'agrégation hivernale. Pour cela, des outils de géostatistique non-linéaire ont été utilisés afin de localiser ces « hotspots » (i.e. zones de forte abondance) spatialement mais également temporellement. Un lien entre distribution des frayères et variables environnementales a également été exploré par une approche de modélisation bayésienne spatio-temporelle.

Le deuxième chapitre concerne le développement d'un modèle bioénergétique visant à simuler la croissance et la mortalité du bar sous forçages environnementaux. Ce modèle a été construit en suivant la théorie DEB. Il se veut applicable pour les bars de l'Atlantique nord-est et a été calibré en utilisant des données de bars sauvages adultes et juvéniles. En vue de développer un modèle pour l'ensemble du cycle de vie, deux jeux de données supplémentaires ont été utilisés concernant la croissance des larves et juvéniles en milieu contrôlé (recherche aquacole). Ce modèle a également permis d'explorer la capacité de survie des jeunes stades exposés au jeûne.

Le troisième chapitre répond à la question de la connectivité entre frayères du large et nourriceries côtières dans l'Atlantique nord-est. Grâce à l'utilisation d'un modèle individu-centré couplé à un modèle hydrodynamique et au modèle de croissance exposé dans le chapitre 2, la dérive des œufs et des larves a été simulée pour sept années (2008-2014). L'analyse des résultats a permis de mettre en évidence les grands patrons de connectivité existants entre les frayères du large (caractérisées dans le chapitre 1) et les nourriceries côtières. Les couples frayère-nourricerie les plus récurrents ont alors été identifiés et considérés comme les zones participant le plus au maintien de la population et nécessitant le plus d'attention. Ce chapitre a également été l'occasion de creuser le lien existant, via la dispersion des jeunes stades, entre les deux stocks évalués annuellement par l'ICES.

Finalement, les grandes questions et limites de chaque chapitre ont été approfondies lors d'une discussion générale. Des perspectives liées à la valorisation de ce travail d'un point de vue gestion de l'espèce ainsi qu'à son amélioration y sont également proposées.

CHAPITRE 1

CARACTÉRISER UN HABITAT ESSENTIEL DE POISSON VIA UNE ANALYSE SPATIO-TEMPORELLE DE DONNÉES DE PÊCHERIE : LE CAS DES FRAYÈRES DU BAR EUROPÉEN

Une version de ce chapitre a été publiée dans *Fisheries Oceanography*

Received: 23 April 2020 | Revised: 18 December 2020 | Accepted: 20 December 2020

DOI: 10.1111/fog.12527

ORIGINAL ARTICLE

FISHERIES OCEANOGRAPHY WILEY

Characterising Essential Fish Habitat using spatio-temporal analysis of fishery data: A case study of the European seabass spawning areas

Chloé Dambrine | Mathieu Woillez | Martin Huret | Hélène de Pontual

RÉSUMÉ DÉTAILLÉ

Les poissons recherchent différentes conditions environnementales au cours de leur cycle de vie pour assurer leurs fonctions vitales (e.g. grandir, se reproduire). Ils vivent donc dans différents habitats (Harden, 1968). Deux de ces habitats sont particulièrement intéressants puisqu'ils participent activement au renouvellement de la population via la reproduction et la croissance des jeunes stades : les frayères et les nourriceries. Il est d'autant plus important de les caractériser qu'un grand nombre d'individus s'y regroupe dans un espace restreint (Dahlgren *et al.*, 2006 ; Domeier, 2012) rendant la population très sensible aux perturbations environnementales et/ou d'origine anthropiques.

L'état inquiétant du « stock Nord » de bar européen (ICES, 2012) lié, entre autres, à une série de mauvais recrutements, fait donc s'interroger sur l'état de ces habitats pour cette espèce. L'enjeu étant alors d'identifier les zones de reproduction du bar et les facteurs qui gouvernent leurs choix afin d'étudier leurs contributions au recrutement et éventuellement d'adapter leurs mesures de gestion (e.g. fermeture de certaines zones à la pêche pendant la période de reproduction).

Généralement, des données issues de campagnes scientifiques lors de la reproduction de l'espèce sont utilisées pour caractériser les zones de ponte (e.g. sur les petits pélagiques; Bernal *et al.*, 2007). Malheureusement, la reproduction du bar a lieu en hiver et aucune campagne dédiée ne permet, à l'heure actuelle, de fournir d'informations quantitatives sur ses frayères.

Dans ce chapitre, nous nous proposons d'étudier les frayères du bar le long de la côte atlantique française à partir de données de pêcherie. Les facteurs environnementaux pouvant expliquer les variations intra- et interannuelles de la distribution spatiale de ces frayères ont également été explorés.

Une méthode de géostatistique non linéaire (Petitgas *et al.*, 2016) utilisée pour détecter les zones de forte agrégation (i.e. hotspots) a été adaptée pour caractériser l'étendue spatiale des frayères de bar sur notre zone d'étude. Pour décrire spatialement les CPUEs (Captures Par Unités d'Effort), ces données ont été transformées en indicatrice en utilisant dix seuils croissants (i.e. de 0.5 à 1000 $kg.h^{-1}$) sur lesquels divers outils mathématiques (e.g. variogrammes, variogrammes croisés) ont été appliqués. Quatre critères devaient être remplis pour qu'un ensemble géométrique A_i, défini par son indicatrice, soit considéré comme un

« hotspot » d'agrégation : (i) le variogramme $\gamma_i(h)$ est structuré, (ii) le variogramme $\gamma_{i+1}(h)$ est déstructuré, (iii) le ratio $\frac{\gamma_{i\times(i+1)}(h)}{\gamma_i(h)}$ est plat et (iv), les résidus de la régression entre $1_{A_{i+1}}(x)$ et $1_{A_i}(x)$ sont déstructurés. Pour chaque mois de chaque année (entre 2008 et 2014), cette analyse a été réalisée permettant de déterminer l'ensemble géométrique A_i représentant les frayères du bar pour une période donnée. Des cartes moyennes de présence/absence de frayères ont ainsi pu être obtenues et des informations sur la période de reproduction du bar ont également pu être déduites en comparant les valeurs des seuils z_i pour chaque mois (i.e. des seuils plus hauts en hiver caractérisent les agrégations de reproduction).

Ainsi, un gradient temporel allant du sud du Golfe de Gascogne et remontant vers la Manche Est au cours de la saison de reproduction a été mis en évidence dans l'occurrence des frayères. De plus, trois zones de frayères actives tout au long de la saison de reproduction ont pu être identifiées : le plateau de Rochebonne, la Manche Ouest et la péninsule du Cotentin. Enfin, concernant la saison de reproduction, j'ai montré qu'elle se terminerait plus tôt dans le Golfe de Gascogne (i.e. en mars) qu'en Manche (i.e. en avril).

Ensuite, le lien éventuel dans le choix des frayères avec des variables environnementales a été exploré via un modèle bayésien spatio-temporel. Huit variables environnementales décrivant les frayères ont été testées : sept variables physiques (i.e. température, salinité, bathymétrie, vitesse des courants, élévation de la surface, taille de la couche de mélange et habitat physique) et une variable biologique (i.e. chlorophylle *a*). De plus, cinq structures spatio-temporelles décrivant l'occurrence des frayères ont également été testées.

La persistance du patron de distribution des frayères a pu être montrée. Ainsi, il semble que la distribution des frayères de bar soit relativement stable. Cependant, les facteurs environnementaux testés lors de l'analyse bayésienne pour expliquer le choix des zones de frayères n'expliquent que peu cette distribution. On peut alors formuler l'hypothèse d'un processus plus mécaniste comme l'apprentissage (Petitgas *et al*. 2006) ou le homing (Griffin, 1953) conduisant à la fréquentation de zones à partir desquelles une dérive fructueuse des œufs et larves peut être obtenue. Cette hypothèse mériterait d'être testée puisque l'analyse provient de données de pêche dont les biais sont nombreux (e.g. couverture spatiale des données, fréquence de fréquentation d'une zone, capturabilité des engins…).

Characterising Essential Fish Habitat using spatio-temporal analysis of fishery data: a case study of the European seabass spawning areas

Chloé Dambrine[1,*], Mathieu Woillez[1], Martin Huret[1], Hélène de Pontual[1]
[1] Ifremer, STH, F29280 Plouzané, France

* Corresponding author.
E-mail address: chloe.dambrine@orange.fr

Abstract

Fish habitats sustain essential functions for fish to complete their life cycle, such as feeding, growing and spawning. Conservation is crucial to maintain fish populations and their exploitation. Since 2013, the spawning stock biomass of the Northern stock of European seabass (*Dicentrarchus labrax*) has been in a worrying state. A series of low recruitments with a persistently high level of fishing has been blamed, raising concerns about the processes involved in seabass reproduction and settlement in nurseries. Here, we characterise seabass spawning areas along the French Atlantic coast using Vessel Monitoring System (VMS) data. A non-linear geostatistical approach was applied, from 2008 to 2014, to detect locations where seabass aggregate for spawning. Occurrence maps of spawning distribution were combined into probability maps to quantify the seasonal and inter-annual variability and to highlight recurrent, occasional and unfavourable spawning areas. We identified three main spawning areas: the Rochebonne Plateau in the Bay of Biscay, the Western English Channel and the North of the Cotentin peninsula in the Eastern English Channel. The correlative link between this geographical distribution and environmental factors was investigated using a Bayesian spatio-temporal model. The spatio-temporal structure accounted for the vast majority of the model predictive skills, whereas environmental covariates had a negligible effect. Our model revealed the persistence of the spatial distribution of spawning areas with intra- and inter-annual variability. Offshore areas appear to be essential spawning areas for seabass, and should be considered in spatial management strategies.

Keywords

European sea bass, *Dicentrarchus labrax*, Non-linear geostatistics, Bayesian spatio-temporal modelling, English Channel, Bay of Biscay, Spawning grounds

1. Introduction

Fish live in different habitats depending on their life stages (Harden, 1968). Finding the right environmental conditions (e.g. temperature, food, oxygenation, etc.) is critical for them to achieve the phases of their life cycle and maximise the vital functions involved (e.g. growth, reproduction, etc.). These environments have been listed as "Essential Fish Habitats" in the Magnuson-Stevens Fishery Act (2007) as follows: "those waters and substrate necessary to fish for spawning, breeding, feeding or growth to maturity". Spawning areas, nurseries, migrations paths (active and passive) and feeding areas are considered essential because the successful renewal of the population relies on their good state. Spawning and nursery areas are characterised by a high concentration of individuals in a restricted area (Dahlgren et al., 2006; Domeier, 2012). It is therefore crucial to understand and describe their spatial and temporal variations to prevent overfishing in these areas when the population is vulnerable.

Following a series of poor recruitments associated with high fishing pressure (ICES, 2012), the spawning stock biomass of European seabass (*Dicentrarchus labrax*) in the North Atlantic is worrying. It raises concerns about our understanding of the habitats of this species. De Pontual *et al.* (2019) confirmed the fidelity of the species to feeding areas, and show evidence of fidelity behaviour to spawning areas. In the North Atlantic, information about European seabass spawning areas are very scarce, and no scientific survey has ever assessed seabass spawning aggregations (e.g. adult or egg sampling). The only data available is from the fisheries. However, several biases have been listed (Maunder *et al.*, 2006) that are related to fishermen's knowledge and intention (targeting or not), gear selectivity, resource catchability and external conditions (e.g. weather conditions, fuel price, management measures, etc.). Besides, these data do not follow a consistent sampling plan, and it is challenging to correlate catches to species abundance in a given area. Thus, it is important to account for these biases when using fishery data to avoid wrong conclusions.

The methods for detecting large fish aggregation or spots of overabundance (hotspots), such as those found in spawning areas, have been reviewed by Nelson & Boots (2008). Most of the time, hotspots are defined after one has applied a species distribution model on catches or densities (e.g. Colloca *et al.*, 2009) or, less frequently, using raw data (e.g. densities from scientific survey; Petitgas *et al.*, 2016). Moreover, according to these authors, in ecology, hotspots are often detected using an arbitrary density or catch threshold above which a species is considered to aggregate. This method was used by Large *et al.* (2009) to study where blue

ling aggregate to reproduce. Since then, attempts have been made to decrease the subjectivity of the threshold approach, while trying to take into account the neighbourhood of the observation. Bartolino *et al*. (2011) used the analysis of the tangent to the cumulative relative frequency distribution (CRFD) curve, whereas Petitgas *et al*. (2016) developed a geostatistical modelling approach. The originality of the geostatistical approach is that it uses spatial structural tools (variogram, cross-variogram), which allow the definition and modelling of the spatial extent of the hotspots with minimal subjectivity. A comparison between these two methods (Petitgas *et al*., 2016) showed that the hotspots highlighted using the geostatistical method are larger and colder, but better defined thanks to the tools used.

The spatial distribution of fish is not random and depends on external (e.g. the environment) and internal (e.g. density-dependence processes) population controls (Planque *et al*., 2011). Species distribution modelling, which is of growing interest in fishery ecology (e.g. Bellido *et al.*, 2008; Brodie *et al.*, 2015), must, therefore, take this into account. Traditionally, Generalized Linear or Additive Models (GLM / GAM) are used to relate the presence or abundance of a species to environmental variables. However, using these models assumes that the observations are independent, which is often not the case in fishery data (Kneib *et al*., 2008). This spatial correlation, therefore, needs to be considered to avoid wrong conclusions. A Bayesian hierarchical spatial or spatio-temporal approach is an suitable tool to account for this spatial dependency. Such approaches are of growing importance in fishery science (e.g. Munoz *et al.*, 2013; Paradinas *et al*., 2015). Compared to frequentist methods, they allow using probability to represent the uncertainty in the inputs and outputs of the model. It is also possible to attribute a random-effect to the spatial component. The use of such methods has been simplified by the development of the Integrated Nested Laplace Approximation (INLA; Rue *et al*., 2009) and its associated R package (Rue *et al*., 2014).

In this paper, our objective was to characterise the spawning areas of the European seabass in the Bay of Biscay – English Channel area. We applied the geostatistical approach of Petitgas *et al*. (2016) to a fishery dataset over the period 2008 – 2014. Studying their seasonal and inter-annual variability, we highlight the most contributing spawning areas. We, then, tested environmental covariates using an INLA geostatistical modelling approach to explain the spatio-temporal distribution of these spawning areas over the whole study area during the spawning season.

2. Material & Methods

2.1 Characterisation of the spawning areas

2.1.1 Data description

Our fishery data represented catches for all vessels that caught seabass at least once a year in the English Channel – Celtic Sea – Bay of Biscay area. The spatial extent of the fishery data is illustrated in Figure 7. On average, 74.5% of the study area was covered by observations each month. The lack of data was mainly due to the ban on fishing along the coast.

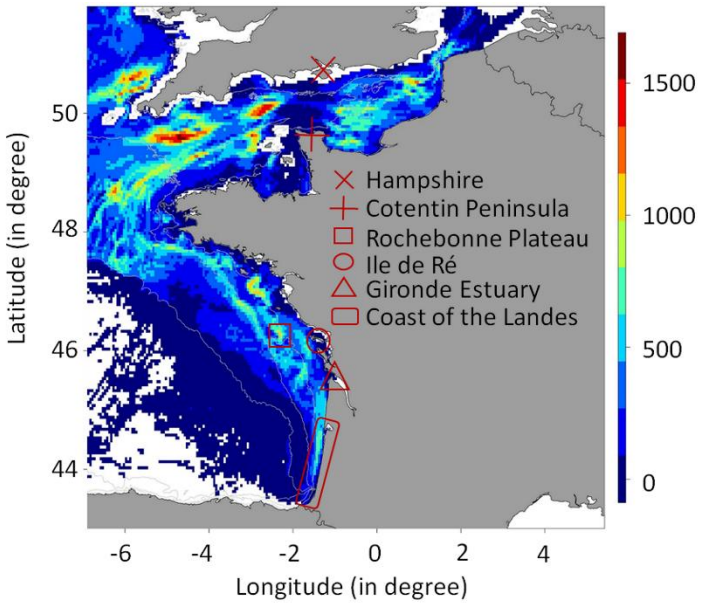

Figure 7. The study area and the spatial extent of the fishery data focused on the Bay of Biscay and the English Channel. Grid cells are coloured depending on their yearly average number of fishing hauls. Grey lines represent the isobaths 100, 200 and 300 m. Red symbols highlight locations of interest.

Data were extracted from the French SACROIS flow (Demanèche *et al*., 2010) for the period 2008-2014. Recent years were not considered since a series of management measures were set since 2015 in the Celtic Sea – English Channel area, and one of them ban pelagic trawling, method known to fish on spawning areas (ICES, 2018). SACROIS is a cross-validation tool that is similar to the approach developed by Hintzen *et al.* (2012). It assembles data from different declarative sources including the French fleet register, annual surveys of fishing activity calendars, logbooks (vessels > 10m) and monthly declarative forms (vessels < 10m), sales and geolocation data (VMS). By comparing the consistency between these information, SACROIS provides the best available data for each fishing trip.

From this flow, we gathered a table containing estimated production data (e.g. quantity of a species broken down in commercial categories (kg), duration of the fishing operations (h), etc.) per week, per square of three nautical miles and per fishing vessel. We summed the data to obtain a fishing duration and a quantity of seabass per month and square. When seabass were absent from the fishing sets, the amount was set to 0 kg. Since a Minimum Conservation Reference Size (MCRS; close to the size of the species at maturity) is applied to seabass catches, and only adult fish migrate to spawning areas (juveniles remain in coastal nurseries), it can be assumed that the proportion of juveniles in the catches was negligible, at least during the spawning period.

Using fisheries data implies having information only where fishermen have prospected. To maintain the broadest spatial coverage in our study, we focused on the gears that presented the highest seabass catch rates on average during the whole year or that targeted seabass in winter. The analysis was restricted to midwater otter (OTM) and pair trawls (PTM), bottom otter (OTB) and pair trawls (PTB), otter twin trawls (OTT), set gillnets (GNS), trammel nets (GTR), purse seines (PS) and Danish seines (SDN). On average, each square of three nautical miles was fished eight times each month. The yearly gear composition and the fishery spatial distribution over the studied period can be found in supplementary material (Figures S1, S2 and S3). The considered fishery remained more or less stable in space and time. The gear composition vary over space (i.e. depending on the location, different gears are dominant). However, the gear composition map is rather stable over time, meaning that we do not expect temporal changes in fishing efficiency and therefore Catch Per Unit Effort (CPUE) estimates. The main gears are OTB, OTT and PTM. They account on average for 43.4%, 28.5% and 8.3% respectively, with PTM presenting the highest average catch rates for seabass (23 $kg.h^{-1}$).

For our analysis, we considered CPUE data ($kg.h^{-1}$) averaged over gears by squares and months. This variable makes it possible to capture the core of the distribution of the seabass spawning areas, even though some biases exist and will be discussed hereafter. For instance, some small spawning areas may be unnoticed because they are not fished or they are exploited by a gear with a lower fishing efficiency than those producing the highest catch rates.

2.1.2 Non-linear geostatistical approach

To detect the seabass spawning areas, we used the hotspots analysis developed by Petitgas *et al.* (2016). As we had no or limited information on the seabass spawning period, we described hotspots for each month of the years in the studied time series. We also split the study area,

because the average of CPUE data differed between the two main ICES management units: the English Channel – Celtic Sea stock (i.e. latitudes ≥ N 48°) and the Bay of Biscay stock (i.e. latitudes < N 48°) and because the value of the highest cut-off depends on the global mean (Petitgas *et al*., 2016).

First, the CPUE variable was coded into indicator functions using ten cut-off values: 0.5, 1, 5, 10, 20, 50, 100, 200, 500 and 1000 kg.h^{-1} of seabass/month/square. For instance, the indicator (i.e. presence/absence) of the geometrical set A_i defined for the cut-off z_i is:

$$1_{A_i}(x) = \begin{cases} 1 \text{ if } Z(x) \geq z_i \\ 0 \text{ if } Z(x) < z_i \end{cases}$$

with $Z(x)$ the CPUE value in the square x. A geometrical set is defined as a collection of distinct objects, in our case CPUE values, for which we have examined how they are shaped or organised in space.

Three geostatistical structural tools, based on these indicators, were used: (i) the simple variogram $\gamma_i(h)$ of the geometrical set A_i, which measures the probability of entering into A_i for various distance vectors h; (ii) the ratio of the cross-variogram of the geometrical sets A_{i+1} and A_i (with $z_{i+1} > z_i$) on the simple variogram of A_i, $\frac{\gamma_{i\times(i+1)}(h)}{\gamma_i(h)}$, which quantifies the transition probability of getting inside A_{i+1} when entering into A_i from distance h, and (iii) the variogram of the residuals of the regression between $1_{A_{i+1}}(x)$ and $1_{A_i}(x)$, which quantifies the spatial behaviour within A_i of the values higher than z_{i+1}.

Then, we searched the geometrical set A_i that represents the hotspots of the spatial distribution of the CPUE values. To do so, we computed the structural tools for the different cut-offs, and then searched the highest cut-off z_i, which fulfilled the following four criteria: (i) the variogram $\gamma_i(h)$ is structured (i.e. increases for the first distance lags and then flattens (I on Figure 8); (ii) the variogram $\gamma_{i+1}(h)$ is unstructured (II on Figure 8); (iii) no edge effect is found with the highest geometrical set (III on Figure 8); and (iv) the residuals are possibly unstructured (IV on Figure 8). However, because of the high data sampling density (i.e. series of gridded maps of CPUE values with a resolution of 3 nmi x 3 nmi), the interpretation of the variograms was sometimes difficult. If the four criteria were not met together, a flat variogram ratio (IV on Figure 8) was considered as the minimal condition to determine which geometrical set should be regarded as a hotspot.

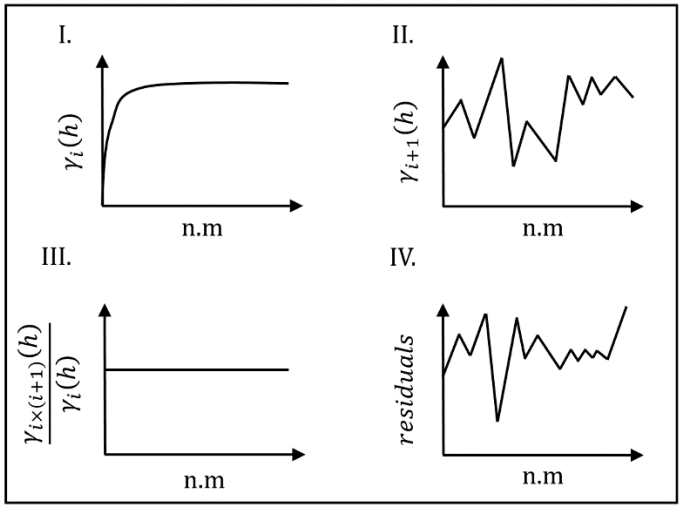

Figure 8. Theoretical situation for which the cut-off z_i of the geometrical set A_i defines a hotspot: I. the variogram $\gamma_i(h)$ is structured (i.e. shows an increase for the first distance lags and then flattens), II. the variogram $\gamma_{i+1}(h)$ is unstructured, III. the variogram ratio $\frac{\gamma_{i\times(i+1)}(h)}{\gamma_i(h)}$ is flat (i.e. $A_{i+1}$is positioned randomly within A_i) and IV. the variogram of the residuals of the regression between $1_{A_{i+1}}(x)$ and $1_{A_i}(x)$ is unstructured.

When finding the cut-off z_i for each month of the seven years (2008 – 2014) in the two areas, we made monthly comparison of the level of the A_i sets that characterise the seabass spawning season. The hypothesis was that higher cut-offs should be found in winter, attesting for the aggregation of seabass to spawn. To check this hypothesis and to confirm the seabass spawning period, we used the gonado-somatic index of seabass in the English Channel (Pawson & Pickett, 1996) and in the Bay of Biscay (ICES, 2018) to keep only months corresponding to the spawning period for each region. For the months of the spawning period, hotspots of the seabass CPUE spatial distribution were considered as seabass spawning areas.

Monthly average maps of seabass spawning areas were produced for each month of the seabass spawning period. To produce those maps, we averaged the value of $1_{A_i}(x)$ between years for each square of a month. The values of $1_{A_i}(x)$ equal to 1 outside the previously defined spawning season were set to 0 to represent fish aggregations for other purposes than reproduction. Our maps thus represent the spawning areas of importance and their variability across years. Spawning areas were classified into three categories depending on the $1_{A_i}(x)$ values in each square, namely: recurring (>0.66) occasionally favourable (0.33-0.66), and unfavourable (<0.33) areas.

2.2 Environmental drivers of the spawning areas distribution

2.2.1 Tested covariates

After characterising seabass spawning areas over the time series, we quantitatively investigated this distribution against environmental covariates. The choice of the covariates was driven by their potential effect on this demersal fish, which has a marked pelagic behaviour, especially during winter-time (Woillez *et al*., 2016; Heerah *et al*., 2017; de Pontual *et al*., 2019). Seabass migrate from coastal areas to offshore areas to spawn (Pawson *et al*., 2007) and one of the main drivers of this migration is temperature (Pickett & Pawson, 1994). We thus considered temperature as well as salinity and bathymetry as covariates pertinent to illustrate a coast to offshore gradient. The qualitative knowledge of seabass spawning areas distribution seems to correspond to very dynamic oceanographic areas. We thus tested current velocities and surface above geoid (as an indicator of eddy activity). We also considered the physical habitat that characterises the global environment of the fish and tested the ocean mixed layer thickness and the chlorophyll-*a* as general descriptors of the environment for eggs and larvae.

Among the covariates tested, two did not vary over time: the bathymetry (SHOM, 2015) and the EUNIS habitats (Hamdi et al., 2010). The EUNIS habitats were simplified in seven or four habitat classes (Tables S1 and S2). The four habitat classes were based on sediment grain size, while the seven habitat classes were also based on the position in the marine vertical zonation and the exposure to currents and swell. We also considered five physical covariates extracted from the Atlantic - European North West Shelf - Ocean Physics Reanalysis (monthly means): temperature (surface, bottom and mean over the entire water column), salinity (surface and mean over the entire water column), current velocity (surface and mean over the entire water column), ocean mixed layer thickness, and surface height above the geoid. The last was a biological covariate: chlorophyll-*a* (monthly mean from satellite observations (daily average) Reprocessed L4 (ESA-CCI)).

We considered two covariates as “not correlated” if their Pearson correlation coefficient was under 0.7.

2.2.2 Model approach

To explore the link between the distribution of seabass occurrences and its environment, we implemented a Bayesian hierarchical spatio-temporal model for each area. To reduce the amount of data involved in the computation, we focused our modelling on the months for which spawning events occurred.

To develop the model, we used the Integrated Nested Laplace Approximation (INLA; Rue *et al*., 2009) approach available in the R-INLA package of the R Statistical Programming software (Rue *et al*., 2014). This approach captures the spatial dependency using Gaussian Random Fields (GRF; e.g. Bakka *et al*., 2018). In statistical modelling, a GRF is fully defined by its mean and covariance. The covariance matrix of a GRF can be constructed based on observation location, but too many observations require a considerable computational cost. Lindgren *et al*. (2011) developed the stochastic partial differential equation (SPDE) approach to reduce these costs. Instead of building a discrete model for the GRF, this approach constructs a continuous indexed approximation of the GRF with a continuous model of Matérn Covariance structure: the SPDE. Computational time is saved because the covariance matrix is not directly computed but deduced from the sparse precision matrix produced with the SPDE. In the R-INLA package (Rue *et al*., 2014), a mesh (i.e. a triangulation of the study area, which is the best compromise between low computational costs and reasonable accuracy of the GRF representation) is used to approximate the SPDE.

2.2.3 Model development

The developed spatio-temporal model is a combination of linear predictors to explain the observed data (i.e. presence/absence of spawning areas):

$$y_{ijk} \sim \mathcal{B}in(\pi_{ijk})$$

$$g^{-1}(\pi_{ijk}) = \beta_0 + \beta_{1:n} x_{ijk} + u_{ijk}$$

with y_{ij} the presence or absence of spawning areas at the location *i* during the month *j* of the year *k*, π_{ijk} the probability of presence, g the logit link function, β_0 the intercept, $\beta_{1:n}$ the linear effects of the covariates x_{ijk}, and u_{ijk} different structures of spatio-temporal random effects. We used an independent zero-mean Gaussian prior for the intercept and the other linear predictors. The spatial component has two parameters τ and κ, which correspond to the total variance and the spatial range, respectively. For them, an independent Gaussian prior was used for the reparametrised log(τ) and 2log(κ).

We first focused on the spatio-temporal structure within the spawning season without considering the inter-annual variability. We tested five different spatio-temporal structures for u_{ij} among those reviewed by Martínez-Minaya *et al*. (2018). In the first case:

$$u_{ij} = w_{ij}$$

with w_{ij} x spatial realisations (i.e. one for each month of the spawning season) that share a common covariance function (same κ and τ). This structure would highlight that the spawning areas are in different zones each month of the spawning season (Paradinas *et al*., 2015).

In the second and third cases:

$$u_{ij} = w_i + v_j$$

with w_i a unique spatial realization and v_j being either a linear random effect (case 2) or a linear temporal trend effect (case 3) on the months. Case 2 would highlight that spawning areas are persistent during the months of the spawning season (Paradinas *et al*., 2015) and case 3, that they persist with an intensity trend over months of the spawning period (Paradinas *et al*., 2016).

Building from earlier model development, the inter-annual variability was added in our analysis as a linear random effect. First, as an independent variable:

$$u_{ijk} = w_i + v_j + x_k$$

with w_i a unique spatial realisation, v_j and $x_k$two linear random effects, for the months and the years, respectively. This structure would highlight that spawning areas persist among months (like previous structure, case 1) but also among years during the spawning season.

Then, as a shared variable for the intra- and inter-annual variability with x levels (i.e. x spawning months × x years analysed):

$$u_{ijk} = w_i + v_{jk}$$

with w_i a unique spatial realisation and v_{jk} a linear random effect for the month *j* of the year *k*. This structure would highlight a persistent pattern in seabass spawning areas distribution with small differences between month and years.

2.2.4 Model evaluation

Models were calibrated using 75% of the dataset. INLA outputs propose the use of the Watanabe-Akaike Information Criterion (WAIC) to evaluate and compare the different combinations. This criterion computes the variance separately for each data point and averages after. It was preferred to the Deviance Information Criterion (DIC), which only averages the variance over a point estimate. The prediction quality of the model was tested using cross-validation over the average logarithm of the Conditional Predictive Ordinate (CPO; Geisser, 1993). The smaller the value of LCPO and WAIC, the better the compromise between fit, predictive quality and parsimony of the model. Hence, the best model was the one with the

lowest LCPO and WAIC values. We also validated the best model on the remaining 25% of our dataset by mapping the predictions *vs.* the observations per month of the spawning season and per year. We finally used boxplots between observations and predictions to assess the ability of the model to predict values of 0 (absence) or 1 (presence).

2.2.5 Model selection strategy

First, we selected the best spatio-temporal structure for each area. We then tested each covariate, together with the selected spatio-temporal structure, as a linear or non-linear (random walk 1 model) predictor, and chose the one that minimized our two criteria. For the covariates available at different depth levels in the water column (i.e. temperature, salinity and current velocity), we selected the level with the lowest two criteria to be used in further combinations. If the covariate did not decrease the WAIC and/or average values of the LCPO compared to the spatio-temporal structure alone, it was not used further in the model construction. Finally, we tested all the combinations of the covariates selected. For each area, we selected the best model as the one representing the best compromise between low WAIC and LCPO values and containing solely relevant variables (i.e. variables whose 95% confidence interval (CI) does not cover 0).

3. Results

3.1 Seabass spawning season

We applied the geostatistical methodology to each month in each of the two areas and for the whole study period. The results for each of the four criteria are summarised in Table S3 for the English Channel and Table S4 for the Bay of Biscay.

Tables 1 and 2 summarise the geometrical sets (i.e. from the set A_1 that corresponds to a cut-off of 0.5 kg.h^{-1} of seabass/month/square to the set A_{10} for a cut-off of 1000 kg.h^{-1} of seabass/month/square) representative of the hotspots of the mean CPUE distribution for each month between 2008 and 2014, in the two areas.

The cut-off value defining the geometrical sets that correspond to hotspots of the CPUE spatial distribution varies depending on years, months and areas from 1 kg.h^{-1} (A_2) to 50 kg.h^{-1} (A_6) of seabass/month/square. As expected, hotspots corresponding to the highest cut-off values (A_5 and A_6) occurred mostly during winter (i.e. asterisks in Tables 1 and 2) and were assumed to characterise the spawning aggregations of seabass. Assuming that fishery data do indeed accurately capture the spawning aggregations within a year and that these cut-offs were selected

correctly, our results indicate that the spawning season occurs between December to April in the English Channel and between January and March in the Bay of Biscay.

*Table 1. Geometrical sets identified as hotspots of the CPUE spatial distribution for the English Channel for each month between 2008 and 2014. * represent the two sets with the highest cut-off values.*

	2008	**2009**	**2010**	**2011**	**2012**	**2013**	**2014**
January	A_5^*	A_5^*	A_6^*	A_5^*	A_5^*	A_6^*	A_4
February	A_5^*	A_5^*	A_5^*	A_6^*	A_5^*	A_6^*	A_2
March	A_5^*	A_5^*	A_6^*	A_5^*	A_5^*	A_6^*	A_3
April	A_5^*	A_5^*	A_5^*	A_5^*	A_5^*	A_5^*	A_5^*
May	A_3	A_3	A_3	A_3	A_3	A_5^*	A_3
June	A_3	A_3	A_3	A_3	A_3	A_2	A_2
July	A_3	A_3	A_2	A_3	A_2	A_2	A_1
August	A_2	A_2	A_2	A_4	A_2	A_2	A_2
September	A_2	A_2	A_3	A_2	A_2	A_2	A_1
October	A_3	A_3	A_2	A_2	A_2	A_2	A_2
November	A_4	A_4	A_5^*	A_4	A_3	A_5^*	A_2
December	A_6^*	A_6^*	A_5^*	A_5^*	A_5^*	A_4	A_2

*Table 2. Geometrical sets identified as hotspots of the CPUE spatial distribution for the Bay of Biscay for each month between 2008 and 2014. * represent the two sets with the highest cut-off values.*

	2008	**2009**	**2010**	**2011**	**2012**	**2013**	**2014**
January	A_3	A_5^*	A_6^*	A_6^*	A_5^*	A_5^*	A_4
February	A_5^*	A_5^*	A_5^*	A_5^*	A_5^*	A_5^*	A_5^*
March	A_5^*	A_5^*	A_5^*	A_5^*	A_4	A_4	A_3
April	A_3	A_4	A_4	A_3	A_3	A_2	A_3
May	A_3	A_3	A_5^*	A_4	A_2	A_3	A_2
June	A_3	A_3	A_4	A_3	A_2	A_3	A_2
July	A_3	A_3	A_3	A_2	A_2	A_3	A_2
August	A_3	A_2	A_3	A_2	A_2	A_2	A_2
September	A_4	A_2	A_3	A_3	A_3	A_3	A_2
October	A_3	A_4	A_3	A_3	A_5^*	A_4	A_4
November	A_3	A_3	A_2	A_5^*	A_4	A_3	A_4
December	A_5^*	A_3	A_3	A_4	A_5^*	A_4	A_4

After considering the gonado-somatic index of European seabass in our two areas, we removed December data from our English Channel analysis, as we assumed that seabass would not be ready to spawn in this month. The seabass spawning season was then only slightly different between the two areas: from January to March in the Bay of Biscay and from January to April in the English Channel.

Besides, as the 2014 cut-off values were low compared to the other years (i.e. not surely highlighting spawning aggregations in winter), particularly in the English Channel, the next steps of our analyses only considered seabass' spawning areas identified over the period 2008 - 2013.

3.2 Important spawning areas

Figures 9 and 10 represent average maps of hotspots during the spawning season.

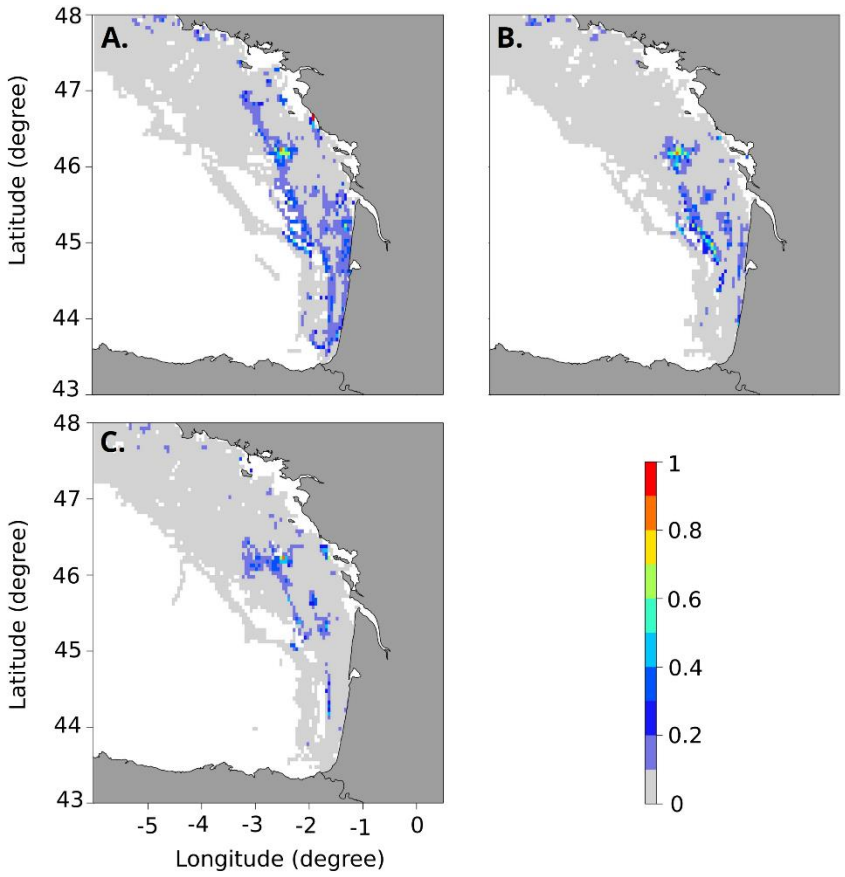

Figure 9. Monthly average maps of seabass spawning areas, from the geostatistical analysis, in the Bay of Biscay during the period 2008-2013: A. January, B. February and C. March. A probability of presence between 0 and 0.33 suggests that the area was rarely favourable every year. In contrast, a probability of presence between 0.66 and 1 indicates that the area was identified as a spawning area for several years. Values in between suggest that the area was occasionally favourable.

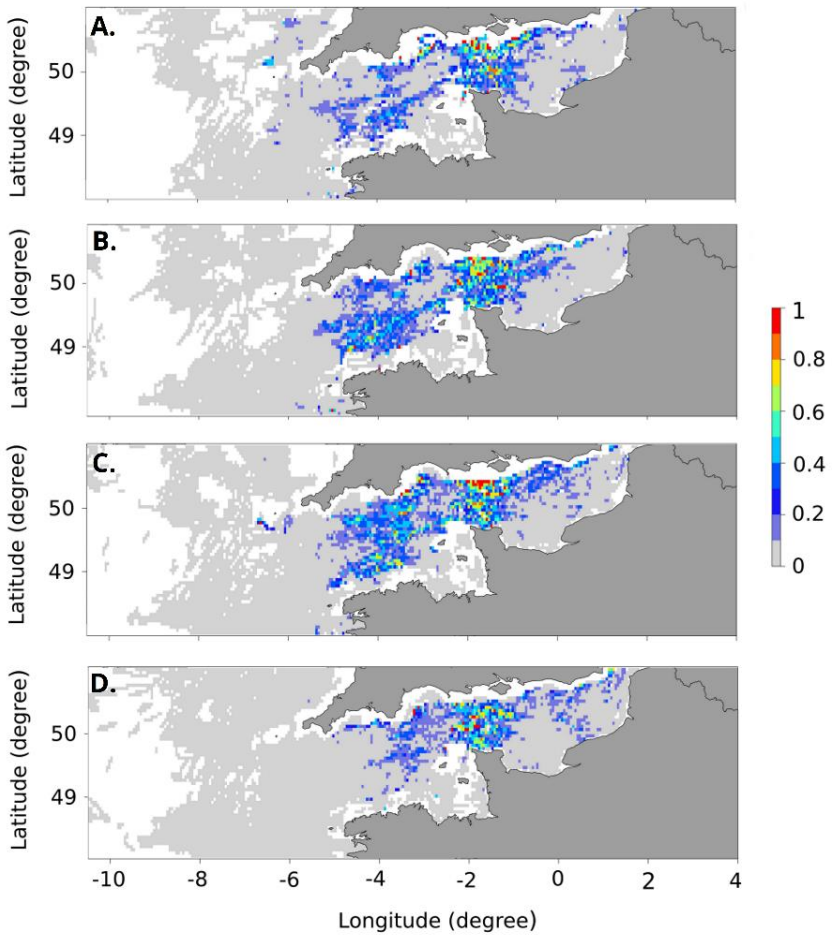

Figure 10. Monthly average maps of seabass spawning areas, from the geostatistical analysis, in the English Channel during the period 2008-2013: A. January, B. February, C. March and D. April. A probability of presence between 0 and 0.33 suggests that the area was rarely favourable every year. In contrast, a probability of presence between 0.66 and 1 indicates that the area was identified as a spawning area for several years. Values in between suggest that the area was occasionally favourable.

In the Bay of Biscay (Figure 9), the Rochebonne Plateau (W 2°28, N 46°12) appeared as an essential spawning area during the entire spawning season (i.e. probability of presence as a spawning area between 0.5 and 0.8). Several occasional spawning areas also appeared along the continental shelf during the entire spawning season and particularly in February (i.e. probability between 0.2 and 0.4). Two additional occasional spots were found with lower probabilities (i.e. probability between 0.1 and 0.5): one in front of the Gironde Estuary (W 1°20, N 45°59) and another one west of Île de Ré (W 1°54, N° 46°21). Last, the Coast of the Landes (between N 44°60, N 43°50) appeared as an occasional spawning area at the beginning of the spawning season (i.e. probability between 0.1 and 0.5). The rest of the Bay of Biscay seems

unfavourable for seabass reproduction, except in some specific areas in the west of Britany (i.e. probability of presence as a spawning area between 0.1 and 0.3).

In the English Channel (Figure 10), the main spawning areas appeared more widespread. The North of the Cotentin peninsula (W 1°71, N 50°27) stood out as a stable spawning area throughout the spawning season (i.e. probability always above 0.6). One area in the south-west of Hampshire showed very high probability in March (probability > 0.9, Fig. 10). The Western English Channel appeared as a recurring spawning area, particularly in February (probability between 0.4 and 0.6). In contrast, the northeastern part of the English Channel showed more occasional and unfavourable areas for seabass reproduction.

These figures show that the distribution of the spawning areas have shifted northward during the spawning season with: (i) a decrease in their extent from January to March in the Bay of Biscay (see also Table 3) and (ii) a dome shaped extentand a shift eastward between January and April in the English Channel (with a peak in February and March; Table 4).

Table 3. The extent of the spawning areas (km^2) for each month of the spawning season in the Bay of Biscay as deduced from the number of squares of three nautical miles highlighted as a spawning area.

	2008	**2009**	**2010**	**2011**	**2012**	**2013**	**Mean**	**Sd**
January	10 248	7 779	926	1 173	2 963	2 160	**4 208**	**3872**
February	5 031	2 438	2 068	1 728	1 481	1 605	**2 392**	**1339**
March	3 611	926	802	1 389	1 450	1 697	**1 646**	**1020**

Table 4. The extent of the spawning areas (km^2) for each month of the spawning season in the English Channel – Celtic Sea as deduced from the number of squares of three nautical miles highlighted as a spawning area.

	2008	**2009**	**2010**	**2011**	**2012**	**2013**	**Mean**	**Sd**
January	12 100	7 130	7 748	13 829	8 828	5 463	**9 183**	**3173**
February	15 619	18 428	13 613	6 050	15 125	5 463	**12 383**	**5367**
March	13 952	19 262	8 519	14 909	16 360	10 094	**13 849**	**3981**
April	8 519	10 649	6 575	5 402	4 043	11 915	**7 851**	**3063**

We observed significant annual variability in the extent of the spawning areas in the Bay of Biscay with a trend towards smaller spawning areas in the latest years (Table 3). A similar pattern was observed for the English Channel (Table 4), with large annual variability and a

trend towards smaller spawning areas over the series, at the exception of January and March 2011 and February and March 2012.

3.3 Environmental drivers explaining the distribution of the spawning areas

The results of the five spatio-temporal structures are presented in Table 5. The best structure corresponds to a persistent spatial distribution with random intensity changing over months and years together (case 5) in the Bay of Biscay and the English Channel.

Table 5. WAIC and mean LCPO values for the five tested spatio-temporal structures.

		English Channel		Bay of Biscay	
Spatio-temporal structure	**Process**	**WAIC**	**LCPO**	**WAIC**	**LCPO**
$u_{ij} = w_{ij}$	Opportunistic monthly spatial distribution during the spawning season	78589	0.2970	12432	0.1048
$u_{ij} = w_i + v_j(1)$	Persistent spatial distribution with random intensity changes over the months of the spawning season	32178	0.1216	8215	0.068
$u_{ij} = w_i + v_j(2)$	Persistent spatial distribution with temporal intensity trend over the months of the spawning season	77614	0.2934	11862	0.096
$u_{ijk} = w_i + v_j + x_k$	Persistent spatial distribution with random intensity changes over months and years separately	31995	0.1209	7648	0.0642
$u_{ijk} = w_i + v_{jk}$	Persistent spatial distribution with random intensity changes over months and years together	31344	0.1185	7526	0.0636

The results of all linear combinations are presented in Table S5 (English Channel) and S6 (Bay of Biscay). We removed from the final model covariates whose 95% CI included zero (i.e. the intercept and the chlorophyll-*a* in the English Channel and the intercept and the bottom grain size in the Bay of Biscay).

Thus, the best models were:

$$g^{-1}(\pi_{ijk}) = \beta_1\, Mld + \beta_2\, UoVo\, S + f(mean\, S) + f(mean\, T) + w_i + v_{jk}$$

in the English Channel and:

$$g^{-1}(\pi_{ijk}) = \beta_1\, Bathy + \beta_2\, Mld + f(mean\, T) + w_i + v_{jk}$$

in the Bay of Biscay.

Figure 11 shows an example of the validation using the remaining 25% of our dataset, in each area (for January 2008). All predictions over the time series are provided in supplementary materials (Figures S4 and S5).

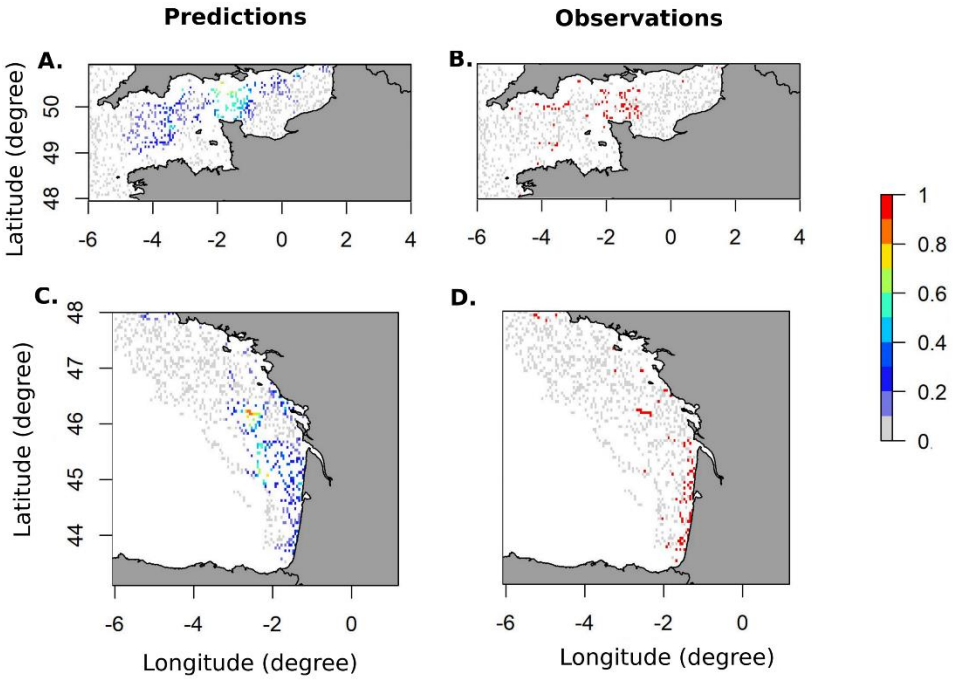

Figure 11. Predicted maps of probabilities for the presence of seabass spawning areas in January 2008 for the English Channel (A&B) and the Bay of Biscay (C&D) with the best spatio-temporal model compared to the maps of observed seabass spawning areas.

The models were efficient in predicting the general pattern of presence of the spawning areas but did not accurately predict their precise location (see low probabilities in Figure 11). This is confirmed in Figure 12, which shows that the models can detect unfavourable and favourable areas. Yet, for the later, the probabilities remain lower than expected, and we would have expected, a better ability to discriminate favourable areas (i.e. probability closer to 1).

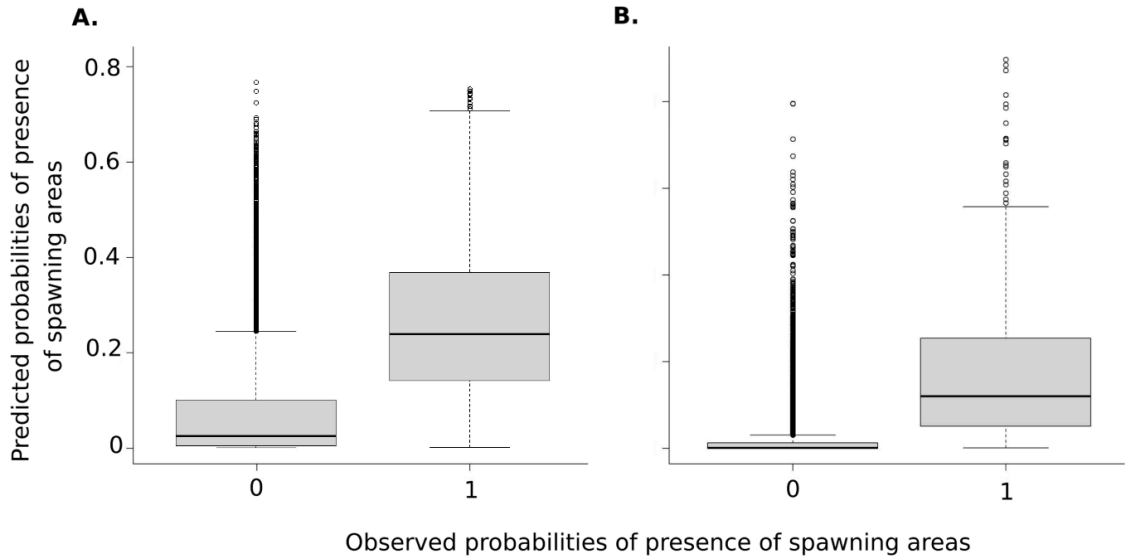

Figure 12. Predicted probabilities of presence of seabass spawning areas vs. *observed seabass spawning areas with the best spatio-temporal model for A. the English Channel and B. the Bay of Biscay.*

Table 6 shows that both covariates (current velocity and mixed layer depth) have a positive effect on the distribution of the spawning areas in the English Channel. In the Bay of Biscay, bathymetry also has a positive effect, while mixed layer depth has a negative effect.

Table 6. Summary of the fixed effects of the best model for the English Channel (two first lines) and the Bay of Biscay (two last lines).

Fixed effect	Mean	Sd	25% Q	97.5% Q
Mld	0.006	0.002	0.002	0.009
UoVoS	3.931	0.894	2.170	5.681
Bathy	0.003	0.001	0.0009	0.006
Mld	-0.005	0.002	-0.009	-0.0008

Figure 13 illustrates the non-linear effect of each environmental covariate on the probability of the presence of seabass spawning areas as predicted by the best model in the English Channel. According to these results, seabass prefer locations with a mixed layer depth between 50 and 90 m, with moderate currents (mostly between 0.15 and 0.17 $m.s^{-1}$), and temperature around 10°C and avoid temperatures around 7°C, they also avoid salinity around 34.

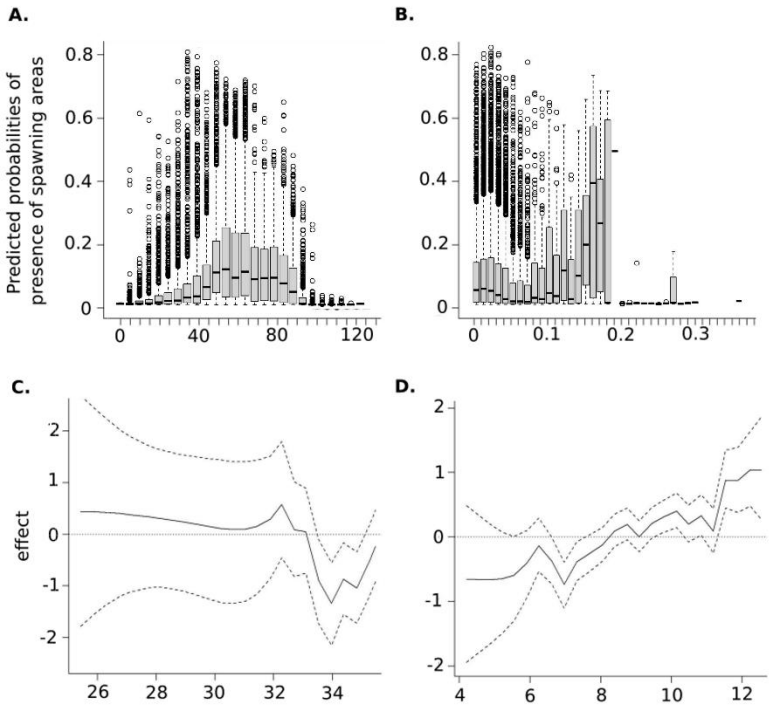

Figure 13. Predicted probabilities of presence with the best model in the English Channel under A. mixed layer depth, B. surface current velocities, C. mean salinity of the water column and D. mean temperature of the water column. For A. and B., each boxplot corresponds to an interval of 5 m for the mixed layer depth and 0.01 m.s^{-1} for current velocities. The rectangles go from the first to the third quartiles and are cut by a horizontal line, which represents the median. The whiskers lead to the outliers, which are represented by dots. For C. and D., dotted lines represent the 25% and 95% quantiles.

Figure 14 shows the effect of the covariates in the Bay of Biscay. Seabass target areas between 30 and 90 m deep, a mixed layer depth of 100 m and shallower, and temperatures around 9-10°C and avoid temperatures around 13°C.

The spatial effect nominal range, the variances of the spatio-temporal effect and the temporal structure are illustrated in Figures S6 (English Channel) and S7 (Bay of Biscay). The mean posterior value of the spatial effect nominal range (i.e. the mean diameter of the spawning areas) is around 170 km in the English Channel and 120km in the Bay of Biscay. The scale of the variances for the spatial and temporal structures are similar from an area to another, with the spatial variances being smaller than the temporal variances. The Gaussian field with Matérn correlation, named the spatial field, is rather smooth, while most of the variability is temporal (intra and inter-annual).

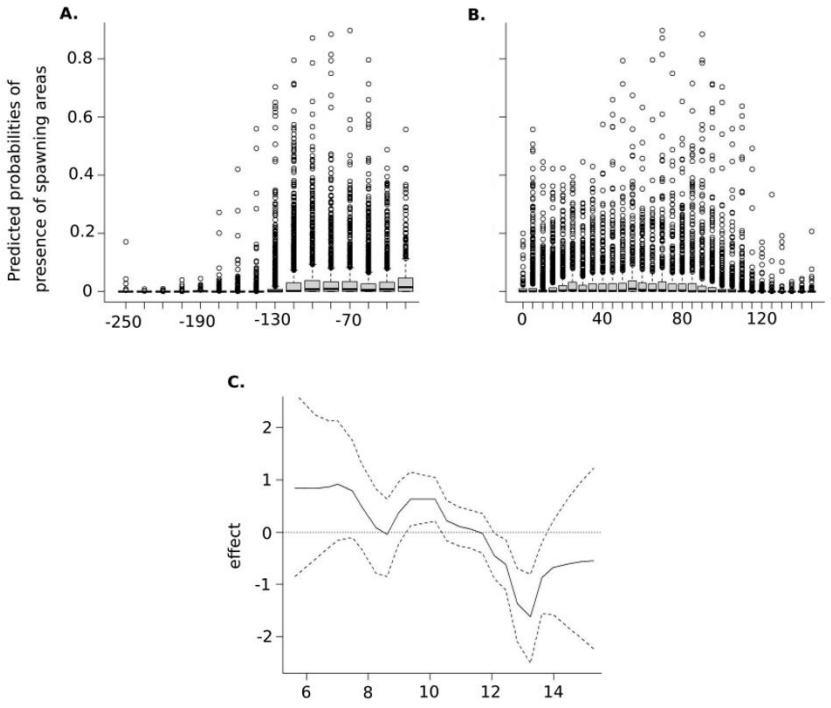

Figure 14. Predicted probabilities of presence with the best model in the Bay of Biscay under A. bathymetry, B. mixed layer depth and C. mean temperature of the water column. For A. and B., each boxplot corresponds to an interval of 15 m for the bathymetry and 5 m for the mixed layer depth. The rectangles go from the first to the third quartiles and are cut by a horizontal line, which represents the median. The whiskers lead to the outliers, which are represented by dots. For C., dotted lines represent the 25% and 95% quantiles.

In the English Channel, the random intensity changes (Figure S6, C) remain very variable across years. In average, random intensity is high for February and March and low for January and April. In the Bay of Biscay (Figure S7, C) the variability of the spatial field during the spawning season moves from high in January to low in March except for years 2010 and 2011 showing higher values in February than in January.

The mean and standard deviation of the persistent spatial field are shown in Figures S8 (English Channel) and S9 (Bay of Biscay). From the values of the posterior mean of the spatial effect, the spatial field itself can locate most of the areas favourable for reproduction. The contribution of each covariate to the prediction ability of the model (Tables 7 and 8) also confirms the importance of the spatial field. In both areas, removing the spatio-temporal structure leads to a model with weak prediction skills (i.e. less than 1% combined). In the English Channel, the spatial structure seems to explain more than the temporal structure, whereas this is the opposite

in the Bay of Biscay. In both cases, the environmental covariates do not explain much of the seabass spawning distribution.

Table 7. Contribution of each covariate to the model predictive skills in the English Channel.

Model	LCPO	Relative variation (%)
Entire model	0.1175629	0
Model without temporal structure	0.1238289	5.33
Model without spatial structure	0.1771387	50.68
Model without spatio-temporal structure	0.2155217	83.32
Model without mean S	0.1178772	0.27
Model without mean T	0.117961	0.34
Model without Mld	0.1176035	0.03
Model without UoVoS	0.1176306	0.06

Table 8. Contribution of each covariate to the model predictive skills in the Bay of Biscay.

Model	LCPO	Relative variation (%)
Entire model	0.0582153	0
Model without temporal structure	0.08210038	41.03
Model without spatial structure	0.07460561	28.15
Model without spatio-temporal structure	0.09887661	69.85
Model without Bathy	0.05837433	0.27
Model without mean T	0.05854458	0.57
Model without Mld	0.0584373	0.38

4. Discussion

The ecology of the wild seabass reproduction is an important research focus for fishery scientists. Reproduction is a critical phase of fish life cycles for population renewal. It is also a phase when a species is most vulnerable to overexploitation as fish aggregate in restricted areas. By sampling eggs and larvae in the English Channel, several studies revealed that seabass reproduce mainly offshore (e.g. Thompson & Harrop, 1987) but that coastal spawning areas also exist (e.g. Kennedy & Fitzmaurice, 1972). Tagging surveys have also confirmed the migration of seabass to offshore spawning areas (Pawson et al., 2007) and highlighted their fidelity to these areas (de Pontual et al., 2019). Managing these areas is therefore critical for the sustainability of seabass populations.

Unlike for many other species such as cod (Andrews *et al*., 2006) or hake (Woillez *et al*., 2007), no quantitative spatial observation independent from fishery data (i.e. scientific survey) occurred in winter to characterise European seabass spawning distribution in the North Atlantic. Only fishermen's knowledge can locate them qualitatively, and fishery data were the only data

available for our study. Therefore, we made the hypothesis that these data would be suitable to capture seabass spawning areas as well as the timing of spawning.

However, CPUE data are known to be non-proportional to fish abundance. The two main types of non-proportionality have been reviewed by Harley *et al*. (2001): (i) hyperstability, which is the most common (i.e. CPUE declines slower than abundance, as observed when fishing effort is concentrated on large fish aggregations), and (ii) hyperdepletion (i.e. CPUE declines faster than abundance, due to different fish behaviour in response to fishing gear). In our study, ignoring CPUE hyperstability in seabass spawning areas could lead to erroneous conclusions about the abundance of the species. We acknowledged the possible biases in our results due to catchability and efficiency differences and changes over time for this multi-gear fishery. However, our objective was to study seabass aggregation behaviour rather than modelling and mapping their abundance. The spatial structure of the tail of the CPUE distribution (i.e. that of a cut-off at high CPUE values) was thus still very informative to indicate spawning aggregations. Besides, fishermen prospecting only known fishing areas have access to limited fish quantities, and some secondary spawning areas may be unnoticed (e.g. in the coastal zone, where VMS based fishing distribution is lower, see Figure 1). There are also differences in fishing efficiency between gears or catchability between fishermen. The detection of core spawning areas may be compromised by fishermen who overestimate the importance of secondary spawning aggregations. However, as pelagic trawlers are the main fleet targeting seabass aggregations in winter, and also the most efficient fleet to catch spawning seabass (see Figures S2 and S3), we believe core spawning areas are correctly detected, while secondary spawning areas may be underestimated or missed (e.g. exploited by a less efficient gear, e.g. gillnets). Then, as the gear composition over space did not change substantially over the period, we considered that our analysis was weakly impacted by the changes in fishing efficiency over time. Our two stage analysis does not account for the differences in fishing effort, and fishermen may conduct more fishing operations in areas with high fish abundance. By aggregating CPUE data over squares and months, preferential sampling should result in higher average CPUE in areas with high fish abundance. As the full range of CPUE values is used to predict the spatial distribution of abundance or biomass, our non-linear geostatistics approach allows us to focus on the most productive areas without trying to correct for biases or errors due to differences in catchability.

With this approach, we have identified the recurring spawning areas of the European seabass along the French Atlantic coast. Our average maps of the presence of spawning areas are in line

with fishermen's empirical knowledge of seabass spawning areas (Drogou, pers. comm.). We also confirmed the persistence of their distribution across months and years using a Bayesian spatio-temporal analysis. We identified three key spawning areas throughout the reproductive season: the Rochebonne Plateau in the Bay of Biscay, the Western English Channel and the North of the Cotentin Peninsula in the eastern English Channel. These results are congruent with the work of Masski (1998), who highlighted significant seabass abundance in the Western English Channel from January to April. Our study is also in agreement with Fritsch (2005), who pointed out to two recurring areas in the Bay of Biscay: the Rochebonne Plateau and the south of the Gironde Estuary. However, the author pointed out the significant variations in seabass aggregations across years in this area. Our study provides critical information for seabass fishery management in the North Atlantic. However, a dedicated scientific survey during the spawning season could improve knowledge on seabass reproduction and provide more information on the spatial distribution and maturity of adults, as well as on the number and stages of eggs.

We also identified a northeast gradient in the occurrence of spawning areas, which changes over time: spawning areas progress northward from the southern section of the Bay of Biscay to the middle of the English Channel during the spawning season. This result is consistent with the work of Thompson & Harrop (1987), who described an eastward gradient of occurrence in the spawning areas of the English Channel from February to the end of June. Our Bayesian spatio-temporal analysis confirmed this result by showing: (i) a seasonal trend with a decrease in the number of spawning areas throughout the spawning season particularly in the Bay of Biscay; and (ii) a non-significant inter-annual variability in the importance of the spatial field for each month of the spawning season.

Unfortunately, the geostatistical method, even if it presents higher cut-offs in winter, does not allow characterising precisely the seabass' spawning season. Indeed, a latitudinal gradient in the beginning of the spawning season is known (e.g. Vinagre *et al*., 2009), which does not appear in our analysis. Based on only one available study that was conducted almost two decades ago (Pawson & Pickett, 1996), we removed December from our analysis in the English Channel as it could rather represent pre-spawning aggregations (Vàzquez & Muñoz-Cueto, 2014) or a shift in the spawning period due to climate change compared to the study. Moreover, we had to remove the year 2014 from our analysis. The low cut-off value observed could be linked to particularly bad weather conditions that impaired French pair trawlers to fish this year (ICES, 2015). However, it could also be linked to changes in the abundance of the species.

Indeed, as explained by Petitgas (1998), the level of fish aggregation can be associated with seabass biomass and the lower cut-off value could reflect lower biomass in 2014. This is in agreement with the 2015 ICES report, which highlights a decrease in the northern seabass spawning stock biomass (SSB) since 2013.

Combining our hotspots detection results and those of the gonado-somatic index, we showed that the seabass spawning season ends earlier in the Bay of Biscay than in the English Channel. This result is congruent with the work of Vinagre *et al*. (2009) showing a latitudinal gradient in the seabass spawning season. However, using our methodology, it was difficult to characterise the exact timing of the spawning season, even if cut-offs appeared lower in spring and summer than in winter and autumn. One way to improve the hotspot methodology for characterising the timing of the seabass spawning season using VMS data only could be the implementation of monthly cross-variograms and the study of the correlation between geometrical sets at different spatial scales. This method could help to highlight how seabass aggregations form, persist and disappear throughout the spawning season. Moreover, we decomposed our analysis in two parts but according to Opitz *et al*. (2018), threshold overrun and environmental predictors could be combined in one modelling approach within INLA.

Our Bayesian spatio-temporal models suggest that the spatio-temporal effect explains most of the distribution of seabass spawning areas. Using a correlative approach, we found that it was difficult to predict seabass spawning areas using the selected environmental variables as they did not explained much of the presence/absence of seabass' spawning areas. The underlying ecological process driving the geographical distribution of seabass spawning areas is not elucidated by available environmental covariates. According to de Pontual *et al*. (2019), we can expect that seabass return to the same spawning areas. Two non-exclusive processes can explain this fidelity behaviour. One is the possibility of a stock memory to ensure good population renewal, referred to as the "Entrainment hypothesis" (Petitgas *et* al. 2006). In the "Entrainment hypothesis", first-time spawners learn the migration routes from old adults to ensure the spatial persistence and the closure of their life cycle. The second is the homing process (Griffin, 1953) in which fish have the innate ability to go and reproduce where they were born. This process could explain the persistence of seabass spawning areas. The question of natal homing could be addressed using near-core otolith microchemistry analysis, as done for several other species (e.g. Artetxe-Arrate *et al.*, 2019). Testing these hypotheses using a mechanistic approach could help identify the environmental forcing characterising the distribution pattern of seabass spawning areas.

For the covariates, our models showed that environmental drivers poorly explained seabass distribution. In both areas, temperature over the water column and mixed layer depth have been selected. In addition, mean salinity of the water column and currents of the surface have been selected in the English Channel, while bathymetry has been selected in the Bay of Biscay. It is difficult to discussed seabass preferences, as covariates do not explain more than 1% of the spawning areas distribution. We thus averaged the value of the covariates selected in each areas during the spawning season for spawning and feeding (i.e. areas at less than 5 km from the coast; e.g. Pawson *et al*., 2007) areas to gain some knowledge on the species ecology. It indicates that, in the English Channel, seabass tend to prefer for reproduction waters with salinity around 35.4 (*vs* 34.3 for feeding), temperature around 9.4°C (vs 8.8°C), currents around 0.03 $m.s^{-1}$ (*vs* 0.04 $m.s^{-1}$) and a mixed layer depth around 59 m (*vs* 18 m). In the Bay of Biscay, seabass tend to prefer for reproduction temperature around 11.3°C (*vs* 10.1°C for feeding), mixed layer depth around 57 m (*vs* 16 m) and bathymetry around 82 m (*vs* 23 m).Higher salinity, bathymetry and mixed layer depth in spawning areas agree with the offshore winter migrations observed by Pawson *et al*. (2007) and de Pontual *et al*. (2019). Adult seabass target coastal areas to feed, because they are rich in food. However, environment in those areas is highly variable (e.g. salinity, temperature, etc.) resulting in a high energy cost for the species. In winter, when temperatures near the coast drop, it is likely that they move from these areas to the open sea and invest all their stored energy in reproduction. Indeed, Pickett & Pawson (1994) identified temperature as the main factor leading to the migration of seabass. Our results tend to confirm this assumption, with seabass targeting areas around 11°C in the Bay of Biscay and areas slightly colder (around 9°C) in the English Channel. These results are in agreement with Pawson *et al*. (2007) who showed that adult seabass might be migrating to seek warmer water (> 9°C) in the English Channel, and de Pontual *et al.* (2019) who found that seabass rarely spent time below 9°C.

Some other limits are worth to notice. The assumptions of the SACROIS flow on the quantity of the species per square are debatable. Indeed, the flow recalculates the position of the fishing events from the VMS data (NB: a vessel is considered to be fishing below 5 knots) to reallocate the fish quantity during the days at sea. The quantity sold at the end of a fishing trip is reallocated homogenously and proportionally to the fishing duration, as averaged across all fishing events, thus smoothing the data. The values of the two gonodo-somatic index used to check the timing of the seabass spawning season are also debatable. Indeed, their value came from studies conducted over one year while Fritsch (2005) shows that fish maturity depends on

environmental conditions and individual morphology, which can vary from year to year. This author also showed that the seabass spawning period as identified using the gonado-somatic index is relatively stable across years in the English Channel. We assumed that the situation was similar in the Bay of Biscay, but further studies are needed to confirm this hypothesis.

Finally, Harden (1968) suggested that returning to the same spawning areas to ensure successful egg and larval drift could be a selective advantage. It is therefore essential to assess if fish consistently spawn in the same areas over time to maximize spawning efficiency and recruitment. If recruitment is a dominant factor in seabass population's dynamics it would help to manage the fished populations. Due to the high inter-annual variability, it would also be relevant to study which areas contribute most to population renewal. Understanding the relationship between the adult stock and recruits is very challenging in fishery science because of high inter-annual variability due to many poorly understood factors (Houde, 2008). A popular tool to study the pelagic larval phase of fish is a spatially explicit Individual-Based Model (IBM). Beraud *et al.* (2018) developed this approach to study the settlement success of European seabass larvae under different hydrological conditions in the English Channel. Combining it to bioenergetics (e.g. Dambrine *et al.*, 2020) would make it possible to take into account the different growth patterns under various environmental conditions. Doing this could help to understand the connectivity between offshore spawning areas and coastal nurseries and provide valuable knowledge for better assessing stock-recruitment relationship and improve fishery management. Characterising and understanding the connectivity between spawning areas and nurseries could help developing better management practices (e.g. areas with monthly fishing ban) and design relevant protected areas.

Acknowledgments

This study was part of the Barfray project funded by the European Maritime and Fisheries Fund (EMFF- OSIRIS N°: PFEA 400017DM0720006), France Filière Pêche (FFP), the French Ministry of Agriculture and Food (MAF) and Ifremer. The authors are grateful to the *Direction des pêches maritimes et de l'aquaculture (*DPMA) and Ifremer (Système d'Informations Halieutiques) who provided the aggregated VMS data. The findings and conclusions of the present paper are those of the authors. This study was conducted using E.U. Copernicus Marine Service Information to collect covariates data. The authors finally thank two anonymous reviewers for their constructive comments that helped to improve the manuscript significantly.

Supplementary Material

Table S1. The EUNIS habitats cluster in seven along the French coast.

EUNIS simplified (7 categories)	Corresponding EUNIS habitat
Circalittoral homogeneous fine	A5.25, A5.26, A5.27, A5.35, A5.36, A5.37
Circalittoral mixed to coarse sediments	A5.14, A5.15, A5.44, A5.45
Circalittoral rocks	A4.1, A4.2, A4.3
Infralittoral homogeneous fine	A5.23, A5.24, A5.33, A5.34
Infralittoral mixed to coarse sediments	A5.13, A5.43
Infralittoral rocks	A3.1, A3.2, A3.3
Interdidal flats	A1, A2, A2.3

Table S2. The EUNIS habitats cluster in four along the French coast.

EUNIS simplified (4 categories)	Corresponding EUNIS habitat
Rock	A1, A3.1, A3.2, A3.3, A4.1, A4.2, A4.3
Mud	A2.3, A5.33, A5.34, A5.35, A5.36, A5.37
Sand	A5.23, A5.24, A5.25, A5.26, A5.27
Sediment	A2, A5.13, A5.14, A5.15, A5.43, A5.44, A5.45

Table S3. Monthly hotspot cut-offs between 2008 and 2014 for the English Channel area with their indicator variograms. "1" means a structured variogram, "0" indicates a pure nugget.

	Hotspot i	Vario i	Vario (i+1)	Vario $\frac{i\times(i+1)}{i}$	Vario res (i, i+1)
01-2008	A5	1	0	0	0
02-2008	A5	1	0	0	0
03-2008	A5	1	0	0	0
04-2008	A5	1	0	0	0
05-2008	A3	1	0	0	0
06-2008	A3	1	0	0	0
07-2008	A3	1	0	0	0
08-2008	A2	1	0	0	0
09-2008	A2	1	0	0	0
10-2008	A3	1	0	0	0
11-2008	A4	1	0	0	0
12-2008	A6	1	0	0	0
01-2009	A5	1	0	0	0
02-2009	A5	1	0	0	0
03-2009	A5	1	0	0	0
04-2009	A5	1	0	0	0
05-2009	A3	1	0	0	0
06-2009	A3	1	0	0	0
07-2009	A3	1	0	0	0
08-2009	A2	1	0	0	0
09-2009	A2	1	0	0	0
10-2009	A3	1	0	0	0
11-2009	A4	1	0	0	0
12-2009	A6	1	0	0	0
01-2010	A6	1	0	0	0
02-2010	A5	1	0	0	0
03-2010	A6	1	0	0	0
04-2010	A5	1	0	0	0
05-2010	A3	1	0	0	0
06-2010	A3	1	0	0	0
07-2010	A2	1	0	0	0
08-2010	A2	1	0	0	0
09-2010	A3	1	0	0	0
10-2010	A2	1	0	0	0
11-2010	A5	1	0	0	0
12-2010	A5	1	0	0	0
01-2011	A5	1	0	0	0
02-2011	A6	1	0	0	0
03-2011	A5	1	0	0	0
04-2011	A5	1	0	0	0
05-2011	A3	1	0	0	0
06-2011	A3	1	0	0	0
07-2011	A3	0	0	0	0

08-2011	A4	1	0	0	0
09-2011	A2	1	0	0	0
10-2011	A2	1	0	0	0
11-2011	A4	1	0	0	0
12-2011	A5	0	0	0	0
01-2012	A5	1	0	0	0
02-2012	A5	1	1	0	0
03-2012	A5	1	0	0	0
04-2012	A5	0	0	0	0
05-2012	A3	1	0	0	0
06-2012	A3	1	0	0	0
07-2012	A2	1	0	0	0
08-2012	A2	1	0	0	0
09-2012	A2	1	0	0	0
10-2012	A2	1	0	0	0
11-2012	A3	1	0	0	0
12-2012	A5	1	1	0	0
01-2013	A6	1	0	0	0
02-2013	A6	1	0	0	0
03-2013	A6	1	0	0	0
04-2013	A5	1	0	0	0
05-2013	A5	1	0	0	0
06-2013	A2	1	0	0	0
07-2013	A2	1	0	0	0
08-2013	A2	1	0	0	0
09-2013	A2	1	0	0	0
10-2013	A2	1	0	0	0
11-2013	A5	1	0	0	0
12-2013	A4	1	0	0	0
01-2014	A4	1	0	0	0
02-2014	A2	1	0	0	0
03-2014	A3	1	0	0	0
04-2014	A5	1	0	0	0
05-2014	A3	1	0	0	0
06-2014	A2	1	0	0	0
07-2014	A1	1	0	0	0
08-2014	A2	1	0	0	0
09-2014	A1	1	0	0	0
10-2014	A2	1	0	0	0
11-2014	A2	1	0	0	0
12-2014	A2	1	0	0	1

Table S4. Monthly hotspot cut-offs between 2008 and 2016 for the Bay of Biscay area with their indicator variograms. "1" means a structured variogram, "0" indicates a pure nugget.

	Hotspot i	**Vario i**	**Vario (i+1)**	**Vario $\frac{i\times(i+1)}{i}$**	**Vario res (i, i+1)**
01-2008	A3	1	0	0	0
02-2008	A5	1	0	0	0
03-2008	A5	1	0	0	0
04-2008	A3	1	0	0	0
05-2008	A3	1	0	0	0
06-2008	A3	0	0	0	0
07-2008	A3	1	0	0	0
08-2008	A3	1	0	0	0
09-2008	A4	1	0	0	0
10-2008	A3	0	0	0	0
11-2008	A3	1	0	0	0
12-2008	A5	1	0	0	0
01-2009	A5	1	0	0	0
02-2009	A5	0	0	0	0
03-2009	A5	1	0	0	0
04-2009	A4	0	0	0	0
05-2009	A3	1	0	0	0
06-2009	A3	1	0	0	0
07-2009	A3	1	0	0	0
08-2009	A2	1	0	0	0
09-2009	A2	1	0	0	0
10-2009	A4	1	0	0	0
11-2009	A3	1	0	0	0
12-2009	A3	1	0	0	0
01-2010	A6	1	0	0	0
02-2010	A5	1	0	0	0
03-2010	A5	1	0	0	0
04-2010	A4	1	0	0	0
05-2010	A5	1	0	0	0
06-2010	A4	1	0	0	0
07-2010	A3	1	0	0	0
08-2010	A3	1	1	0	0
09-2010	A3	1	0	0	0
10-2010	A3	1	0	0	0
11-2010	A2	1	0	0	0
12-2010	A3	1	1	0	0
01-2011	A6	1	0	0	0
02-2011	A5	1	0	0	0
03-2011	A5	1	0	0	0
04-2011	A3	1	0	0	0

05-2011	A4	1	0	0	0
06-2011	A3	1	0	0	0
07-2011	A2	1	0	0	0
08-2011	A2	1	0	0	0
09-2011	A3	1	0	0	0
10-2011	A3	0	0	0	0
11-2011	A5	1	0	0	0
12-2011	A4	1	0	0	0
01-2012	A5	1	0	0	0
02-2012	A5	1	0	0	0
03-2012	A4	1	1	0	0
04-2012	A3	1	0	0	0
05-2012	A2	1	0	0	0
06-2012	A2	1	0	0	0
07-2012	A2	1	0	0	0
08-2012	A2	1	0	0	0
09-2012	A3	0	0	0	0
10-2012	A5	1	0	0	0
11-2012	A4	1	0	0	0
12-2012	A5	1	0	0	0
01-2013	A5	1	0	0	0
02-2013	A5	1	0	0	0
03-2013	A4	1	0	0	0
04-2013	A2	1	0	0	0
05-2013	A3	1	0	0	0
06-2013	A3	1	0	0	0
07-2013	A3	1	0	0	0
08-2013	A2	1	0	0	0
09-2013	A3	1	1	0	0
10-2013	A4	1	0	0	0
11-2013	A3	1	0	0	0
12-2013	A4	1	0	0	0
01-2014	A4	1	0	0	0
02-2014	A5	1	0	0	0
03-2014	A3	1	0	0	0
04-2014	A3	1	0	0	0
05-2014	A2	1	0	0	0
06-2014	A2	1	0	0	0
07-2014	A2	1	0	0	0
08-2014	A2	1	0	0	0
09-2014	A2	1	0	0	0
10-2014	A4	1	1	0	0
11-2014	A4	1	0	0	0
12-2014	A4	1	0	0	0

01-2015	A4	1	0	0	0
02-2015	A5	1	0	0	0
03-2015	A3	1	0	0	0
04-2015	A5	1	0	0	0
05-2015	A2	1	0	0	0
06-2015	A2	1	0	0	0
07-2015	A2	1	0	0	0
08-2015	A3	1	0	0	0
09-2015	A4	1	0	0	0
10-2015	A3	1	0	0	0
11-2015	A4	1	0	0	0
12-2015	A4	1	0	0	0
01-2016	A4	1	0	0	0
02-2016	A4	1	0	0	0
03-2016	A4	0	0	0	0
04-2016	A3	1	0	0	0
05-2016	A2	1	0	0	0
06-2016	A2	1	0	0	0
07-2016	A2	1	0	0	0
08-2016	A2	1	0	0	0
09-2016	A2	1	0	0	0
10-2016	A3	1	0	0	0
11-2016	A3	1	0	0	0
12-2016	A3	1	0	0	0

*Table S5. Summary of the models tested for the English Channel. Bathy: bathymetry, Chl: surface chlorophyll-a, Mld: mixed layer depth, mean S: mean salinity of the water column, mean T: mean temperature of the water column, and UoVoS: surface current velocities. The subscripts lin and rw1 indicate whether the variable was tested as a linear predictor or following a random walk 1 model. * indicates the best model.*

Model	WAIC	M(LCPO)
$Intercept + Bathy_{lin} + Chl_{rw1} + w_i + v_{jk}$	31309,85	0,1183778
$Intercept + Bathy_{lin} + Mld_{lin} + w_i + v_{jk}$	31316,46	0,118366
$Intercept + Bathy_{lin} + Mean\ S_{rw1} + w_i + v_{jk}$	31248,38	0,1181076
$Intercept + Bathy_{lin} + Mean\ T_{rw1} + w_i + v_{jk}$	31209,57	0,117961
$Intercept + Bathy_{lin} + UoVoS_{lin} + w_i + v_{jk}$	31319,93	0,1183781
$Intercept + Chl_{rw1} + UoVoS_{lin} + w_i + v_{jk}$	31302,45	0,1183121
$Intercept + Mld_{lin} + Chl_{rw1} + w_i + v_{jk}$	31307,72	0,118332
$Intercept + Mld_{lin} + UoVoS_{lin} + w_i + v_{jk}$	31305,3	0,1183221
$Intercept + Mean\ S_{rw1} + Chl_{rw1} + w_i + v_{jk}$	31243,21	0,1180881
$Intercept + Mean\ S_{rw1} + Mld_{lin} + w_i + v_{jk}$	31234,39	0,1180548
$Intercept + Mean\ S_{rw1} + Mean\ T_{rw1} + w_i + v_{jk}$	31134,9	0,1176787
$Intercept + Mean\ S_{rw1} + UoVoS_{lin} + w_i + v_{jk}$	31226,68	0,1180257
$Intercept + Mean\ T_{rw1} + Chl_{lin} + w_i + v_{jk}$	31215,45	0,1179831
$Intercept + Mean\ T_{rw1} + Mld_{lin} + w_i + v_{jk}$	31201,67	0,1179312
$Intercept + Mean\ T_{rw1} + UoVoS_{lin} + w_i + v_{jk}$	31199,17	0,1179217
$Intercept + Bathy_{lin} + Chl_{rw1} + Mld_{lin} + w_i + v_{jk}$	31307,32	0,1183305
$Intercept + Bathy_{lin} + Chl_{rw1} + Mean\ T_{rw1} + w_i + v_{jk}$	31206,98	0,1179514
$Intercept + Bathy_{lin} + Chl_{rw1} + UoVoS_{lin} + w_i + v_{jk}$	31300,43	0,1183044
$Intercept + Bathy_{lin} + Mld_{lin} + Mean\ T_{rw1} + w_i + v_{jk}$	31192,64	0,1178997
$Intercept + Bathy_{lin} + Mean\ S_{rw1} + Chl_{rw1} + w_i + v_{jk}$	31236,75	0,1180637
$Intercept + Bathy_{lin} + Mean\ S_{rw1} + Mld_{lin} + w_i + v_{jk}$	31234,04	0,1180535
$Intercept + Bathy_{lin} + Mean\ S_{rw1} + Mean\ T_{rw1} + w_i + v_{jk}$	31128,54	0,1176547
$Intercept + Bathy_{lin} + Mean\ S_{rw1} + UoVoS_{lin} + w_i + v_{jk}$	31225,19	0,11802
$Intercept + Bathy_{lin} + UoVoS_{lin} + Mld_{lin} + w_i + v_{jk}$	31301,07	0,1183069

$Intercept + Bathy_{lin} + UoVoS_{lin} + Mean\ T_{rw1} + w_i + v_{jk}$	31196,75	0,1179125
$Intercept + Mld_{lin} + Chl_{rw1} + UoVoS_{lin} + w_i + v_{jk}$	31286,84	0,1182531
$Intercept + Mean\ S_{rw1} + Chl_{rw1} + UoVoS_{lin} + w_i + v_{jk}$	31214,45	0,1179795
$Intercept + Mean\ S_{rw1} + Mld_{lin} + Chl_{rw1} + w_i + v_{jk}$	31227,58	0,118029
$Intercept + Mean\ S_{rw1} + Mld_{lin} + UoVoS_{lin} + w_i + v_{jk}$	31209,61	0,117912
$Intercept + Mean\ S_{rw1} + Mean\ T_{rw1} + Chl_{rw1} + w_i + v_{jk}$	31133,92	0,1176751
$Intercept + Mean\ S_{rw1} + Mean\ T_{rw1} + Mld_{lin} + w_i + v_{jk}$	31121,75	0,1176291
$Intercept + Mean\ S_{rw1} + Mean\ T_{rw1} + UoVoS_{lin} + w_i + v_{jk}$	31114,84	0,1176029
$Intercept + Mean\ T_{rw1} + Chl_{rw1} + UoVoS_{lin} + w_i + v_{jk}$	31191,99	0,1178951
$Intercept + Mean\ T_{rw1} + Mld_{lin} + Chl_{rw1} + w_i + v_{jk}$	31200,96	0,1179285
$Intercept + Mean\ T_{rw1} + Mld_{lin} + UoVoS_{lin} + w_i + v_{jk}$	31187,36	0,1178771
$Intercept + Bathy_{lin} + Mld_{lin} + Chl_{rw1} + UoVoS_{lin} + w_i + v_{jk}$	31288,21	0,1182583
$Intercept + Bathy_{lin} + Mean\ S_{rw1} + Chl_{rw1} + UoVoS_{lin} + w_i + v_{jk}$	31212,59	0,1179724
$Intercept + Bathy_{lin} + Mean\ S_{rw1} + Mld_{lin} + Chl_{rw1} + w_i + v_{jk}$	31226,32	0,1180242
$Intercept + Bathy_{lin} + Mean\ S_{rw1} + Mld_{lin} + UoVoS_{lin} + w_i + v_{jk}$	31211,15	0,117967
$Intercept + Bathy_{lin} + Mean\ S_{rw1} + Mean\ T_{rw1} + Chl_{rw1} + w_i + v_{jk}$	31116,98	0,1176111
$Intercept + Bathy_{lin} + Mean\ S_{rw1} + Mean\ T_{rw1} + Mld_{lin} + w_i + v_{jk}$	31120,29	0,1176235
$Intercept + Bathy_{lin} + Mean\ S_{rw1} + Mean\ T_{rw1} + UoVoS_{lin} + w_i + v_{jk}$	31104,78	0,117565
$Intercept + Bathy_{lin} + Mean\ T_{rw1} + Mld_{lin} + Chl_{rw1} + w_i + v_{jk}$	31199,92	0,1179245
$Intercept + Bathy_{lin} + Mean\ T_{rw1} + Chl_{rw1} + UoVoS_{lin} + w_i + v_{jk}$	31201,72	0,1179307
$Intercept + Bathy_{lin} + Mean\ T_{rw1} + Mld_{lin} + UoVoS_{lin} + w_i + v_{jk}$	31188,12	0,11788
$Intercept + Mean\ S_{rw1} + Mld_{lin} + Chl_{rw1} + UoVoS_{lin} + w_i + v_{jk}$	31200,67	0,1179274
$Intercept + Mean\ S_{rw1} + Mean\ T_{rw1} + Chl_{rw1} + UoVoS_{lin} + w_i + v_{jk}$	31114,16	0,1176004
$Intercept + Mean\ S_{rw1} + Mean\ T_{rw1} + Mld_{lin} + Chl_{rw1} + w_i + v_{jk}$	31120,86	0,1176258
$Intercept + Mean\ S_{rw1} + Mean\ T_{rw1} + Mld_{lin} + UoVoS_{lin} + w_i + v_{jk}$	31104,04	0,1175621
$Intercept + Mean\ T_{rw1} + Mld_{lin} + Chl_{rw1} + UovoS_{lin} + w_i + v_{jk}$	31186,42	0,1178736
$Intercept + Bathy_{lin} + Mean\ S_{rw1} + Mld_{lin} + Chl_{rw1} + UoVoS_{lin} + w_i + v_{jk}$	31201,94	0,1179321

$Intercept + Bathy_{lin} + Mean\ S_{rw1} + Mean\ T_{rw1} + Chl_{rw1} + UoVoS_{lin} + w_i + v_{jk}$	31111,74	0,1175912
$Intercept + Bathy_{lin} + Mean\ S_{rw1} + Mean\ T_{rw1} + Mld_{lin} + Chl_{rw1} + w_i + v_{jk}$	31119,48	0,1176205
$Intercept + Bathy_{lin} + Mean\ S_{rw1} + Mean\ T_{rw1} + Mld_{lin} + UoVoS_{lin} + w_i + v_{jk}$	31104,78	0,117565
$Intercept + Bathy_{lin} + Mean\ T_{rw1} + Mld_{lin} + Chl_{rw1} + UoVoS_{lin} + w_i + v_{jk}$	31187,23	0,1178767
$Intercept + Mean\ S_{rw1} + Mean\ T_{rw1} + Mld_{lin} + Chl_{rw1} + UoVoS_{lin} + w_i + v_{jk}^{*}$	31103,23	0,1175591
$Intercept + Bathy_{lin} + Mean\ S_{rw1} + Mean\ T_{rw1} + Mld_{lin} + Chl_{rw1} + UoVoS_{lin} + w_i + v_{jk}$	31103,78	0,1175612

*Table S6. Summary of the models tested for the Bay of Biscay. Mean T: mean temperature of the water column, UoVoS: surface current velocities, Mld: mixed layer depth, and Hab4:bottom grain size. The subscripts lin and rw1 indicate whether the variable was tested as a linear predictor or following a random walk 1 model. * indicates the best model.*

Model	*WAIC*	*M(LCPO)*
$Intercept + Bathy_{lin} + Hab4_{lin} + w_i + v_{jk}$	7508.28	0.061346027
$Intercept + Bathy_{lin} + Mld_{lin} + w_i + v_{jk}$	7515.871	0.05995349
$Intercept + Bathy_{lin} + Mean\ T_{rw1} + w_i + v_{jk}$	7469.867	0.06042965
$Intercept + Bathy_{lin} + UoVoS_{lin} + w_i + v_{jk}$	7520.876	0.06079494
$Intercept + Mld_{lin} + Hab4_{lin} + w_i + v_{jk}$	7509.647	0.06064174
$Intercept + Mld_{lin} + UoVoS_{lin} + w_i + v_{jk}$	7523.34	0.06100687
$Intercept + Mean\ T_{rw1} + Hab4_{lin} + w_i + v_{jk}$	7464.225	0.06094378
$Intercept + Mean\ T_{rw1} + Mld_{lin} + w_i + v_{jk}$	7476.666	0.06025134
$Intercept + UoVoS_{lin} + Hab4_{lin} + w_i + v_{jk}$	7514.301	0.06579151
$Intercept + Bathy_{lin} + Mld_{lin} + Hab4_{lin} + w_i + v_{jk}$	7505.343	0.05992618
$Intercept + Bathy_{lin} + Mld_{lin} + UoVoS_{lin} + w_i + v_{jk}$	7517.943	0.05999463
$Intercept + Bathy_{lin} + Mean\ T_{rw1} + Hab4_{lin} + w_i + v_{jk}$	7458.491	0.06003248
$Intercept + Bathy_{lin} + Mean\ T_{rw1} + Mld_{lin} + w_i + v_{jk}$	7470.713	0.05971278
$Intercept + Bathy_{lin} + UoVoS_{lin} + Hab4_{lin} + w_i + v_{jk}$	7509.999	0.06271318
$Intercept + Mean\ T_{rw1} + Mld_{lin} + Hab4_{lin} + w_i + v_{jk}$	7464.585	0.06011221
$Intercept + Mean\ T_{rw1} + Mld_{lin} + UoVoS_{lin} + w_i + v_{jk}$	7478.914	0.06015953
$Intercept + Mean\ T_{rw1} + UoVoS_{lin} + Hab4_{lin} + w_i + v_{jk}$	7466.339	0.06096489
$Intercept + Mld_{lin} + UoVoS_{lin} + Hab4_{lin} + w_i + v_{jk}$	7511.805	0.06065239
$Intercept + Bathy_{lin} + Mean\ T_{rw1} + UoVoS_{lin} + w_i + v_{jk}$	7471.95	0.06020014
$Intercept + Bathy_{lin} + Mld_{lin} + UoVoS_{lin} + Hab4_{lin} + w_i + v_{jk}$	7507.417	0.06006405
$Intercept + Bathy_{lin} + Mean\ T_{rw1} + Mld_{lin} + Hab4_{lin} + w_i + v_{jk}$	7459.558	0.05972331
$Intercept + Bathy_{lin} + Mean\ T_{rw1} + Mld_{lin} + UoVoS_{lin} + w_i + v_{jk}$	7472.997	0.05963177
$Intercept + Mean\ T_{rw1} + Bathy_{lin} + UoVoS_{lin} + Hab4_{lin} + w_i + v_{jk}$	7460.611	0.05995768
$Intercept + Mean\ T_{rw1} + Mld_{lin} + UoVoS_{lin} + Hab4_{lin} + w_i + v_{jk}$	7466.783	0.06000379
$Intercept + Mean\ T_{rw1} + Bathy_{lin} + UoVoS_{lin} + Hab4_{lin} + Mld_{lin} + w_i + v_{jk}$	7461.84	0.05959102
$Mean\ T_{rw1} + Bathy_{lin} + Mld_{lin} + w_i + v_{jk}^{*}$	7470.864	0.0582153

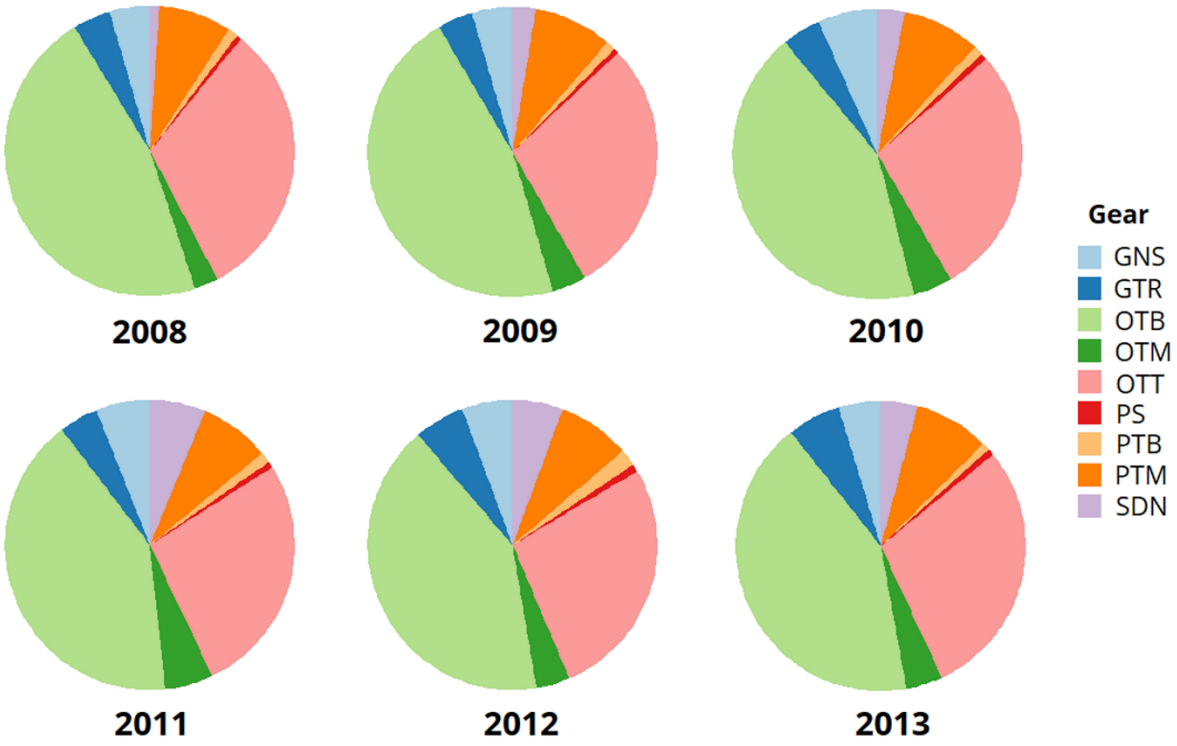

Figure S1. Yearly gear composition in the study area (No. of fishing events). GNS: set gillnets, GTR: trammel nets, OTB: bottom otter, OTM: midwater otter, OTT: otter twin trawls, PS: purse seines, PTB: bottom pair trawls, PTM: midwater pair trawls, and SDN: Danish seines.

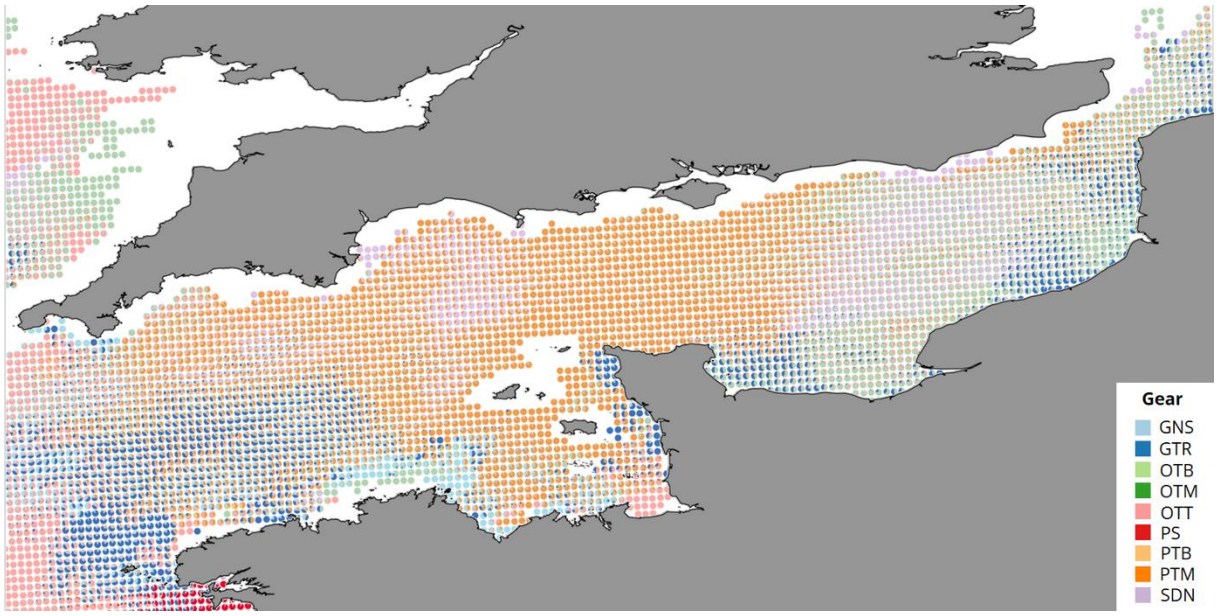

Figure S2. Fishery distribution (No. of fishing events per square of three nautical miles) throughout the time series in the English Channel.

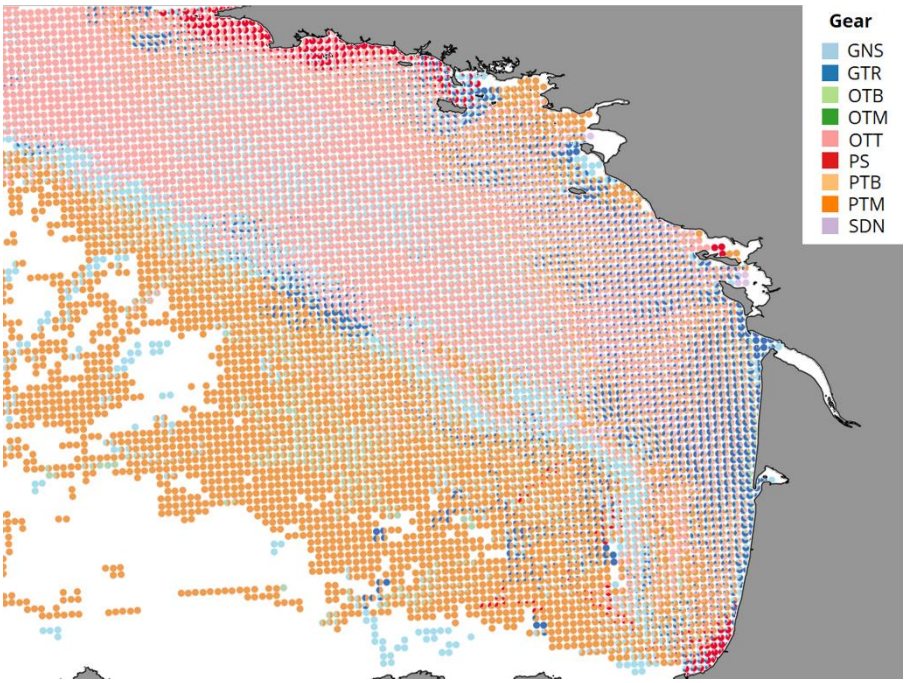

Figure S3. Fishery distribution (No. of fishing events per square of three nautical miles) throughout the time series in the Bay of Biscay.

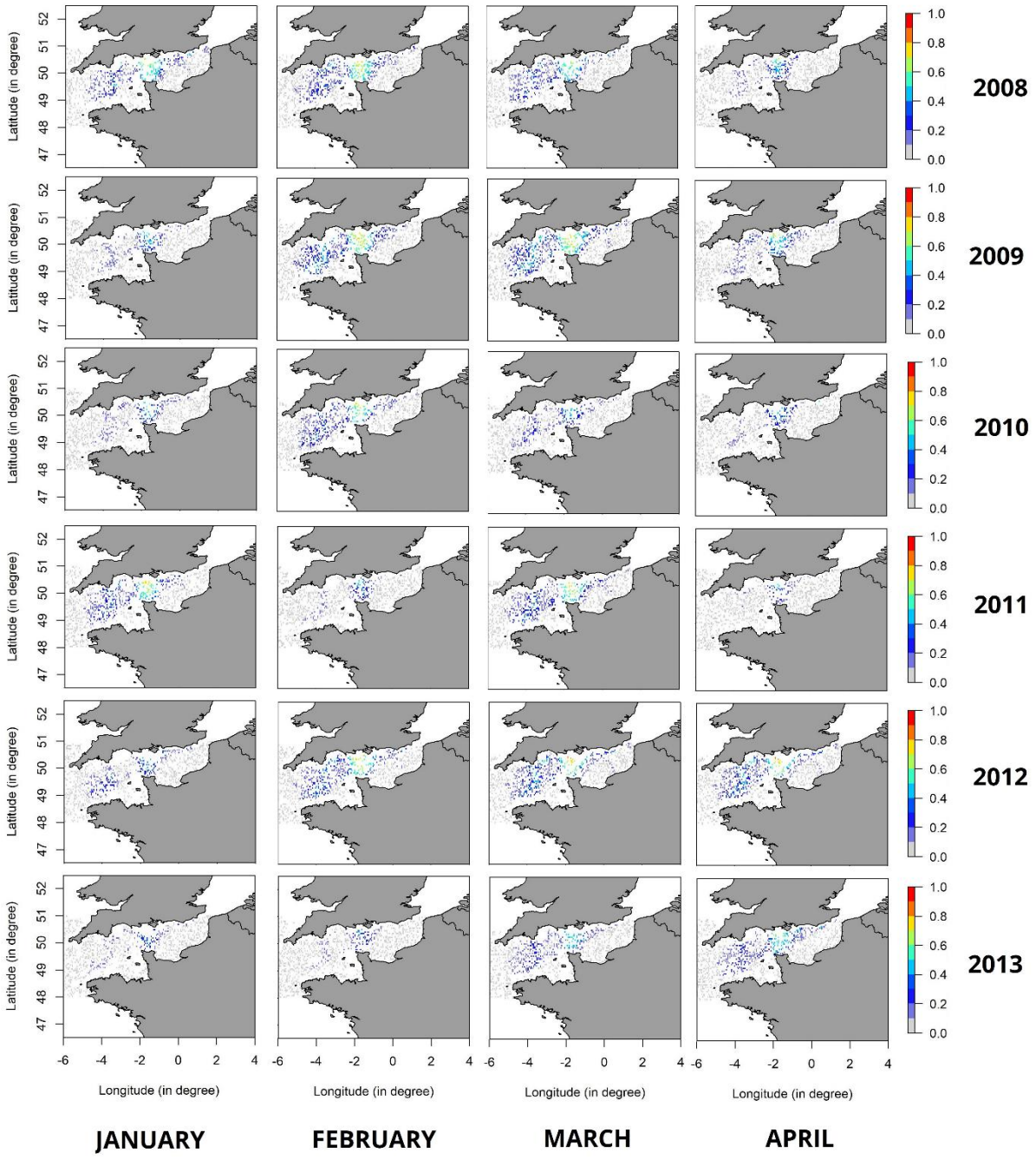

Figure S4. Predicted maps of the probability of presence of seabass spawning areas for each spawning month of the time series (2008-2013) in the English Channel with the best spatio-temporal model.

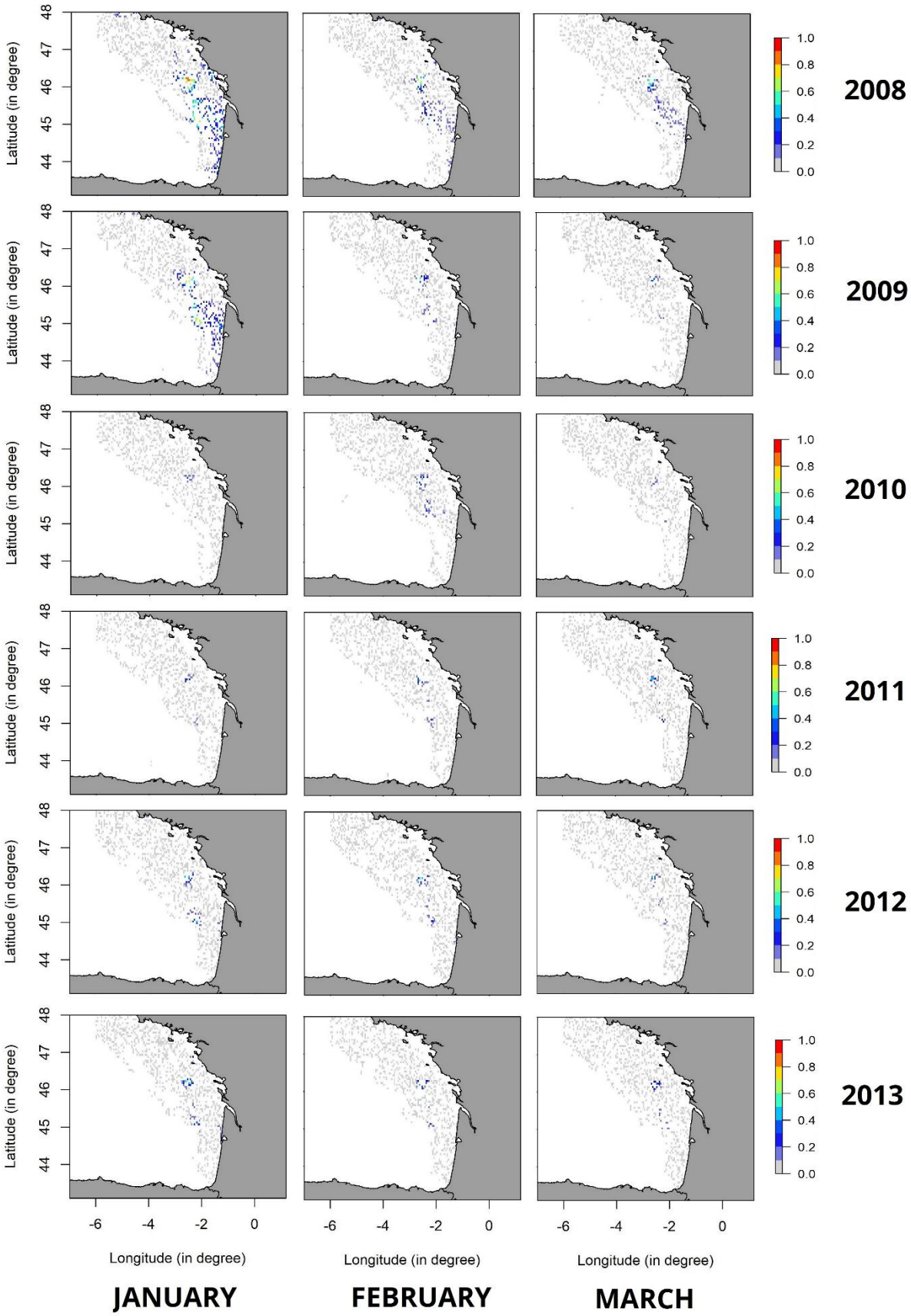

Figure S5. Predicted maps of the probability of presence of seabass spawning areas for each spawning month of the time series (2008-2013) in the Bay of Biscay with the best spatio-temporal model.

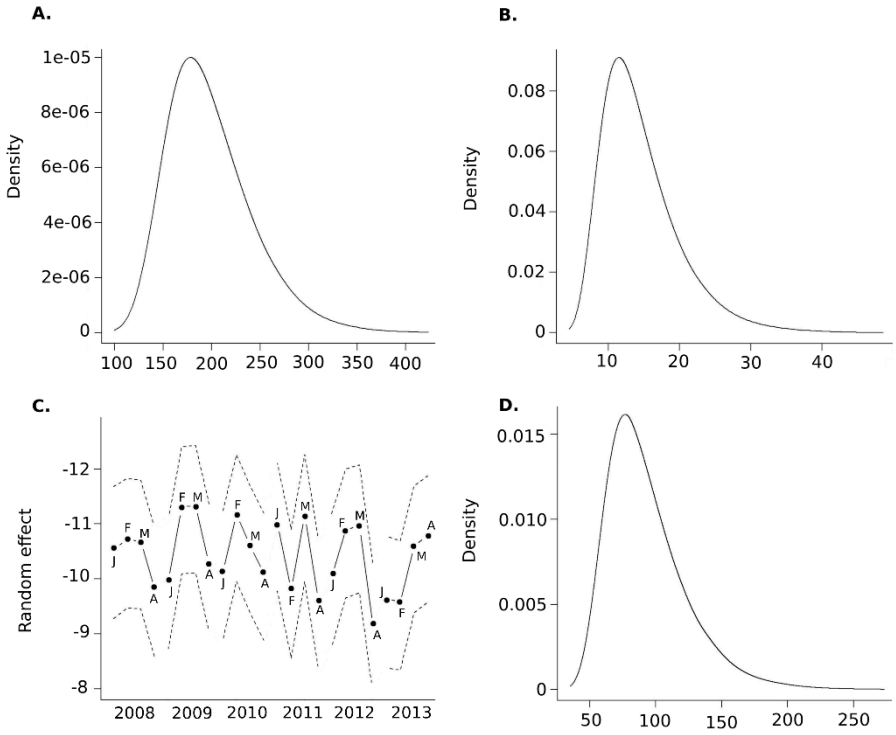

Figure S6. Posterior distribution in the English Channel of A. the spatial effect nominal range (km), B. the spatial effect nominal variance, C. the temporal effect (for months of the spawning period) and D. the temporal effect variance. Note that the scale is different on each figure. For C., dotted lines represent the 25 and 95% quantiles.

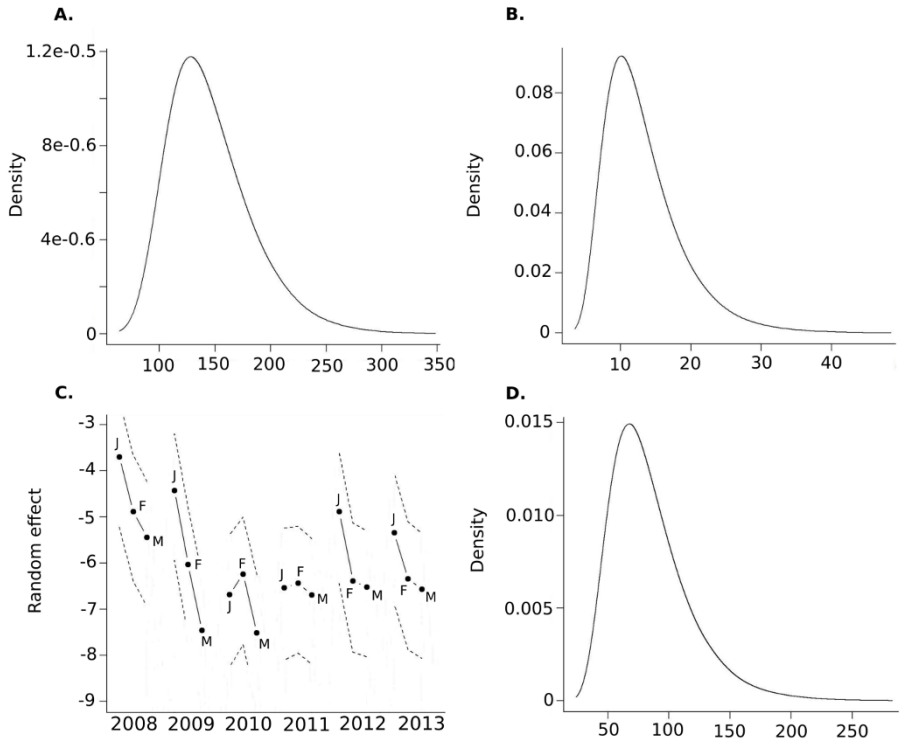

Figure S7. Posterior distribution in the Bay of Biscay of A. the spatial effect nominal range (km), B. the spatial effect nominal variance, C. the temporal effect (for months of the spawning period) and D. the

temporal effect variance. Note that the scale is different on each figure. For C., dotted lines represent the 25 and 95% quantiles.

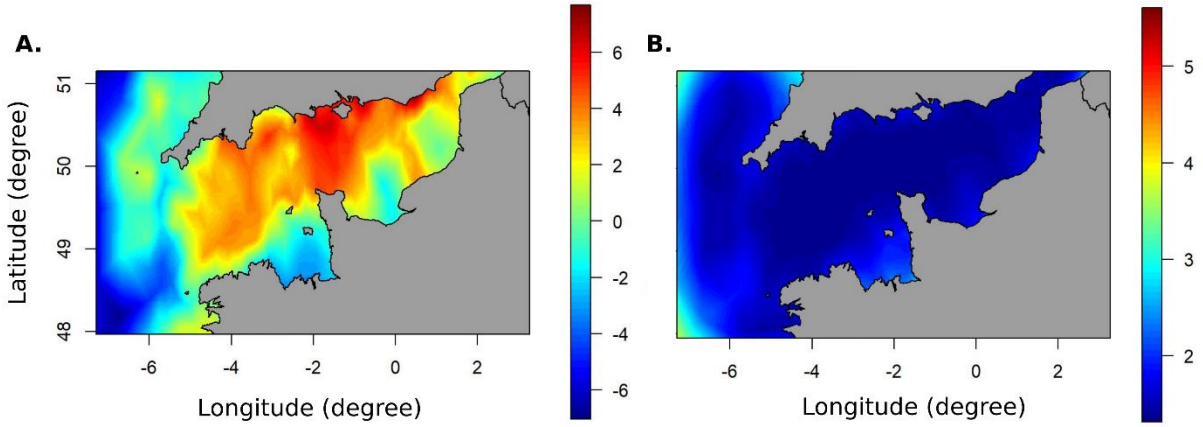

Figure S8. Posterior A. mean and B. standard deviation of the spatial effect in the English Channel.

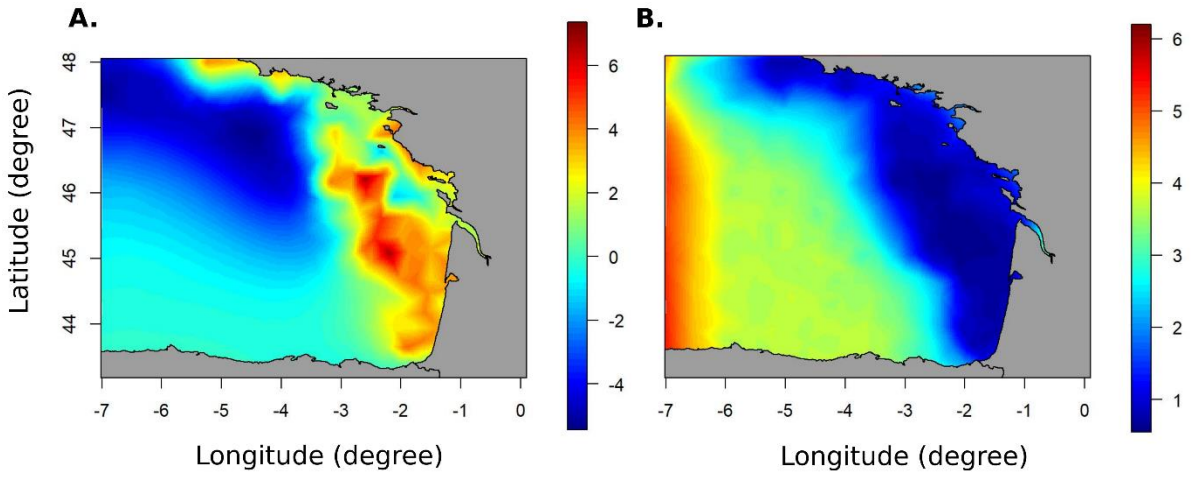

Figure S9. Posterior A. mean and B. standard deviation of the spatial effect in the Bay of Biscay.

CHAPITRE 2

CONTRIBUTION D'UN MODÈLE BIOÉNERGÉTIQUE POUR ÉTUDIER LA CROISSANCE ET LA SURVIE DU BAR EUROPÉEN DANS LA ZONE GOLFE DE GASCOGNE - MANCHE

Une version de ce chapitre a été publiée dans *Ecological Modelling*

Ecological Modelling 423 (2020) 109007

Contents lists available at ScienceDirect

Ecological Modelling

journal homepage: www.elsevier.com/locate/ecolmodel

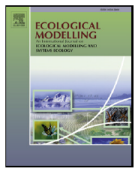

Contribution of a bioenergetics model to investigate the growth and survival of European seabass in the Bay of Biscay – English Channel area

Chloé Dambrine[a,*], Martin Huret[a], Mathieu Woillez[a], Laure Pecquerie[b], François Allal[c], Arianna Servili[d], Hélène de Pontual[a]

RÉSUMÉ DÉTAILLÉ

Dans le chapitre précédent, les zones de ponte du bar ont été caractérisées le long de la façade atlantique française. Leurs relations dynamiques avec les nourriceries peuvent alors être étudiées en utilisant un modèle de dérive larvaire (e.g. Huret *et al*., 2010).

Cependant, la dispersion des œufs et larves est complexe et dépend de nombreux facteurs environnementaux (Houde, 2008). Parmi ces facteurs, nous trouvons les courants, mais également la température et la disponibilité en nourriture qui vont impacter la croissance et la survie des individus. Pour quantifier le processus d'arrivée des bars sur nourricerie, qui dépend fortement de la survie des jeunes stades (Chambers & Trippel, 2012), il serait alors intéressant d'introduire dans le modèle de dérive une croissance et une mortalité différentielles des individus en fonction de l'environnement.

Les modèles bioénergétiques semblent être de bons candidats pour satisfaire cet objectif puisqu'ils conditionnent les performances individuelles (e.g. croissance, survie) à des variables environnementales (i.e. température et disponibilité en nourriture). Parmi eux, les modèles suivant la théorie DEB (Dynamic Energy Budget ; Kooijman, 2010) sont particulièrement intéressants, notamment car les fonctions vitales des individus sont décrites par un nombre limité d'équations différentielles dont les paramètres peuvent être calibrés à partir de données facilement mesurables : la taille et le poids aux âges.

Ce chapitre s'attache à calibrer un modèle DEB sur l'ensemble du cycle de vie du bar de la façade atlantique française. La calibration a intégré des données de bars sauvages adultes et juvéniles ainsi que des données de larves et juvéniles élevés en milieu contrôlé. Le modèle est capable de reproduire la durée des différents stades de vie, la croissance des individus, le nombre de fois où les individus se reproduisent par année, la survie du bar au jeûne ainsi qu'une des principales différences rencontrées dans les traits de vie de l'espèce : les poissons d'élevage sont matures plus tôt que les poissons sauvages (i.e. 3 à 4 ans contre 6 ans en moyenne pour les femelles, respectivement). Les performances du modèle ont enfin été testées sur des données indépendantes de jeunes stades de vie et valident la future utilisation du modèle dans le modèle de dérive larvaire.

La croissance et la survie des larves et des juvéniles a été explorée en exposant numériquement les individus à des températures et des niveaux de nourriture variables, y compris un jeûne total. Nous avons pu montrer que les premiers stades de vie du bar ont une forte capacité à faire face à la privation de nourriture : le modèle a estimé qu'après ouverture de la bouche, les larves pouvaient survivre 17 jours à 15°C sans nourriture disponible. Cependant, une fois métamorphosées (i.e. arrivées sur nourricerie), cette capacité est largement réduite et un niveau de nourriture suffisant est nécessaire rapidement pour assurer leur survie. Ainsi, une des hypothèses expliquant les dernières années de mauvais recrutements pourrait être, entre autres, un manque ou un changement de nourriture disponible sur les nourriceries.

La variabilité individuelle a également été explorée en ajustant le taux d'assimilation maximum spécifique. Nous avons constaté que les larves et les juvéniles ayant une capacité d'assimilation plus élevée survivaient mieux à de faibles niveaux de nourriture lorsque la température est plus élevée.

Enfin, la calibration, ayant intégré des individus sauvages, a permis de montrer que les bars ne se nourrissaient pas *ad libitum* dans le milieu naturel (i.e. réponse fonctionnelle $f < 1$). Ce résultat permet d'estimer un autre paramètre pour le bar (i.e. la constante de demi-saturation X_k d'un modèle de type Holling type II) à intégrer dans le modèle de dérive larvaire et permettant de relier la disponibilité en nourriture (i.e. le zooplancton pour les larves) avec ce qui est effectivement ingéré par l'individu.

Contribution of a bioenergetics model to investigate the growth and survival of European seabass in the Bay of Biscay – English Channel area

Dambrine Chloé[1,*], Huret Martin[1], Woillez Mathieu[1], Pecquerie Laure[2], Allal François[3], Servili Arianna[4], de Pontual Hélène[1]

[1] Ifremer, Laboratoire de Biologie Halieutique, Unité de Sciences et Techniques Halieutiques, Centre Ifremer Bretagne, ZI de la Pointe du Diable – CS 10070, 29280 Plouzané, France
[2] Univ Brest, CNRS, IRD, Ifremer, LEMAR, F-29280 Plouzané, France
[3] MARBEC, Univ Montpellier, CNRS, Ifremer, IRD, Palavas-les-Flots, France
[4] Ifremer, Univ Brest, CNRS, IRD, LEMAR, F-29280 Plouzané, France

* Corresponding author
E-mail address: chloe.dambrine@orange.fr

Abstract

The European seabass (*Dicentrarchus labrax*) is a species of particular ecological and economic importance. Stock assessments have recently revealed the worrying state of the "Northern stock", probably due to overfishing and a series of poor recruitments. The extent to which these poor recruitments are due to environmental variability is difficult to assess, as the processes driving the seabass life cycle are poorly known. Here we investigate how food availability and temperature may affect the growth and survival of wild seabass at the individual scale. To this end, we developed a bioenergetics model based on the Dynamic Energy Budget (DEB) theory. We applied it to seabass population of the Northeast Atlantic region (Bay of Biscay – English Channel area) throughout their entire life cycle. We calibrated the model using a combination of age-related length and weight datasets: two were from aquaculture experiments (larvae and juveniles raised at 15 and 20°C) and one from a wild population (juveniles and adults collected during surveys or fish market sampling). By calibrating the scaled functional response that rules the ingestion of food and using average temperature conditions experienced by wild seabass (obtained from tagged individuals), the model was able to reproduce the duration of the different stages, the growth of the individuals, the number of batches and their survival to starvation. We also captured one of the major differences encountered in the life traits of the species: farmed fish mature earlier than wild fish (3 to 4 years old *vs.* 6 years old on average for females, respectively) probably due to better feeding conditions and higher temperature. We explored the growth and survival of larvae and juveniles by exposing the individuals to varying temperatures and food levels (including total starvation). We show that early life stages of seabass have a strong capacity to deal with food deprivation: the model estimated that first feeding larvae could survive 17 days at 15°C. We also tested individual variability by adjusting the specific maximum assimilation rate and found that larvae and juveniles with higher assimilation capacity better survived low food levels at a higher temperature. We discuss our results in the context of the recent years of poor recruitment faced by European seabass.

Keywords

Dicentrarchus labrax, Northeast Atlantic, Dynamic Energy Budget theory, Growth, Starvation, early-life stages

1. Introduction

European seabass (*Dicentrarchus labrax*) is a species of high economic value in Europe which production relies primarily on aquaculture (81,852 t in 2016; EUMOFA, 2018) and fishing. Both commercial and recreational anglers target seabass, and fishing pressure has rapidly increased from 2,000 t in the late 1970s to more than 9,000 t in 2006, before becoming stable around 6,000 t in 2013 (ICES, 2012). Since then, the state of the "Northern stock" (one of the four stocks defined by ICES, i.e. Irish Sea, Celtic Sea, English Channel and southern North Sea) has been worrying, as highlighted by the rapid decline in spawning stock biomass and a series of poor recruitments probably due to continued excessive fishing pressure.

The resilience of fish populations is based on their ability to complete their life cycle and maintain abundance through recruitment (Peck *et al*., 2014). The recruitment success is partly determined by the reproductive potential of the adults and by the survival rate of early life stages (Chambers *et al*., 2012), which strongly relies on environmental conditions. According to Houde (1987), eggs, yolk-sac larvae, larvae and juveniles are the most vulnerable stages due to high rates of predation, starvation and other dietary deficiencies, or to deleterious oceanographic conditions that transport them to unsuitable environments. However, despite their ecological and economical importance, the recruitment dynamics of the European seabass early life stages is still poorly known. Besides, this species is reported to spawn in winter (Fritsch *et al.*, 2007 ; Pawson *et al.*, 2007), when environmental conditions can be considered as suboptimal in terms of temperature and food availability, which raises questions about eggs and larvae survival during the planktonic phase.

Bioenergetics models are suitable tools to study the impact of environmental variability on the recruitment success of seabass early life stages. They make it possible to study biological and physiological processes on an individual scale in relation to the environment by translating the specific environmental conditions experienced by the fish into individual performance (growth, survival and investment in reproduction). To achieve this, bioenergetics models quantify the energy fluxes between an organism and its environment. In particular, models using the Dynamic Energetic Budget (DEB) theory (Kooijman, 2010) translate an individual's physiological functions into a reduced number of differential equations. It allows the construction of a dynamic model related to the environment without having to conduct laboratory experiments to quantify input (i.e. ingestion and assimilation) and output (i.e. excretion, respiration and locomotion) fluxes as in the Scope For Growth (SFG) models

(Winberg, 1956), and it relies only on existing length and weight-at-age data. Besides, in this theory, the rules of energy conservation are followed and the flux of energy to reproduction is explicitly described.

DEB models are commonly used to study some of the fish physiological characteristics (e.g. Jusup *et al.*, 2011), and they are useful to investigate the impacts of environmental changes (i.e. temperature and food availability) on fish growth and reproduction (e.g. Pecquerie *et al.*, 2009 and Pethybridge *et al.*, 2013). Lika *et al.*, (2014) and Stavrakidis-Zachou *et al.*, (2018) successfully parametrized DEB models for seabass. They used data from Mediterranean farmed seabass and focussed on early life stages (i.e. larvae and juveniles). Our primary aim in the present study was, therefore, to develop a DEB model for wild European seabass using full life cycle data. Besides, given the worrying state of the northern stock revealed by ICES, we chose to apply the model to the Northeast Atlantic and to focus on a region stretching from the Bay of Biscay to the English Channel. Preliminary analyses revealed that fitting the model of Stavrakidis-Zachou et al. (2018) to our Northeast Atlantic dataset resulted in an overestimation of seabass growth, particularly for the juveniles (see Supplementary Material). This, along with the recognized genetic differences between Mediterranean and Atlantic populations (Tine *et al.*, 2014) argued for compiling new data and estimating new DEB parameters for wild European seabass.

To reach our aim, we calibrated an 'abj' DEB model using length and weight data, from both farmed (larvae and juveniles) and wild (juveniles and adults) Atlantic specimens. We then evaluated the model's ability to reproduce very distinct life-history traits displayed by farmed and wild individuals. We applied the model to study two key processes: the growth and survival of early life stages. We evaluated the survival capacity of seabass larvae and juveniles to a range of temperatures and food levels. We also introduced individual variability to study its impact on larval survival in limited food conditions.

2. Material & methods

2.1 The 'abj' DEB model applied to seabass

The standard DEB model (Kooijman, 2010, chapter 2) quantifies the metabolic dynamics of an individual organism during its entire life cycle and describes the processes of growth, maintenance and reproduction. Here, we used an 'abj' model (Marques *et al*., 2018), which is a standard DEB model with a metabolic acceleration between birth and metamorphosis. Two forcing variables drive the 'abj' model: temperature and food availability. The conversion between food availability and ingestion is obtained using the Holling type II functional response:

$$f = \frac{X}{X_K + X} \qquad (1)$$

where X is the food density and X_K the half-saturation constant. f can take values between 0 (food deprivation) and 1 (feeding *ad libitum*).

An individual is described by four state variables: the reserve energy (E, J), the structural volume (V, J), the maturity (E_H, J) - which is the cumulative energy invested to become more complex (i.e. development of new organs, installation of regulation systems; Kooijman, 2010, chapter 2) - and the reproduction buffer (E_R, J). Links between these variables are summarised in Figure 15.

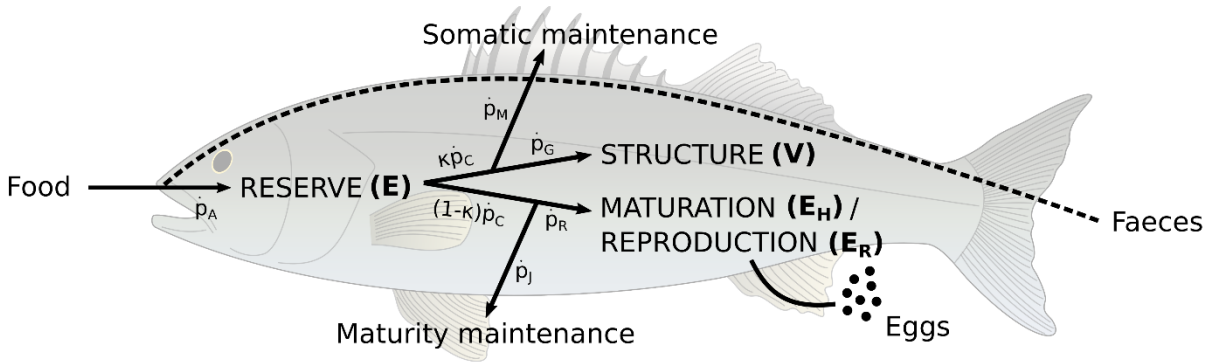

Figure 15. Schematic representation of the standard DEB model applied to European seabass. Arrows represent energy fluxes (J/d, Table 10*).* Table 10 *records the dynamics of the state variables E, V, E_H and E_R.*

The dynamics of the state variables are described by differential equations (Table 9), which were solved using the finite-difference method with the Euler numerical scheme.

Table 9. Equations of the 'abj' model including the dynamics of the four state variables, the metabolic acceleration, the six energy fluxes (J/d) and the shape correction function. Brackets [] represent quantities per unit of structural volume and braces {} represent quantities per unit of structural surface area.

Reserve dynamics	$\frac{dE}{dt} = \acute{p}_A - \acute{p}_C$
Structural length dynamics	$\frac{dL}{dt} = \frac{\acute{p}_G}{3L^2[E_G]}$
Maturity level dynamics	$\frac{dE_H}{dt} = \acute{p}_R$ if $E_H < E_H^p$ else $\frac{dE_H}{dt} = 0$
Reproductive buffer dynamics	$\frac{dE_R}{dt} = \acute{p}_R$ if $E_H \geq E_H^p$ else $\frac{dE_H}{dt} = 0$
Metabolic acceleration	if $E_H < E_H^h$ $s_M = 1$ if $E_H^h \leq E_H < E_H^j$ $s_M = L/L_b$ if $E_H \geq E_H^j$ $s_M = L_j/L_b$
Assimilation flux	$\acute{p}_A = s_M\{\acute{p}_{Am}\} f L^2$ if $E_H \geq E_H^b$ else $\acute{p}_A = 0$
Mobilisation flux	$\acute{p}_C = \frac{E}{L^3} \frac{s_M \acute{v}[E_G]L^2 + [\acute{p}_M]L^3}{[E_G] + \frac{\kappa E}{L^3}}$
Somatic maintenance flux	$\acute{p}_M = [\acute{p}_M]L^3$
Growth flux	$\acute{p}_G = \kappa \acute{p}_C - \acute{p}_M$
Maturity maintenance flux	$\acute{p}_J = \acute{k}_J E_H$
Maturation or reproduction flux	$\acute{p}_R = (1-\kappa)\acute{p}_C - \acute{p}_J$
Shape correction function	$\delta_M(L) = \delta_{Mj} + (\delta_{Mb} - \delta_{Mj}) \frac{L_j - L}{L_j - L_b}$

An organism assimilates the food energy following the flux $\acute{p}_A$(J/d) and added to the energy reserve (molecules waiting to be used to fuel metabolic processes). The stored energy is then mobilised (flux $\acute{p}_C$, J/d) for somatic maintenance and growth with the fraction κ, while the rest (1-κ) is used for maturity maintenance and maturation (juveniles) or reproduction (adults). Maintenance always has priority over the other processes. In other words, if the costs of somatic and/or maturity maintenance cannot be paid from reserve, the individual dies of starvation. Table 9 summarises the equations of the standard DEB model fluxes.

The standard DEB model works for isomorphs, i.e. organisms that do not change in shape. We assume that this is the case during the period from egg to non-feeding larval stages, as well as from juvenile to adult stages. This means that the shape coefficient ($\delta_M$that links the volumetric length (L, cm) and the physical length (L_w, cm) by $L = \delta_M L_w$ (Kooijman, 2010) is constant. For feeding-larvae, the change in shape is given by the shape correction function (Table 9, Augustine *et al*., 2011) with δ_{Mb} and δ_{Mj} corresponding to the shape coefficients for eggs/non-feeding larvae and juveniles/adults, respectively, and L_b and L_j corresponding to the volumetric lengths at birth (*sensu* DEB, i.e. mouth opening) and metamorphosis, respectively. L_b and L_j are saved during the simulation and used in post-treatment to calculate the shape correction function (Table 9).

The metabolic acceleration (Table 9) accounts for the exponential growth increase of the larvae until metamorphosis. It affects the maximum surface-area-specific assimilation rate $\{\acute{p}_{Am}\}$ (J.cm^{-2}.d^{-1}) and the energy conductance $\acute{v}$ (cm.d^{-1}), thereby, the acceleration of growth relies on an increasing amount of intake and reserve mobilization during the larval stage.

The temperature affects all the fluxes as enzymatic processes are accelerated within a given temperature range. According to Kooijman (2010), we used the extended Arrhenius relationship to quantify the temperature effect on all fluxes:

$$\acute{k}(T) = \acute{k}(T_1) exp\left(\frac{T_A}{T_1} - \frac{T_A}{T}\right)\left(\frac{1+exp\left(\frac{T_{AL}}{T_1} - \frac{T_{AL}}{T_L}\right)+exp\left(\frac{T_{AH}}{T_H} - \frac{T_{AH}}{T_1}\right)}{1+exp\left(\frac{T_{AL}}{T} - \frac{T_{AL}}{T_L}\right)+exp\left(\frac{T_{AH}}{T_H} - \frac{T_{AH}}{T}\right)}\right) \qquad (2)$$

with $\acute{k}$ a physiological rate, T the absolute temperature in Kelvin, T_1 a reference temperature of 293.15 K, T_A the Arrhenius temperature, T_L and T_H the critical lower and upper boundaries of the thermal tolerance range (respectively 10°C and 28°C, in Kelvin in the model), and T_{AL} and T_{AH} the Arrhenius temperatures for these boundaries.

The standard DEB model operates over the entire life cycle and differentiates three life stages: embryo, juvenile and adult. As each one of these DEB stages may include different biological stages, and because we aim to study the early life stages, we considered five life stages: the egg and non-feeding larval stage (does not feed or reproduce, i.e. the embryo *sensu* DEB), feeding larva and juvenile stage (feeds but does not reproduce, i.e. juvenile *sensu* DEB) and the adult stage (feeds and reproduces). Transitions between stages occur at specific thresholds of maturity E_H. An egg hatches at $E_H = E_H^h$, a non-feeding larva starts feeding at$E_H = E_H^b$, the metamorphosis occurs at $E_H = E_H^j$ and a juvenile becomes mature at $E_H = E_H^p$.

During the two first life stages, an individual lives on its reserves ($\dot{p}_A = 0$). After the mouth opening, the flux $\dot{p}_A$ depends on food availability. The energy in reserve (E_0, J) for an egg was estimated at 2.8 J using the biochemical composition of seabass eggs from wild genitors acclimatized to captivity for 4 to 6 years (Devauchelle & Coves, 1988). We acknowledge that genetic selection, as well as experimental conditions, may have modified the energy content of the eggs used in our experiments as compared to the value of Devauchelle & Coves (1988), and that wild eggs may also have different energy content, but with no means of estimating these differences, we used the best available information. Moreover, this value was included in the range proposed by Riis-Vestergaard (2002), who developed a generalization to calculate the energy density of marine pelagic fish eggs by averaging the energy density as a function of the percentage of the oil globule compared to the total egg volume.

As specified in Kooijman (2010, chapter 2), strategies to handle E_R are species-specific and the management of this buffer can be adapted in each DEB model. Hereafter, we summarised the rules used in this model. For adults, the spawning season was set between January and May to cover all potential spawning over the entire study area (from the Bay of Biscay to the English Channel). The energy of one batch is defined as:

$$E_B = N_B E_0 Ww \qquad (3)$$

with N_B the relative batch fecundity (N_B = 104 eggs/g of female; Stéphane Lallement, 2018 pers. comm.), E_0 the energy of an egg and W_w the wet weight of the individual:

$$W_w = d_v L^3 + \frac{E}{\rho_E \frac{d_v}{d_{vd}}} + \frac{R}{\rho_R \frac{d_v}{d_{vd}}} \qquad (4)$$

with d_v, d_{vd}, ρ_E and ρ_R as defined in Table 12.

According to (Mayer *et al*., 1990), seabass can produce between two and four batches per year. For simplicity and because it does not change the seasonal bioenergetic the reproduction buffer was emptied once a year, as soon as it contained enough energy, during the spawning season. Then, this energy was converted into a number of batches following the equation:

$$n = \frac{E_R \kappa_R}{N_B E_0 Ww} \qquad (5)$$

with n the number of batches, κ_R the fraction of reproduction energy fixed in eggs (Table 10) and E_R, N_B, E_0, W_w as defined previously.

In the case of prolonged starvation, various levels of response can be considered (Kooijman, 2010; chapter 4). Here, we chose to continue the standard reserve dynamics until death occurred. The κ-rule for allocation was kept unchanged. No shrinkage occurred.

2.2 Calibration of a model adapted to the Atlantic wild seabass population

2.2.1 Data description

Length-at-age and weight-at-age datasets were used to calibrate the DEB model. Data for wild seabass were available in the Ifremer database 'Bargeo'. This database contains all biological measurements and estimated biological parameters (length, weight, age, puberty, sex, etc.) of wild individuals collected for Ifremer at fish markets, by observers at sea, or during scientific cruises catching adult (CGFS and EVHOE) or juvenile (NOURDEM) seabass. Over the period 2000-2016, a total of more than 8,000 individuals (3,402 from the English Channel and 4,948 from the Bay of Biscay) aged between 6 months and 22 years were sampled and considered for this analysis. In the database, the age is provided in years. For the model, age was converted to a value corresponding to the number of days between the day of capture and the hypothesis that the individuals were born on February the 2nd.

Length-at-age and weight-at-age data collected during aquaculture experiments carried out by Ifremer (PFOM/ARN lab) were added to the dataset. Two experiments on larvae and juveniles were considered (Howald *et al*., 2019); the first with individuals between one week and four years old, fed *ad libitum* at a temperature of 15°C (then varying for juveniles but for sake of simplicity, considered as constant around 15°C for the whole experiment), and the second with individuals between 1 week and 8 months old raised at 20°C and fed *ad libitum*.

2.2.2 Parameters estimation

A fundamental assumption when calibrating the 'abj' DEB model for wild seabass was that the model structure and parameters would be similar between wild and domestic strains. Although genetic selection in aquaculture may have changed the growth pattern of domestic strains, our datasets could not account for such differences between strains. Differences can, therefore, only be explained by variations in the forcing variables (temperature and food availability) that are driving the model.

The calibration process was performed by fitting the growth patterns of three average individuals to two experimental (Howald *et al.*, 2019) and one wild datasets. For the experimental datasets, temperature and food availability were kept constant with the scaled

functional response (*f*) equal to 1 (i.e. larvae and juveniles fed *ad libitum*), and a temperature of either 15°C or 20°C, depending on the experiment. For the wild dataset, *f* was unknown and considered as a parameter to estimate. At this stage, we assumed that *f* does not evolve seasonally for seabass, based on the observation that there was no significant weight evolution over the year in our dataset. For the temperature, we used data collected by wild tagged seabass and published by Heerah *et al*. (2017) and de Pontual *et al*. (2018). In these studies, electronic tags recorded, at high frequency (approx. every 90 seconds), the temperature and depth experienced by 1220 European seabass along the Atlantic French coast between 2010 and 2012, and 2014 and 2016. A maximum of two years of data were recorded due to battery capacity. Our aim with this data was to reconstruct a climatology, as accurate as possible, of the temperatures experienced by adult seabass in the wild. For each day of the year, we averaged the temperature experienced by all individuals with a temperature record (Figure 16). Annual variations were not taken in consideration because the temperature data did not cover the temporal range of the length and weight-at-age data extracted from the Ifremer database.

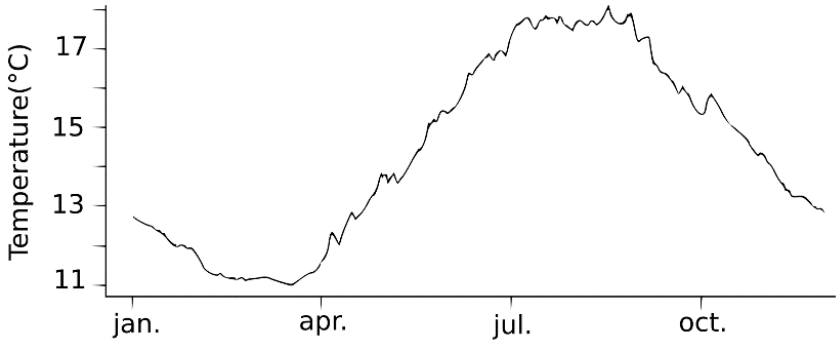

Figure 16. Temperature climatology reconstructed from tagged seabass, and used for the "wild" dataset during calibration (see Methods).

For parameter estimation, we used the global estimation method CMAES (Covariance Matrix Adaptation Evolution Strategies) (Bäck & Schwefel, 1993) with the Fortran library pCMALib (Müller *et al*., 2009). As detailed in Gatti *et al*. (2017), this method estimates the best set of parameters across the entire parameter space, even in the case of a large number of parameters (15 in this study). The cost function to minimize is the sum of two terms:

$$Fcost = \sum_i^{datasets} \sum_j^{stages} \sum_k^{variables} \frac{1}{n_{obsi,j,k}} \sum_l^{n_{obsi,j,k}} \left(\frac{x_{i,j,k,l} - y_{i,j,k,l}}{\sigma_{obsi,j,k}} \right)^2 + \sum_m^{thresholds} \left(\frac{x_m - z_m}{\sigma} \right)^2 \quad (6)$$

The first term represents the fitting of the length- and weight-at-age data for our three datasets, whereas the second term represents the fitting of literature data for length at hatching, mouth opening, metamorphosis and puberty. In the first term, x is the model predictions, y the

observations, and $\sigma_{obsi,j,k}$ and $n_{obsi,j,k}$, the standard deviations and the number of observations of variable k for stage j and dataset i, respectively. The standard deviations were calculated for each dataset and stage, as it depends on the environmental conditions experienced by the individuals and on their age/length (i.e. the value is linked to the mean). The variables are length and weight, whereas the stages are larvae (both non-feeding larvae and feeding larvae), juveniles and adults. The adult stage lasts much longer than the other stages (fifteen years *vs*. three months for larvae and six years for juveniles in our calibration) with sizes and weights covering a broad range of values. To better balance the fit with the duration of each stage, we have divided this stage into three equal periods of five to six years (i.e. the duration of the juvenile stage), which has the effect of increasing the weight of the oldest individuals, who are the rarest (i.e. only 46 individuals over 16 years old *vs.*1,470 between 11 and 16 years old and 4,800 between 6 and 11 years old). In the second term, x is the length prediction for the different thresholds of E_H, z is the corresponding length at hatching at 15°C (Regner & Dulcic, 1994), mouth opening at 15°C (Kennedy & Fitzmaurice, 1972), metamorphosis in the wild (Barnabé, 1990) and puberty in the wild (Drogou, 2018 pers. comm.), while σ is a standard deviation calculated for length at puberty and set arbitrarily for the others lengths.

As we had no information on reproduction at different food levels, we chose to use the general value for animals following Marques *et al.* (2018), and set the maturity maintenance rate coefficient, that control the sink of reserve linked to maturity ($\acute{k}_j$, equal to 0.002 d^{-1}. We were also missing information to calibrate the energy density for structure (ρ_V) and reserve (ρ_E). We calculated those parameters by following Lika *et al.* (2011) and set $\rho_V = \rho_E = 23431$ $J.g^{-1}$. We also set the specific density of the wet mass (d_v) and dry mass (d_{vd}) at 1 $g.cm^{-3}$ and 0.2 $g.cm^{-3}$, respectively.

We then optimized 15 parameters: κ, $\{\acute{p}_{Am}\}$, $\acute{v}$, $[E_G]$, $[\acute{p}_M]$, T_A, E_H^h, E_H^b, E_H^j, E_H^p, δ_{Mb}, δ_{Mj}, T_{AL}, T_{AH} and f for the wild dataset. The description of these parameters and their values after optimization are summarised in Table 10 as well as the parameters we set in our model, based on data from the literature.

Table 10. Comparison of the 15 optimized and 8 fixed DEB parameters used in this study of European seabass with the values published by Stavrakidis-Zachou, et al (2018). All rates are expressed at T_1 = 293.15 K (=20°C). Brackets [] indicate quantities per unit of structural volume and braces {} indicate quantities per unit of structural surface area.

Symbol	This study (1)	Stavrakidis-Zachou *et al.*'s model (2)	$\frac{(1)-(2)}{(2)}$	Unit	Definition
κ	0.478	0.56	-0.15	-	Allocation fraction to soma
$\{\dot{p}_{Am}\}$	109.7 / 581.4 *	85.44 / 585.85 *	0.28 / -0.008 *	$J.cm^{-2}.d^{-1}$	Specific maximum assimilation rate
$\acute{v}$	0.023 / 0.122 *	0.041 / 0.282 *	-0.44 / -0.57 *	$cm.d^{-1}$	Energy conductance
$[E_G]$	6678	5230	0.28	$J.cm^{-3}$	Specific costs for structure
$[\acute{p}_M]$	18	19.6	-0.08	$J.cm^{-3}.d^{-1}$	Volume-specific somatic maintenance rate
T_A	7002	7998	-0.12	K	Arrhenius temperature
E_H^h	0.047	0.14	-0.66	J	Maturity threshold at hatching
E_H^b	0.306	1.61	-0.81	J	Maturity threshold at birth
E_H^j	45.7	526.16	-0.91	J	Maturity threshold at metamorphosis
E_H^p	2507273	2510000	0	J	Maturity threshold at puberty
δ_{Mb}	0.058	/	/	-	Shape coefficient for eggs and non-feeding larvae
δ_{Mj}	0.16	0.148	0.08	-	Shape coefficient for juveniles and adults
T_{AL}	38563	22974	0.68	K	Arrhenius temperature at low boundary
T_{AH}	89833	87590	0.03	K	Arrhenius temperature at high boundary
f	0.833	/	/	-	Scaled functional response for wild data
T_L	283.15 (Claireaux & Lagardère, 1999)	274	0.03	K	Critical lower boundary of thermal tolerance range
T_H	301.15 (Claireaux & Lagardère, 1999)	303	-0.01	K	Critical upper boundary of thermal tolerance range
κ_R	0.95 (Kooijman, 2010)	0.95	0	-	Fraction of reproduction energy fixed in eggs
$\acute{k}_j$	0.002 (Marques *et al*., 2018)	0.002	0	d^{-1}	Maturity maintenance rate coefficient
ρ_V	23431 (Lika *et al*., 2011)	23431	0	$J.g^{-1}$	Energy density for structure
ρ_E	23431 (Lika *et al*., 2011)	23431	0	$J.g^{-1}$	Energy density for reserve
d_v	1 (Kooijman, 2010)	1	0	$g.cm^{-3}$	Specific density of wet structure
d_{vd}	0.2 (Kooijman, 2010)	0.2	0	$g.cm^{-3}$	Specific density of dry structure

* values before/after acceleration

For initializing the model, we used the parameters from Lika *et al.* (2014). As the parameter T_{AH} modifies the correction factor even before reaching the upper critical temperature T_H, we kept T_{AH} in the list of parameters to be estimated. Claireaux & Lagardère (1999) showed that above 20°C, metabolic fluxes start to decrease; we, therefore, considered that the dataset of larvae raised at 20°C contained information for estimating T_{AH}. Our estimated value appeared very similar to the value of Stavrakidis-Zachou *et al*. (2018).

2.2.3 Model validation

Seven checks were performed to validate our optimized parameter set in comparison to the literature. First, we checked whether the duration of the egg stage agreed with the literature (Devauchelle & Coves, 1988):

$$D = 414.455 - 119.728lnT \quad (7)$$

with D the incubation duration in hours and T the temperature in degree Celsius. We then checked if birth (*sensu* DEB, i.e. mouth opening) at 19°C and 9°C occurred around 4 and 14 days post-hatching, respectively (Barnabé et *al*., 1976). We also looked at the survival of larvae without food at 19°C and controlled that the number of batches was within the range of two to four batches per year, as shown by in Mayer *et al*. (1990). Finally, we checked the age at first maturity in aquaculture at 15°C and in the wild, and verified that the growth efficiency ($\kappa_G = \frac{d_{vd}\rho_v}{[EG]}$ (8)) was close to 0.8 (Marques *et al*., 2018) and below 1 (to ensure mass conservation).

For model validation, we used an independent length-at-age and weight-at-age dataset for Atlantic seabass larvae raised in aquaculture since egg fertilization with temperatures varying during the whole experiment (Figure 17) and individuals fed *ad libitum* (f = 1) (Allal *et al*., unpublished, Ifremer - MARBEC lab). To validate the model, hypothesis tests were made on the parameters of the regression between observed and predicted values for both length and weight.

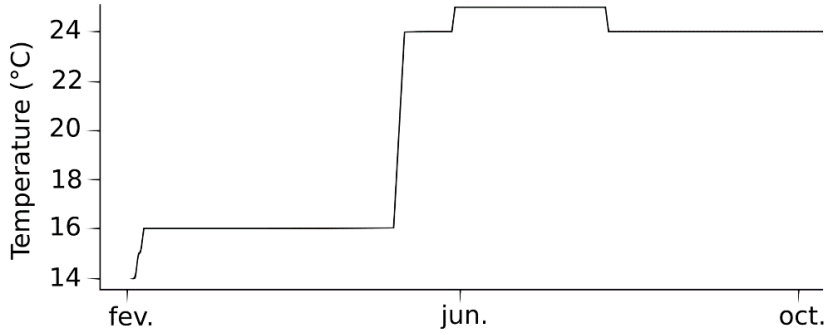

Figure 17. Temperatures experienced by young seabass in the experiment of Allal et al. *(unpublished) and used to validate our DEB model with an independent dataset.*

2.3 Using the model to investigate the effects of varying temperatures and food levels on young seabass

To evaluate the impact of food availability and temperature on the survival of seabass early life stages, we carried out three numerical experiments.

Experiment 1 focused on the ability of young seabass to survive starvation. Here, we numerically analysed the ability to survive starvation as a function of i) the timing of spawning and ii) the state of the individual when food deprivation begins. We considered 12 spawning dates (one for each month of the year) to test the impact of the environment (i.e. mostly temperature) on the survival of young seabass to starvation. We also initiated the food deprivation at four different states (mouth opening and 1, 2 and 3 months after mouth opening) to assess how this affects survival to food deprivation. The temperature was similar to that used for the wild dataset calibration (Figure 16) and food was set similar to the *f* calibrated for the wild dataset (Table 10) until starvation begins (*f = 0*).

Experiment 2 numerically investigated whether the life history of larvae during their drift (i.e. the planktonic phase) would have an impact on their survival capacity to starvation once they have reached the nursery. To this end, we tested different scenarios of temperature (10, 15, 20 and 25 °C) and food level (*f* = 1 or *f* = 0.2) before starting food deprivation (at 1.2 cm, i.e. the minimal size of larvae observed in English Channel nurseries, Jennings & Pawson, 1992).

Experiment 3 numerically investigated how the environmental conditions affect the growth of seabass larvae and their potential to reach a nursery. Larvae are considered to survive and recruit if, after three to four months (the average drift time according to, Reynolds *et al*., 2003), they reach a minimum size of 1.2 cm (Jennings & Pawson, 1992). We used the scenario of experiment 2 and the environmental conditions of our "wild" dataset (i.e. the calibrated *f* and T of Figure 16) and checked the size of the larvae after 110 days. Some level of individual variability was also introduced in this experiment to assess the properties of our model at an individual scale and evaluate the sensitivity of the model to variations of one DEB parameter only. Technically, we studied the impact of changing the specific maximum assimilation rate $\{\dot{p}_{Am}\}$ on the growth of larvae. We choose this parameter as the main source of individual variability following the body size scaling relationships defined by the DEB theory (Kooijman 2010, chap. 8). These body size scaling relationships stipulate that among species, only the specific maximum assimilation rate and the different maturity levels covary with maximum length, the other primary parameters being constant (Kooijman 2010, chap. 8, Pecquerie *et al*.

2011). Here, we applied this reasoning to individuals of the same population based on the observed variability of maximum sizes within the population. For each scenario, we simulated 30 individuals with different values of $\{\acute{p}_{Am}\}$. The 30 values were determined to obtain individuals with an asymptotic length ($L_{w\infty}$, eq.9) between 58 and 94 cm. The target was a normal distribution centred around 80 cm (the asymptotic length for our study area (Bertignac, 1987).

$$L_{w\infty} = f\frac{L_m}{\delta_{Mj}} = f\frac{\kappa\{\acute{p}_{Am}\}s_M}{[\acute{p}_M]\delta_{Mj}} \qquad (9)$$

with $f, \kappa, \{\acute{p}_{Am}\}, s_M, [\acute{p}_M]$and δ_{Mj} as detailed in Table 10.

3. Results

3.1 Model calibration

The DEB model fitted well our three length-at-age datasets, as illustrated in Figure 18 for all life stages. For wild larvae, the age in days was not available and our estimation assumed that they were all born in February. This could partly explain why some individuals at the age of about 200 days are longer than others at the age of 500 days (Figure 18). Another explanation could be inter-annual growth variability.

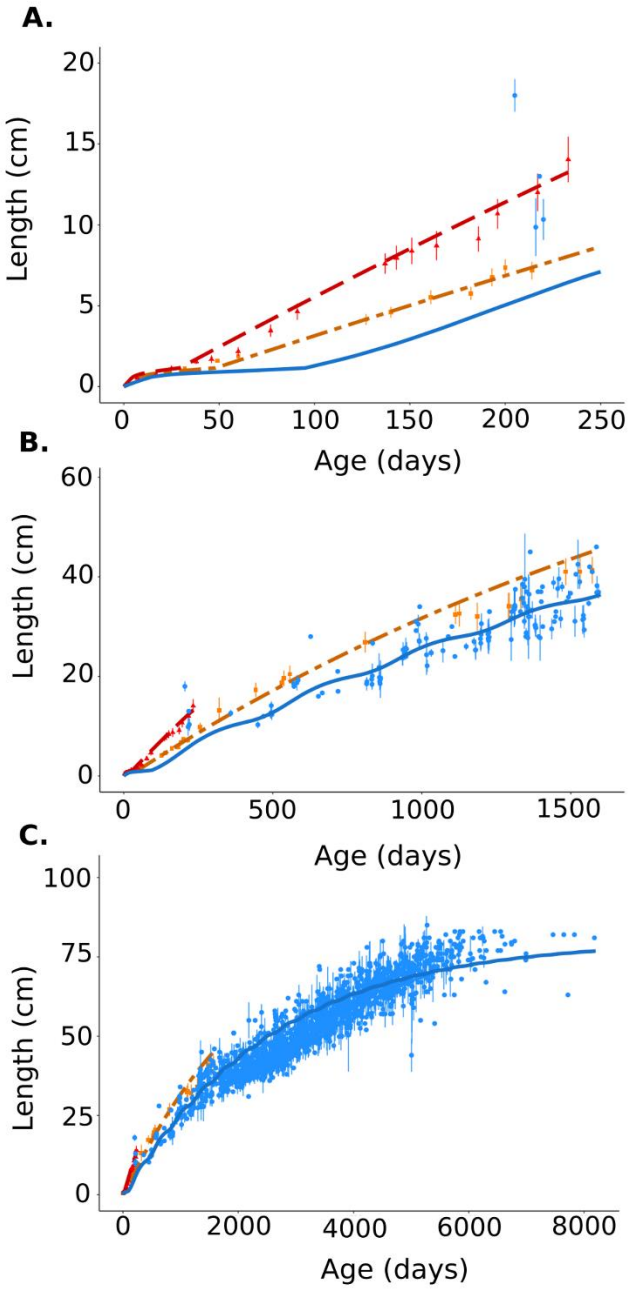

Figure 18. Model fitted to the three "length-at-age" datasets: A) 0-250 days, B) 0-1,600 days and C) 0-8,200 days. Triangles, squares and dots represent mean observations with their standard deviation (not used for calibration). Lines represent model predictions for the aquaculture experiment at 20°C (red/longdash), the aquaculture experiment at 15°C (orange/twodash), and the "wild" dataset (blue/solid).

The model underestimated the weight for all datasets, and Figure 19 shows that the absolute difference between the model and the data increases with time.

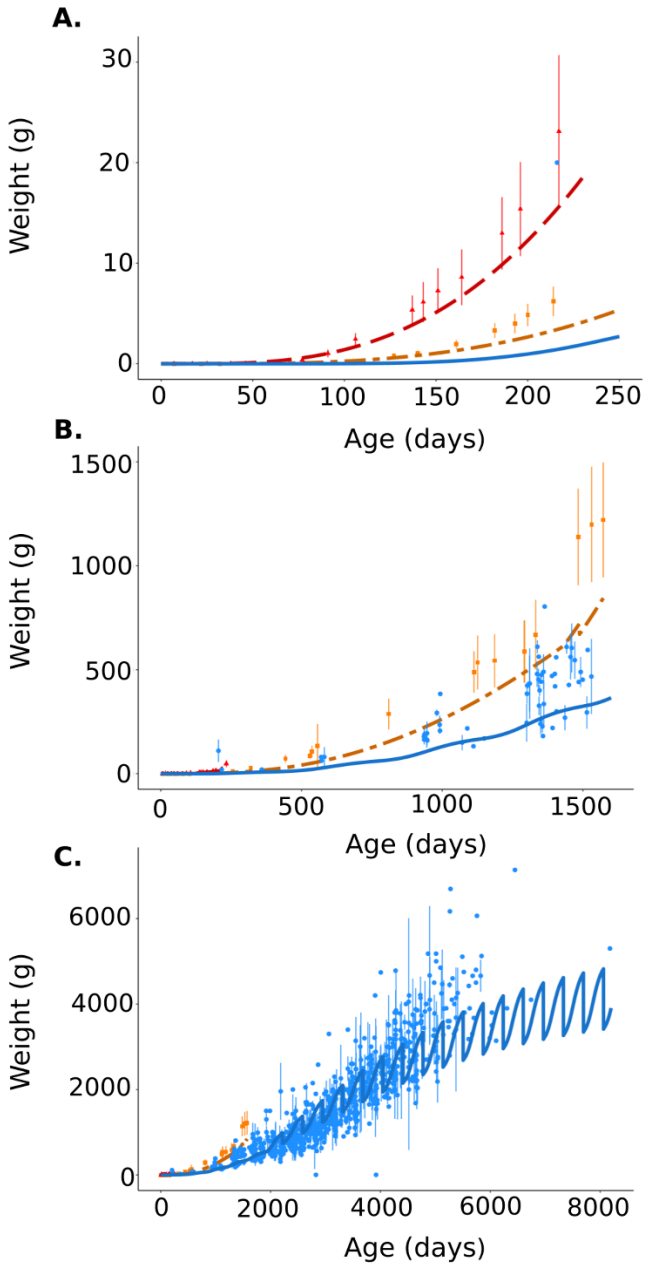

Figure 19. Model fitted to the three" weight-at-age" datasets: A) 0-250 days, B) 0-1,600 days and C) 0-8,200 days. Triangles, squares and dots represent mean observations with their standard deviation (not used for calibration). Lines represent the model predictions for the aquaculture experiment at 20°C (red/longdash), the aquaculture experiment at 15°C (orange/twodash), and the "wild" dataset (blue/solid).

The relative difference appeared very variable, with a mean difference of 67% for larvae and 10% for juveniles at 20°C, and of 13% for larvae and 15% for juveniles at 15°C. For the wild dataset, the mean difference was 18% for juveniles, 21% for adults 6 to 11 years old, and 6% for the two other groups of adults. We then run a regression between observed and predicted

weight values for the first months of life (0-110 days) as we focused on the first life stages. Our results demonstrate that the model reproduces the observations well at 15°C but slightly overestimates the weight at 20°C *(*Figure 20).

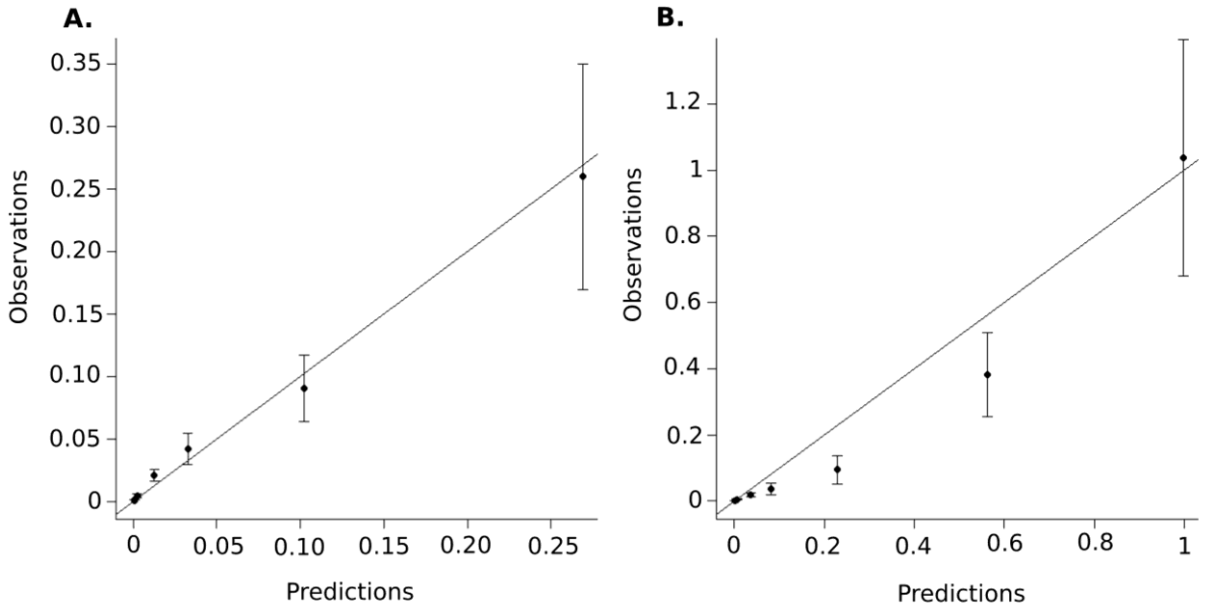

Figure 20. Plot of observed weight values with their standard deviation error bars (y-axis) vs. predicted weight values (x-axis) compared to the 1:1 line for the 0-110 days time period: A) experiment at 15°C and B) experiment at 20°C.

The root-mean-squared errors (RMSE) were 0.007 at 15°C and 0.08 at 20°C. The relative differences for larvae about three to four months old, at 15 and 20°C, were 7% on day 127 and 9% on day 106, respectively. This level of errors was judged acceptable. We thus kept this parameterization for the rest of the study.

Our model was able to produce some interesting results: individuals from aquaculture experiments mature earlier than individuals from the wild (Table 11). This can be seen on the modelled weight curves (Figure 19) as the curves show sudden stalls when the reproduction occurs (i.e. a batch of eggs is released).

3.2 Model validation

Our model was used to predict a large number of observable properties for which we found corresponding values in the literature. These properties were not used during the calibration procedure and were used as validation data (Table 11). The number of days for the first stages was well reproduced as well as reproduction properties (i.e. number of batches and age at first spawning in different conditions). The survival time was slightly overestimated (i.e. 11 days at 19°C *vs*. 8 days in experimental conditions).

Table 11. Quantities derived from the calibrated 'abj' DEB model (f=0.833) and values from the literature used for comparison and validation.

Quantities derived from the calibrated model	Value	Literature
Duration of the egg stage (days)	4/3*	3.759/2.324* (Devauchelle & Coves, 1988)
Number of days post-hatching before mouth opening at 15°C	5	7 (Barnabé *et al.*, 1976)
Larval survival at 19°C without food (days)	11	7-8 (Zambonino, 2018 pers. comm.)
Age at first spawning in the wild (years)	6	6 (Kennedy & Fitzmaurice, 1972 ; Pawson & Pickett, 1996)
Number of batches per year (in the wild)	4	2-4 (Mayer *et al.*, 1990)
Age at first spawning at 15°C (years)	4	4 (Servili, 2018 pers. comm.)
Growth efficiency	0.7	0.8 (Marques *et al.*, 2018)

* values at 15°C / 20°C

We also validated our model using an independent dataset of growth data (length and weight) at varying temperatures (Allal *et* al., unpublished) (Figure 21).

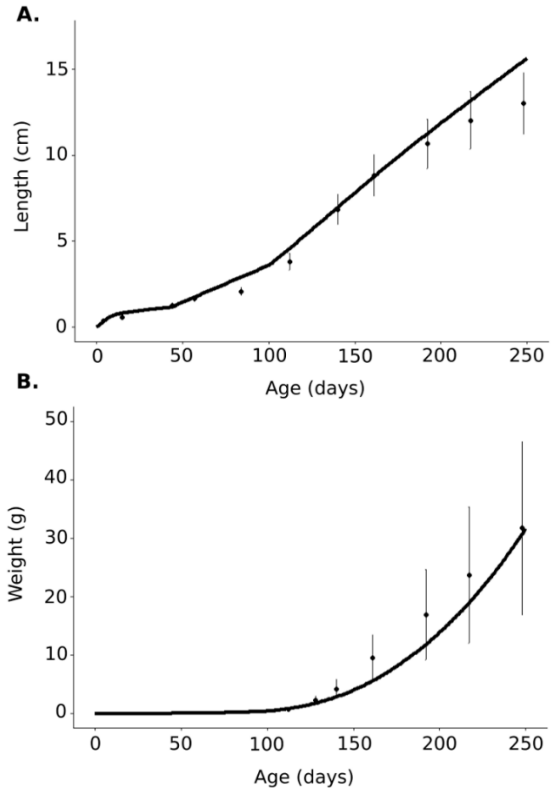

Figure 21. Validation of our model (line) using an independent dataset (dots with their standard deviation) for A) length and B) weight. Individuals were fed ad libitum *and raised at temperatures shown on Figure 17.*

The model predicted the growth values well with a relative error of 4.4% for length and 7.6% for weight. The regression between observed and predicted values were y = 0.90x + 0.06 with R^2 = 0.99 for length, and y = 1.05x + 1.82 with R^2 = 0.97 for weight. The Student's t-test revealed that the intercept was not significantly different from 0. The new equations were y = 0.90x for length and y = 1.14x for weight and the regression validated.

3.3 Survival of larvae and early juveniles to starvation

The ability of larvae and early juveniles to survive starvation was tested at different times of starvation onset (i.e. different spawning months and ages, cf. Experiment 1).

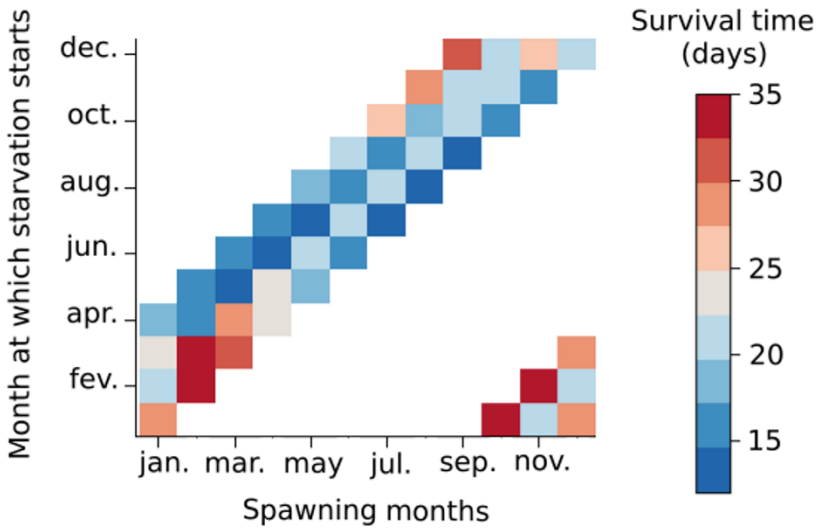

Figure 22. Experiment 1: Starvation survival time of seabass larvae (in days) relative to the spawning month (x-axis) and the month at which starvation starts (directly at mouth opening, or 1, 2 or 3 months after mouth opening) (y-axis). The feeding level corresponds to f = 0.833 *(estimated from the calibration procedure) and the temperature follows Figure 16.*

Our results demonstrate that the season at which starvation occurs is the main factor explaining the survival of the larvae with the longest survival times occurring when starvation happens in winter (lowest temperatures). Besides, when starvation starts straight at mouth opening, individuals born during the first months of the year appear to survive starvation longer than those born in the middle or at the end of the year (19-34 days *vs*. 13-22 days). When food deprivation starts at one month old, the same pattern is observed, although slightly shifted towards autumn; larvae appear to endure starvation better between October and April than during the rest of the year (22-33 days *vs*. around 20 days). On the other hand, if starvation starts at three months old, individuals born during summer and autumn appear more resistant to starvation than the others (16-25 days in July and 22-34 days in October *vs*. 12-16 days in

April). We also observed that larvae (or juveniles) are more sensitive to starvation when food deprivation starts about two months after birth (blue squares in Figure 22).

3.4 Effect of temperature and food history on the survival of young seabass

Figure 23 shows the impact of temperature and food history on the survival of seabass larvae as tested during experiment 2.

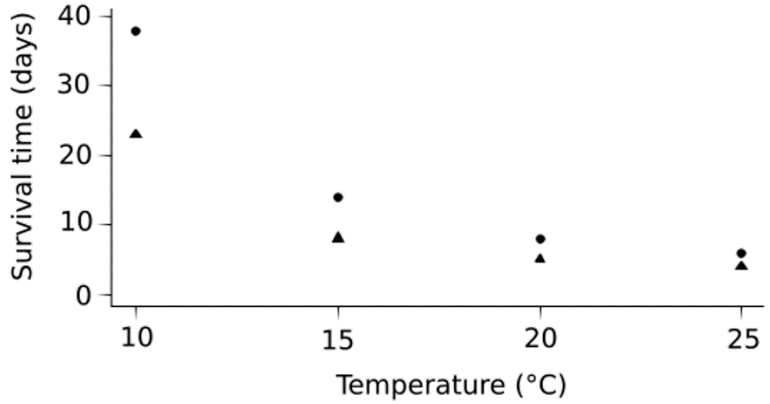

Figure 23. Experiment 2: Starvation survival time of seabass larvae when food deprivation begins at recruitment size (L = 1.2 cm) according to experimental temperature and feeding history: f=1 (dots) and f=0.2 (triangles).

As implied by the DEB theory, we observed that the survival capacity of larvae decreases with temperature as well as the energy in reserve. At the end of the experiment, larvae fed at $f = 1$ had 46 J on average whereas those fed at $f = 0.2$ had 8 J on average. Our results also indicate that, larvae fed ad libitum ($f = 1$) survive starvation longer than those fed at $f = 0.2$. Finally, the difference in survival time between the two experiments decreased with temperature. The individuals fed *ad libitum* at 10°C surviving 15 days longer than those fed at $f = 0.2$ whereas at 25°C, they survived only 2 more days.

3.5 Effect of temperature, food history and individual variability on the growth of young seabass

Experiment 3 tested the impacts of temperature and food history on the growth of larvae and assessed variability at the individual scale. As explained in the methods, we consider that a larva successfully survived if it reached 1.2 cm in length (the recruitment size) within 110 days. Figure 24 illustrates the mean sizes reached by the 30 individuals with different $\{\acute{p}_{Am}\}$ in the eight environmental conditions after 110 days.

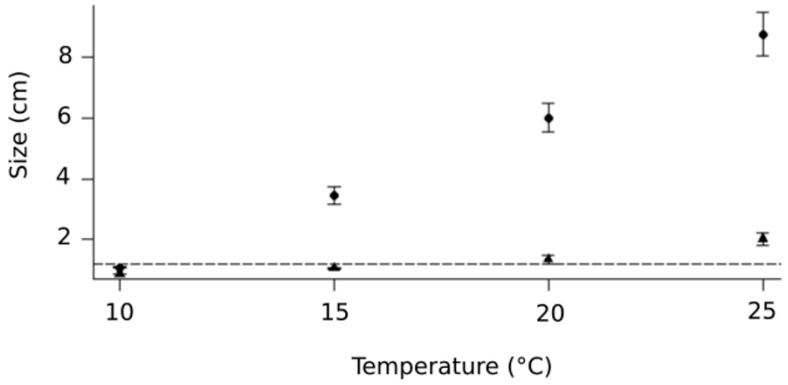

Figure 24. Experiment 3: Mean sizes and standard deviations for 30 individuals with different $\{\acute{p}_{Am}\}$ according to experimental temperatures and feeding history: f=1(dots) and f=0.2 (triangles). The dotted line represents the target size of 1.2 cm.

At 10°C, neither the individuals fed *ad libitum*, nor those fed at f = 0.2 survived until recruitment. At 15°C, the 30 individuals fed *ad libitum* survived while all the others "died". At 20°C, the 30 individuals fed *ad libitum* all survived, while only seven of those fed at f = 0.2 (those with an asymptotic length of more than 84 cm) would have survived the planktonic larval phase (Figure 25). Finally, at 25°C, all individuals survived in both populations. In the conditions of the "wild" dataset, the seven smaller individuals (i.e. those with an asymptotic length of less than 73 cm) did not survive (Figure 25).

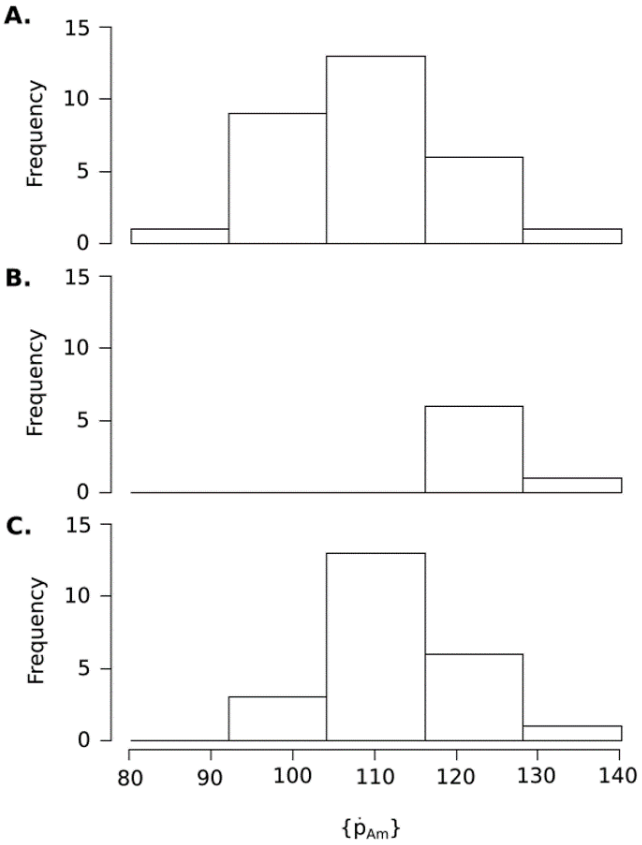

Figure 25. Experiment 3: Distribution of individuals according to their specific maximum assimilation rate. A) initial population; B) and C) individuals that would have reached at least 1.2 cm-long on day 110 and either fed at f = 0.2 and raised at 20°C (B) or fed and raised using the environmental conditions experienced by the wild dataset (i.e. calibrated f and T as shown in Figure 16)(C).

4. Discussion

The DEB parameters for Atlantic European seabass were estimated with a robust method based on an evolutionary algorithm. The estimation was performed using three Atlantic population datasets: two from aquaculture experiments and one from the wild. Using this approach, we estimated food availability (i.e. the scaled functional response; $f = 0.833$) for the wild individuals of our study area (Bay of Biscay – English Channel). The model predicted a large number of properties, which were in agreement with data from the literature. Notably, farmed individuals appeared to grow faster and reach full maturity earlier than wild individuals, mainly because they are fed *ad libitum* and raised at higher temperatures. The model was then used to carry out three experiments that demonstrated (i) higher starvation survival rates when eggs are hatch in winter, (ii) the importance of food throughout the planktonic phase and (iii) the need of food in spring in nurseries.

For this study, we performed a new parametrization of the European seabass DEB model and compared the parameters to the model of Stavrakidis-Zachou *et al.* (2018) (Table 10*).* The two calibrations showed differences in the fish lengths and ages at hatching, birth, metamorphosis and puberty (Table 12).

Table 12. Comparison of lengths and ages at hatch, birth, metamorphosis and puberty, as predicted using the parameters of this study (wild seabass), with those of farmed seabass (Stavrakidis-Zachou et al.*, 2018).*

	This study	**Stavrakidis-Zachou *et al.*, 2018**
Length at hatching (cm)	0.32	0.22
Length at birth (cm)	0.58	0.5
Length at metamorphosis (cm)	1.2	3.4
Length at puberty (cm)	42	53.38
Age at hatch at 15°C (d)	5	3.92
Age at birth at 19°C (dph)	6	6
Age at metamorphosis at 19°C (dph)	34	70
Age at puberty at 19°C (d)	959	723

The individuals of the Stavrakidis-Zachou *et al.* (2018)'s model grow faster: they reach puberty earlier, even if their puberty length is longer (i.e. 53.38 cm against 42 cm). Similarly, we noted differences in lengths at metamorphosis, a stage transition that is complicated to determine and which occurs earlier in individuals with an Atlantic origin. This observation is in agreement with Darias *et al*. (2008) who highlighted significant changes in the transcriptome of Atlantic seabass larvae at 20°C between days 17 and 31 post-hatching, and which could correspond to metamorphosis. Overall, our model improves the predictions of Atlantic seabass growth (in length); however, weight predictions can still be improved.

We used our model to study fish growth in relation to temperature and food availability. Generally, individuals in aquaculture grow faster because they are well fed and raised at higher temperatures (e.g. Person-Le Ruyet *et al*. 2004), and they reach full puberty earlier (e.g. Pawson, 2000) than wild populations. Our DEB model was able to reproduce these characteristics (Figures 18 & 19) with an initial spawning at six years old (for females), which is close to previous observations in Atlantic seabass populations (Kennedy & Fitzmaurice, 1972; Pawson & Pickett, 1996), whereas, according to puberty tests, the initial spawning of farmed female seabass is around three to four years old (e.g. Forniés *et al*., 2001; Servili, 2018 pers. comm.).

We then used the model to explore the effects of selected environmental factors (i.e. food and temperature) on egg and larval biological traits in the wild, including growth and survival. The aim was to provide some understanding of the poor recruitment events experienced by seabass in the Northeast Atlantic since 2010 (ICES, 2018). The spawning season of seabass occurs in winter (Fritsch *et al*, 2007; Pawson *et al*, 2007), which was put forward by Warlen & Burke (1990) as an advantage for the migration of the larvae to nurseries. Indeed, drifting larvae encounter fewer predators or competitors for food during winter and when they reach nursery estuaries in spring, temperatures start rising, which allows them to achieve faster growth. However, in winter in our study area, the seawater temperature is colder and phytoplankton and zooplankton are less abundant than during spring and autumn when planktonic production is the highest (Pingree & Garcia-Soto, 2014). This led us to use our DEB model to assess the effect of temperature and food availability on the growth and survival of early life stage**s** (i.e. planktonic phase) and in the nurseries.

During our first experiment, which tested the ability of seabass larvae to survive food deprivation, we observed that individuals born between January and April-May coped better with total food deprivation than individuals born later (Figure 22). On the other hand, if starvation starts when larvae reach their nurseries (i.e. at about three to four months old), individuals born at the beginning of the year appear less resistant to starvation (Figure 22). This means that if spawning takes place in winter, the seabass larvae or young juveniles that reach nurseries in summer need food to survive. With experiment 2, we investigated the impact of temperature and food history during the planktonic phase on starvation survival in the nurseries. Our results indicate that at low temperatures, the food history of the larvae affects their capacity to survive starvation in nurseries (Figure 23*)*. In the wild, since the drift occurs in winter when food is scarce, the availability of food at nurseries seems to be essential for the survival of the recruits according to our results. These findings indicate that low food levels at nurseries could be one of the factors explaining the poor recruitments observed over the past few years. Besides, according to Martinho *et al*. (2009) and Vinagre *et al*. (2009), factors that most influence the good recruitment of seabass in nurseries are high river runoff and heavy rainfall, which probably support planktonic production through nutrients inputs.

With experiment 3, we investigated the impact of temperature and food history during the drift on the growth of seabass larvae. Again, we observed that individuals raised at low temperatures require sufficiently good environmental conditions (i.e. temperature and food) during the first three to four months of their life to grow to size of at least 1.2 cm in length and

reach nurseries alive. These results indicate that between 10 and 15°C (i.e. winter temperatures), food availability is a key factor for seabass larvae to grow sufficiently and reach nurseries alive. It is possible that the spawning period of the European seabass may be timed by a trade-off between optimal temperatures and food availability during the drift.

Introducing individual-scale variability in experiment 3 did not significantly change the effect of environmental conditions. Figure 24 shows that at 10, 15 and 25°C, the variability inserted in the simulation did not change the model response and all individuals either survived or died. On the other hand, at 20°C, the response varied depending on the individual assimilation rate. Figure 25 shows that at a very low food level, only individuals with high assimilation capacity (i.e. high $\{\acute{p}_{Am}\}$) can survive a drift at 20°C. In the context of climate change with rising temperatures and lower food level in the North Atlantic (Bopp *et al*., 2013), our results tend to suggest that individuals with a higher assimilation rate will be better able to recruit than others.

Conclusion

For the first time, a DEB model was calibrated for Northeast Atlantic wild European seabass. The use of aquaculture experiments and wild population datasets for calibration provided a robust estimation of the DEB parameters. Our original approach reproduce known traits differences between wild seabass and farmed seabass, with the latter growing faster and reaching full puberty earlier. Food availability is a model input which is difficult to assess in the wild. However, through our calibration procedure, we were able to calculate an estimate showing that wild individuals are not fed *ad libitum*. The model also provided evidence of the seabass' tolerance to temperature and food level variations, confirming the adaptation of this fish to winter spawning in the open ocean. Indeed, in our model, larvae were able to survive long-term food deprivation. We related it to their capacity to survive a drift of about three months with difficult environmental conditions (i.e. low temperature and low food levels). We also stress the need for abundant food in the nurseries for the survival of individuals and suggest that a lack of food could explain the low recruitment of the past years. The future application of this model is to link it to a spatially explicit model at the individual scale to study the connectivity between different seabass functional areas and in particular, between spawning areas and nurseries.

Acknowledgments

This study was part of the Barfray project funded by the European Maritime and Fisheries Fund (EMFF- OSIRIS N°: PFEA 400017DM0720006), France Filière Pêche (FFP), the French Ministry of Agriculture and Food (MAF) and Ifremer. DST data were provided by the Bargip project funded by the FFP, MAF and Ifremer. The authors are very grateful to the Ifremer labs PFOM/ARN (Physiologie Fonctionnelle des Organismes Marins) and MARBEC (MARine Biodiversity, Exploitation and Conservation), and H2020 AQUAEXCEL^{2020} (No. 652831) for providing aquaculture data on seabass larvae and juveniles which greatly improved the quality of the model. The authors also thank Romain Lopez for his thorough review of seabass physiology. The authors finally thank Dr. C. Recapet and one anonymous reviewer for their constructive comments that helped to improve the manuscript significantly.

Supplementary material

Testing the Mediterranean European seabass DEB model from Stavrakidis-Zachou *et al.* 2018 with our wild Atlantic European seabass length dataset

The DEB model was twice successfully parametrized for European seabass (Lika *et al.*, 2014 and Stavrakidis-Zachou *et al.*, 2018). The DEB parameter values from those studies were extracted from aquaculture data and applied to the Mediterranean Sea.

To test this model on our wild seabass dataset, we calculated the von Bertalanffy parameters $L_{w\infty}$ (the ultimate physical length, cm, eq. 9) and k (the growth rate, d^{-1}, eq. A.1).

$$k = \frac{\dot{v}}{3\left(\frac{\kappa\{\dot{p}_{Am}\}}{[\dot{p}_M]}\right)\left(f+\left(\frac{[E_G]\dot{v}}{\kappa\{\dot{p}_{Am}\}}\right)\right)} \qquad \text{(A.1)}$$

With f = 1, these parameters were equal to 113.1 and 0.00102, respectively. To model a $L_{w\infty}$ of 80.4 cm, such as estimated by Bertignac (1987), we found that f should be around 0.71. We then compared this model (f = 0.71 and T reconstructed from tagged wild seabass, *Fig.*2) with our wild seabass dataset and observed growth rates too fast for juveniles (*Fig. S1*). These results highlighted the need to compile new data and obtain new parameter estimates.

It is also worth noting that the egg energy had to be increased from 2.8 J (i.e. the value calculated following Devauchelle & Coves (1988)) to 3.8 J in the model of Stavrakidis-Zachou *et al.* (2018) for individuals to hatch.

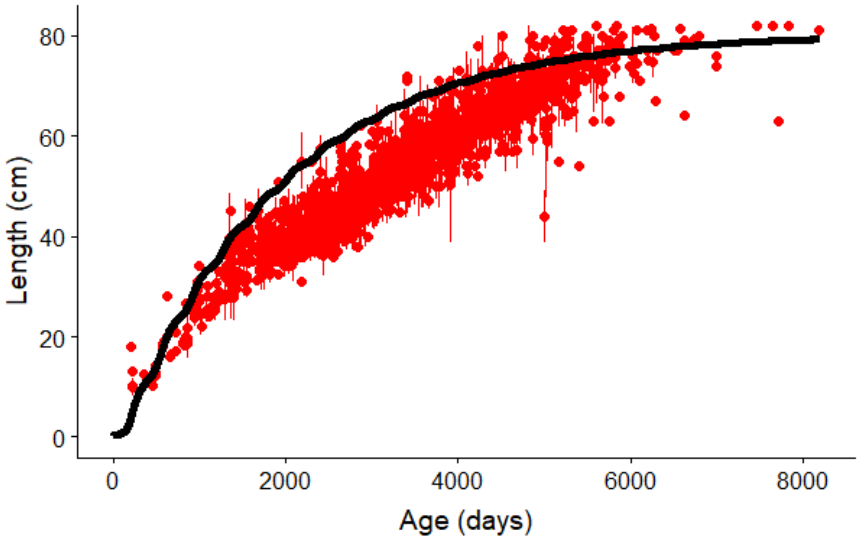

Figure S10. Fit using the DEB model of Stavrakidis-Zachou et al. *(2018) (black line) at f=0.71 and T reconstructed from tagged seabass, to our length-at-age dataset for wild seabass (red dots with their standard deviation error bars).*

CHAPITRE 3

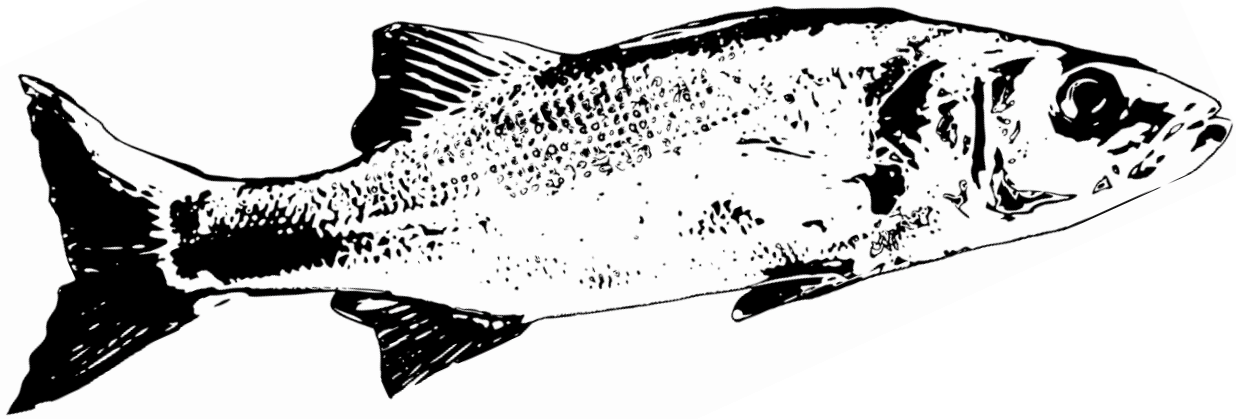

UN MODÈLE DEB-IBM POUR MODÉLISER LA CONNECTIVITÉ ENTRE LES FRAYÈRES ET LES NOURRICERIES DU BAR EUROPÉEN DANS L'ATLANTIQUE NORD-EST

Une version de ce chapitre est en préparation pour soumission à l'*ICES Journal of Marine Science*

RÉSUMÉ DÉTAILLÉ

Les poissons, pouvant vivre dans des habitats variés en fonction de leurs besoins physiologiques (Harden Jones, 1968), ont besoin que la connectivité entre ceux-ci soit maintenue afin d'assurer le bouclage de leur cycle de vie et le maintien de leur population (Rijnsdorp *et al*., 2009; Sinclair, 1988). La caractérisation des habitats fréquentés par une espèce ainsi que l'étude de leur connectivité sont donc essentielles pour une bonne gestion.

Le bar est une espèce partiellement migratrice dont les adultes sont fidèles à leurs zones d'alimentation estivales (Pawson *et al*., 2007 ; de Pontual *et al*. 2019) ainsi qu'à leurs zones de reproduction (de Pontual *et al*., 2019). Certains individus vont migrer au large pour se reproduire (Pawson *et al*. 2007 ; de Pontual *et al*. 2019), les nourriceries étant côtières, la dispersion des œufs et larves constitue alors un processus important pour assurer la connectivité pour cette espèce. Son maintien étant essentiel pour le recrutement de l'espèce.

L'étude de ce processus est complexe puisqu'il repose sur de nombreux facteurs dont les interactions sont difficilement quantifiables. Houde (1987, 2008) explique que la dérive des œufs et larves est une phase sensible, entre autre, au manque de nourriture, à la prédation ainsi qu'aux conditions océanographiques défavorables. Pour étudier l'influence combinée de ces facteurs sur la dispersion des jeunes stades de vie, les sciences halieutiques ont utilisé des modèles couplés physique et biologique (Gallego *et al*., 2007).

Dans le chapitre 1, les frayères du bar ont été caractérisées et leur persistance a pu être montrée. Dans le chapitre 2, un modèle bioénergétique de type DEB a été développé simulant la croissance et la mortalité du bar européen en Atlantique nord-est et étant applicable aux jeunes stades de vie. Le présent chapitre va présenter le couplage de ces approches dans un modèle de dérive larvaire permettant de simuler la dérive des œufs et larves de bar soumis à différentes conditions environnementales afin d'étudier la connectivité résultante entre les frayères et les nourriceries de cette espèce.

Nous avons pour cela couplé un modèle individu-centré (IBM) comprenant un module bioénergétique à un modèle hydrodynamique (MARS3D ; Lazure & Dumas, 2008) et un modèle biogéochimique (POLCOMS-ERSEM ; Holt *et al*., 2001 ; Butenschön *et al*., 2016) simulant les courants et les conditions environnementales (i.e. température et disponibilité en

nourriture) en Manche et dans le golfe de Gascogne. La caractérisation des frayères a permis d'obtenir des zones de lâcher d'individus réalistes ainsi que la délimitation de la saison de reproduction. L'IBM a permis de suivre les trajectoires de plusieurs individus (via un module lagrangien ; Huret *et al*., 2010) dont la croissance et la mortalité étaient différentielles en fonction des conditions environnementales rencontrées (via un module bioénergétique ; Dambrine *et al*., 2020). La sensibilité du succès de colonisation des nourriceries a été étudiée à l'aide de différent scenarios (i.e. mois et année de dérive, comportement vertical des larves, taille à atteindre, durée maximale de dérive et distance à la côte). Un scenario de base a été défini pour étudier la connectivité entre frayères et nourriceries : être à moins de 5 km des côtes et mesurer plus de 1.2 cm avant 90 j de dérive (Jennings & Pawson, 1992).

À l'aide de ce modèle, nous avons simulé la dérive des jeunes stades de vie du bar entre 2008 et 2014 en Manche et dans le golfe de Gascogne. Des zones de frayères et de nourriceries importantes ont été identifiées en estimant la proportion de larves émises par une frayère qui colonise effectivement une nourricerie ainsi que la proportion de larves colonisant une nourricerie particulière. Le succès de colonisation des nourriceries a été montré comme supérieur en Manche même si les mois de janvier et février affichent des pourcentages de colonisation très faibles (~0%) dans cette zone. Une variabilité interannuelle a également été montrée, les hivers doux semblant favoriser la colonisation des nourriceries. Malgré tout, le succès de colonisation reste relativement faible sur la zone d'étude (souvent <1%), les frayères côtières affichant de meilleurs taux de succès (en moyenne sur tous les scenarii 0.46%) que celles du large (en moyenne sur tous les scenarii 0.38%).

En étudiant la connectivité via le scenario de base, il est apparu que les frayères récurrentes (Dambrine *et al*., in revision) étaient en fait celles qui permettaient de disséminer les individus dans le plus grand nombre de nourriceries. Il est également apparu une connectivité entre les frayères du nord du golfe de Gascogne et les nourriceries de Manche ouest mais peu récurrente. Seul le plateau de Rochebonne semble alimenter régulièrement (4 ans sur les 7 testées) et de manière importante (en moyenne 40 occurrences) des nourriceries en mer d'Iroise.

Ces résultats ont pour objectif d'améliorer les connaissances sur les habitats liés au recrutement du bar, dont l'état est inquiétant ces dernières années dans le stock Nord, afin d'aider les gestionnaires dans leur prise de décisions (e.g. encadrement de la pêche pendant la saison de reproduction, protection de zones de nourriceries…).

A DEB-IBM to model the connectivity between spawning and nursery areas of European seabass in the Northeast Atlantic

Chloé Dambrine[1,*], Martin Huret[1], Mathieu Woillez[1], Hélène de Pontual[1]

[1] Ifremer, STH, F29280 Plouzané, France

* Corresponding author.
E-mail address: chloe.dambrine@orange.fr

Abstract

A bioenergetics module was embedded in a particle-tracking model to simulate the growth and drift of eggs and larvae of European seabass for seven years (2008-2014) in the Bay of Biscay – English Channel area. The connectivity patterns were investigated based on a large number of defined spawning areas, throughout the spawning season, and with several scenarios of settlement success that allow for variability. Estimating the proportion of settlers from spawning areas that effectively settle and the number of settlers per nurseries, we highlighted the importance of the vertical behaviour to define nurseries in the Bay of Biscay. Comparing two thermally and windily contrasted year (2010 and 2014), we showed that mild winters favoured the settlement success and increased the connectivity, particularly in the English Channel. Using different scenarios, we showed that the settlement success is better in the English Channel than in the Bay of Biscay. We also highlighted intra- and inter-annual variability but generally, the percentage of settlement was low (< 1%), coastal spawning areas presenting better success than offshore ones. These results may guide management strategies highlighting important recurring spawning and nursery areas for the species that could deserve particular protection measures.

Keywords

Early-life stages, Individual-Based Modelling, Dispersal, Settlement variability, English Channel, Bay of Biscay, *Dicentrarchus labrax*, European sea bass

1. Introduction

Fish need different environmental conditions to grow, survive and reproduce. Thus, they usually live in different stage-specific habitats (Harden Jones, 1968). When habitats are geographically distant, connectivity between them is key to ensure the closure of fish life cycles and populations' sustainability (Rijnsdorp *et al*., 2009; Sinclair, 1988).

Active and passive movements sustain the connectivity between stage-specific habitats. Adults realise active movements while Early Life Stages (ELS) dwell passively with currents. This larval dispersal is recognised as a highly sensitive period with high mortality rate (Houde, 2008). It mostly explains the inter-annual variability of fish recruitment that leads to strong fluctuation in stock size (Hjort, 1914; Rijnsdorp *et al*., 1992). Thus, studying the recruitment process implies understanding the factors influencing the variability of ELS drift and survival (e.g. Cury & Roy, 1989; Cowen & Sponaugle, 2009). Among other factors, Houde (1987 & 2008) pointed out predation, starvation and deleterious oceanographic conditions to explain ELS vulnerability.

To study the influence of these factors on the dispersal patterns, coupled physical-biological models of ELS have been used for several decades in fisheries science (Gallego *et al*., 2007). Within this modelling framework, dispersal is simulated under the influence of hydrodynamic forces and on biological and behavioural traits. In details, Individual Based Models (IBMs; Grimm & Railsback, 2005) coupled to a Lagrangian particle-tracking module within a hydrodynamic 3 dimensional model have been widely used to explore (i) the larval dispersal duration (e.g. Bonhommeau *et al*., 2009), (ii) the larval vertical behaviour (e.g. Fox *et al*., 2006; Sentchev & Korotenko, 2007), (iii) the dispersal kernels (e.g. Koutsikopoulos *et al*., 1991; Ellien *et al*., 2000; Huret *et al*., 2010), (iv) the connectivity within a population (e.g. Savina *et al*., 2009; Rochette *et al*., 2012; Lacroix *et al*., 2013) or (v) the impacts of larval traits on connectivity (e.g. Barbut *et al*., 2019).

European seabass (*Dicentrarchus labrax*) is a species with high economical value, that has been facing a worrying state in its Northern stock (i.e. Irish Sea, Celtic Sea, English Channel, and southern North Sea) since 2013. High levels of fishing pressure together with a series of low recruitments (ICES, 2012) have been pointed out to explain the rapid decline in the spawning stock biomass. As seabass is a partial migratory species that can travel hundreds of kilometres to reproduce (Pawson *et al*., 2007; de Pontual *et al*., 2019), it is important to understand the connectivity between its habitats that support spawning and juvenile growth to

study its populations sustainability. Adult seabass shows localised residency and inter-annual fidelity to coastal foraging areas (Pawson *et al*., 2007; de Pontual *et al*., 2019). In winter, a seemingly important proportion of them migrate offshore to spawn (Pawson *et al*., 2007). Fidelity to these spawning habitats has recently been evidenced (de Pontual *et al*., 2019) as well as a seasonal and inter-annual persistence in the distribution of the spawning areas (Dambrine *et al*., 2021). Thus, the spatial dynamics of seabass adult population seems well structured. From both offshore and coastal spawning areas, eggs and larvae are transported by currents, a proportion of them then settle in coastal nurseries. Thus, characterising seabass larval dispersal is key to quantify the connectivity patterns from spawning areas and settlement success in nurseries.

Beraud *et al*. (2018) first modelled the dispersal of eggs and larvae in the ICES Northern stock. Comparing two thermally contrasted years (i.e. 1996 and 1997) allowing for comparisons between model's outputs and field data, they showed that central western English Channel (WEC) spawning areas are connected to nurseries in England and France and that warm years favour connectivity from central EC to eastern English Channel (EEC). In the absence of better information, eggs were uniformly distributed in areas with temperature above the 9°C isotherm, mortality was not explicitly included and growth and development rates were function of the temperature.

In this study, we aimed at improving the characterisation of the connectivity patterns between spawning and nurseries areas, by developing a modelling framework to provide quantitative responses on seabass dispersal and its variability. From previously identified spawning areas (Dambrine *et al*., 2021), we studied the dispersal of seabass eggs and larvae both in the Bay of Biscay (BoB) and English Channel (EC) areas over seven-years (2008-2014). We used a coupled particle tracking model with a bioenergetics module based on the Dynamic Energy Budget theory (Kooijman, 2010), allowing the simulation of the growth and mortality of seabass ELS under both temperature and food constraints (Dambrine *et al*., 2020).

More specifically, we studied the average connectivity between spawning areas and nurseries and we answered the following questions: Is there difference in the connectivity pattern between two thermally and windily contrasted years? What is the intra- and inter-annual variability of the dispersal? Are there any differences in the efficiency between offshore and coastal spawning areas? Is there any exchanges due to larval dispersal between the two seabass stocks currently assessed by ICES? Variability to respond these questions was added using different scenarios of dispersal success.

2. Material & methods

The larval drift model is a coupled physical–biological model. A particle-tracking module coupled to a 3D hydrodynamic model provide the transport of particles. This individually based approach then follows the individuals in space and time, and along their life history by including a bioenergetics module that simulates the growth and mortality of individuals forced by temperature and food availability. Figure 26 illustrates the modelling approach, which is further detailed below.

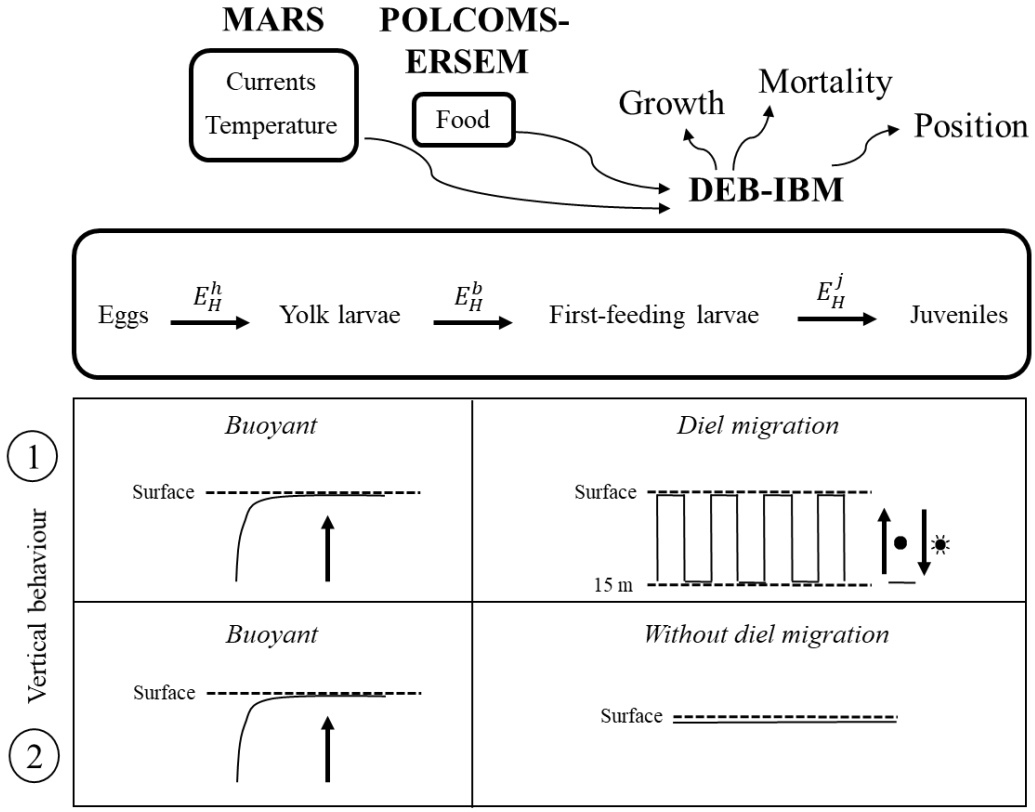

Figure 26. Scheme of the modelling approach: a hydrodynamic model (MARS) simulates the temperature and currents whereas a biogeochemical model (POLCOMS-ERSEM) provides the food availability; a bioenergetics model (DEB) controls the growth, the mortality and transitions between stages (i.e. depending on threshold of maturity $E_H^{h,b,j}$); two vertical behaviour were tested: in both cases, eggs and yolk larvae remain in the surface whereas first-feeding larvae and juveniles can either perform a diel migration or remain in the surface.

2.1. The hydrodynamic model

The 3D hydrodynamic model MARS (Model for Application at Regional Scale, Lazure & Dumas, 2008) was set up for the years 2008 to 2014 in the EC – BoB area. The geographic extent of the domain spans from 43.2°N to 52.3°N, and from 8°W to 5.2°E. The model grid has a 2.5 km resolution on the horizontal, with 40 sigma layers on the vertical. The surface elevation at the boundaries are obtain from a 2D model run from Portugal to Norway. Open boundary

conditions for temperature and salinity were derived from the Mercator Ocean models GLORYS2v2 (1992-2009) and PSY2v4 (2010-2014). Atmospheric forcing (i.e. wind fields, air temperature, atmospheric pressure, cloud cover and relative humidity) were extracted from the Météo-France models ARPEGE (2008-2011, resolution of 0.5° every six hours) and ARPEGE-HR (2012-2014, resolution of 0.1° every hours). Daily river discharges from rivers, including the Rhin, Seine, Loire, Dordogne, and Garonne, were included in the model. Every year a physical spin-up of four months initiated from a hydrological solution of the hydrodynamic model Mercator.

2.2. The particle-tracking module

A Lagrangian particle-tracking module (Huret *et al*., 2010) is coupled on-line with the hydrodynamic model. Particles are affected by advection in 3D and vertical diffusion. The latter is based on a random-walk computed from the eddy diffusivity coefficient following Visser (1997), and with a time-step of ~1s to avoid accumulation at the bottom or surface boundaries (Ross & Sharples, 2004).

2.3. The bioenergetics individual-based model (DEB-IBM)

2.3.1. The DEB model

We used a bioenergetics model to account for the effects of temperature and food availability on seabass growth. We coupled a Dynamic Energy Budget (Kooijman, 2010) model to the particle-tracking module. The parameters of the DEB model were calibrated in Dambrine *et al*. (2020) for wild European seabass in our study area. This model was validated to simulate seabass larval growth. Its equations and parameters can be found in Tables S7 & S8.

The DEB model was developed for seabass entire life cycle, here we focused on ELS. Transitions between stages occur at specific thresholds of maturity (i.e. the state variable E_H, which is the cumulative energy invested to become more complex, units: J). Mortality occurs when the costs of maintenance cannot be paid from reserve (E, units: J). Temperature affects all fluxes following the extended Arrhenius relationship (Kooijman, 2010). Conversion between food availability and ingestion is derived from the Holling type II functional response:

$$f = \frac{X}{X+X_k}$$

with X the food density ($mgC.m^{-3}$) and X_k the half-saturation constant.

The food density (X) was the sum of daily average micro- and meso-zooplankton extracted from the POLCOMS-ERSEM model (Holt *et al*., 2001; Butenschön *et al*., 2016) between 0 and 25m. The food availability was estimated by Dambrine *et al*. (2020) over the full lifecycle to be on average 0.833 for European seabass in our study area. Thus, to have a variable food availability over space and time, we had to estimate the half saturation constant (X_k) that relate X to *f*. We chose X_k so that *f* equals to 0.833 on average in winter between 2008 and 2014. The value of X_k was equal to 1.3.

2.3.2. Larval vertical behaviour

As illustrated in Figure 26, vertical migrations are stage dependent. The eggs and non-feeding larvae are considered positively buoyant (i.e. their density was set equal to the one of sea surface), remaining in the upper water column (Pickett & Pawson, 1994). Feeding larvae and juveniles (although generally simulations stopped before this stage) are supposed to perform diel vertical migrations (Schurmann *et al*., 1998) between 0 and 15m with a velocity of $1cm.s^{-1}$. This behaviour with vertical migration between day and night is recognised for larvae of some fish species (e.g. demersal fishes; Faillettaz, 2015 and pelagic ones; Stenevik *et al*., 2007). Without information in the literature about diel vertical migration of seabass larvae in the wild and as Jennings & Pawson (1992) showed that seabass larvae in the EC were mostly caught at 15 m depth during the day, we considered this behaviour as the most likely.

2.3.3. Settlement success

From Jennings & Pawson (1992), we defined the settlement success as following: a larva is supposed to settle if it still alive within a period of 90 days after spawning and reaches 1.2 cm, within 5 km from the coast. As soon as the four criteria are met, larva's coordinates are saved and represent its settlement location. If they cannot be met together, then the individual is considered lost for settlement. This definition of settlement success was subsequently considered as the "base-case scenario", while alternatives are detailed below.

2.4. Spawning areas and season

According to Dambrine *et al*. (2021), the spawning period was set between January and March in the BoB and between January and April in the EC, for the spawning areas displayed on Figure 27. For each month of the spawning period, the spawning locations were the 3*3 nautical miles squares that had been identified at least once, between 2008 and 2013, as spawning areas by Dambrine *et al*. (2021).

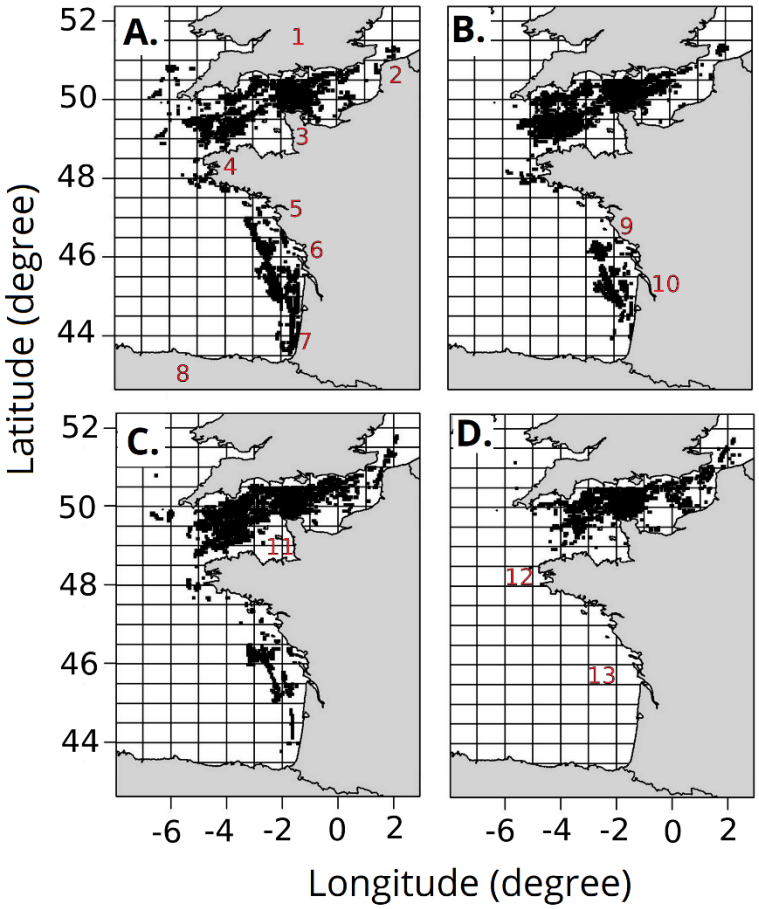

Figure 27. Location of the spawning areas for January (A), February (B), March (C) and April (D) from Dambrine et al. *(2021). ICES rectangles and the main locations used in the results are also provided. 1. United Kingdom (UK), 2. Pas de Calais, 3. Cotentin, 4. Britanny, 5. Loire Estuary, 6. Charente Estuary, 7. Landes, 8. Spain, 9. Sables d'Olonne, 10. Gironde Estuary, 11. Jersey/Guernesey, 12. Iroise Sea, 13. Rochebonne Plateau.*

Each week during the spawning season (i.e. 16 released dates), from each spawning locations, 15 particles were released at random depth (between 0 and 25 m). In total, each week, 27 510 particles were released in January, 26 280 in February, 27 180 in March and 14 850 in April.

2.5. Model experiments

Each particle was followed for 110 days and provided a unique trajectory. To characterise the spatio-temporal variability of seabass ELS dispersal, we tested different settlement scenarios by changing (i) the size to reach, (ii) the maximum drift time and (iii) the distance to the coast. Sensitivity was assessed with respect to the base-case scenario as follow: +/- 10 days (i.e. 80 and 100 days) and +/- 0.3 cm (i.e. 0.9 and 1.5 cm TL) and settlement at 20 km from the coast. We also evaluated the effect of the vertical behaviour (comparing the

dispersal of larvae with or without this process implemented). Combining all modalities of size, maximal drift time, distance to the coast and vertical behaviour, a set of 252 scenarios were obtained, as summarized in Table 13.

Table 13. Scenarios of settlement success run from 2008 to 2014. There were three modalities of size to reach and maximal drift time and two modalities of distance from the coast and vertical behaviour for a total of 252 simulations.

Size to reach (cm)	Maximal drift time (days)	Distance from the coast (km)	Vertical migration
0.9 / 1.2 / 1.5	80 / 90 / 100	5 / 20	Yes / No

2.6. Model output analysis

To synthetize and get more robust results, we used ICES statistical rectangles (Figure 27) instead of individuals' coordinates. To do so, initial and final coordinates of each particle were referenced to the coordinates of the centre of the ICES rectangle to which it belongs.

Constructing maps of the proportion of seabass settlement success per spawning areas (i.e. number of individuals from a spawning area that effectively settle divided by the total number of individuals from this spawning area) and of the number of settlers per nurseries (i.e. number of individuals settling in a nursery divided by the total number of individual born in the study area), we investigated model's sensitivity to the larval vertical behaviour.

We also estimated the settlement success' temporal variability and studied the efficiency's differences between coastal and offshore spawning areas. Significance in the results were tested using t-test.

As Beraud *et al*. (2018) showed the importance of temperature and wind in the settlement success of European seabass in the EC, we focused on two contrasted years to study the connectivity of ELS in our study area. We used years 2010 (i.e. cold winter with a negative North Atlantic Oscillation index) and 2014 (i.e. warm winter with a positive NAO index). We also tested the influence of spawning temperature in the connectivity pattern by removing the spawning areas with a temperature < 9°C (i.e. temperature under which seabass spawning might not happen according to Pickett & Pawson, 1994). The connectivity results were mapped using connectivity diagrams (e.g. Le Corre *et al*., 2020) with the base-case scenario. This representation allows summarizing (i) the main links between spawning and nursery grounds

predicted by the model in 2010 and 2014, (ii) the strength of those links, and (iii) the self-recruitment (i.e. proportion of settlers from an ICES rectangle that settle in it).

3. Results

3.1. Effect of the larval vertical behaviour

The contribution efficiency of spawning areas in supplying nurseries weakly depends on larval vertical behaviour (Figure 28). Indeed, the percentage of settlement remains the same for each spawning area, except for a small area in the WEC. The most efficient spawning areas are in the southern BoB, the southern Brittany and the WEC (percentage of settlement around 1%).

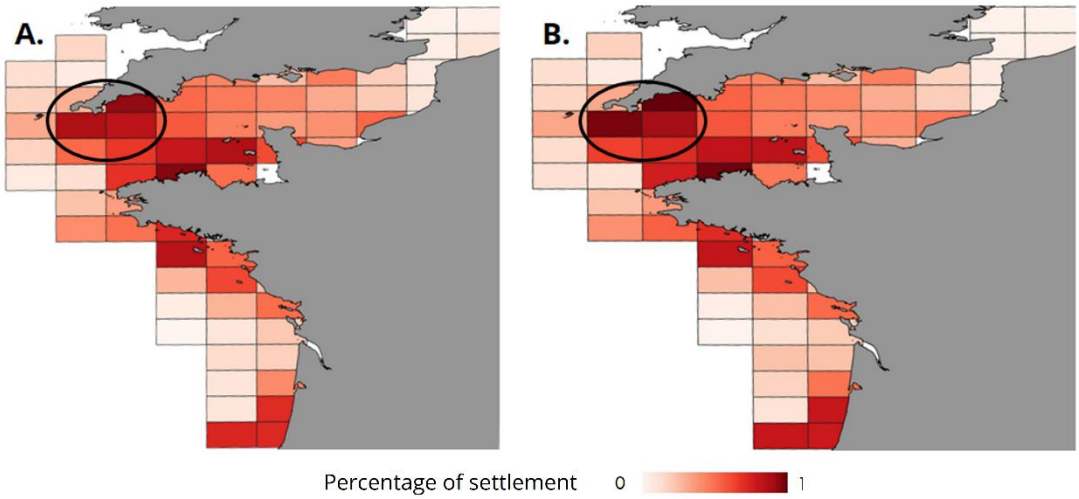

Figure 28. Percentage of larval settlement from seabass spawning areas at the scale of ICES rectangles for simulations with A) larvae performing diel vertical migration and B) larvae remaining at surface. The colour of each rectangle represents the number of individuals that effectively settled divided by the total number of individuals. The value is averaged over all simulations (Table 13). Ellipse represents the area in the EC for which the percentage differs slightly.

On the contrary, the larval vertical behaviour discriminates the nurseries based on their settlement success, yet only within the BoB (Figure 29). For example, with the diel vertical migration, nurseries in the south of Brittany, the Loire estuary and the north of Spain show better percentages of settlement (0.2-1% compared to 0.05-0.1%). On the contrary, some nurseries have lower settlement success: those off the coast of the Landes have their percentage decreased from 0.4-0.6% to 0.1-0.4% with addition of the diel vertical migration.

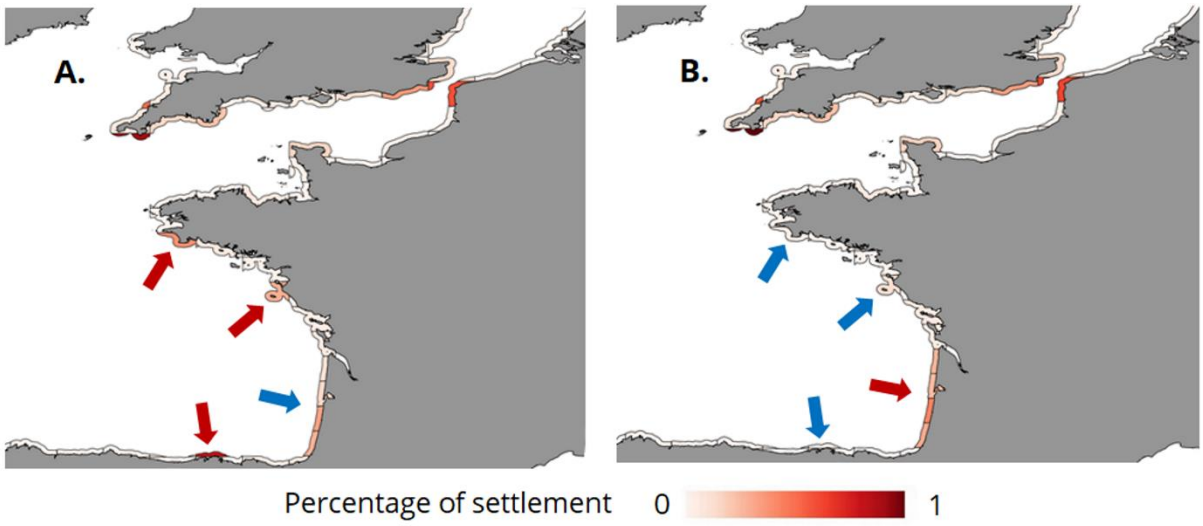

Figure 29. Percentage of larval settlement on seabass nurseries at the scale of ICES rectangles for A) larvae performing diel vertical migration and B) larvae remaining at surface. The colour of each rectangle represents the number of individuals that settle in a nursery divided by the total number of individual and weighted by the surface of the nursery in the ICES rectangle. The value is averaged over all simulations. Blue arrows represent nurseries with lower percentage of settlement whereas red one represent areas with better percentage of settlement.

3.2. Connectivity differences between two contrasted years

We only consider here the base-case scenario. On both years 2010 and 2014 (Figure 30), there is no connectivity between spawning areas in the EC and nurseries in the BoB. Spawning areas are linked to their closer nurseries (e.g. spawning areas in the south of the BoB are mostly linked to nurseries in this area, same for spawning areas with nurseries in the north of the BoB, the WEC and the EC).

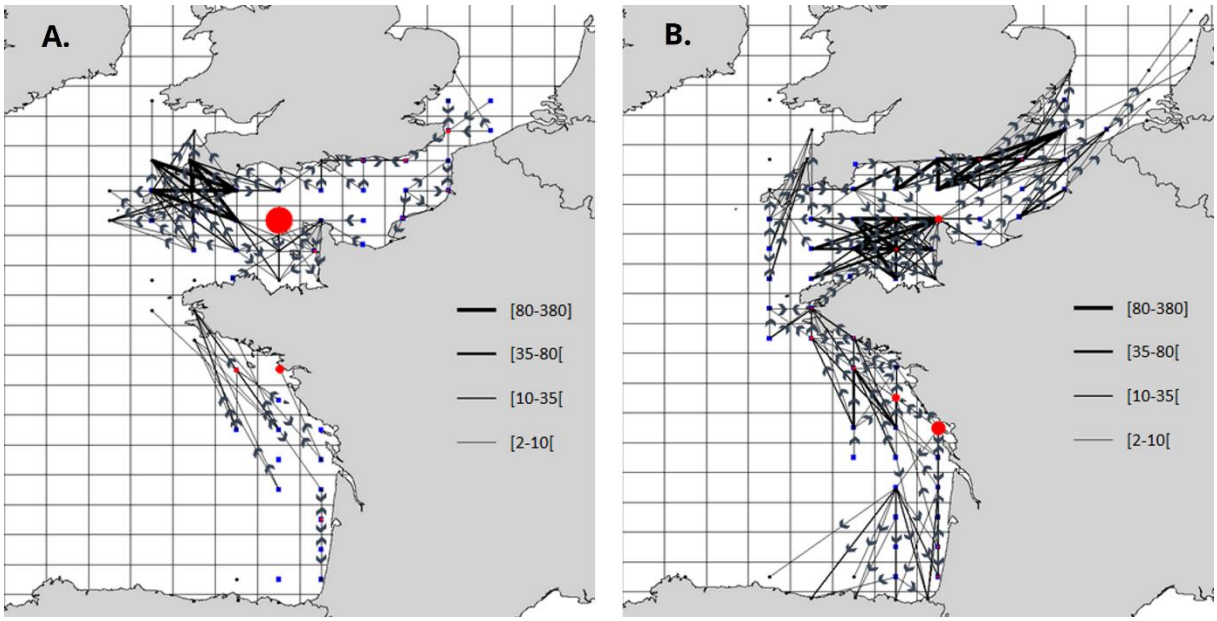

Figure 30. Diagrams of connectivity using the base-case scenario for years 2010 (A; cold winter with negative NAO index) and 2014 (B; warm winter with positive NAO index); blue squares represent the spawning areas; black circles represent the nurseries; black lines represent the links between a spawning area and a nursery, their size are proportional to the number of individuals that perform that link; red circles represent self-recruitment, their size are proportional to the number of individuals that was born in an ICES rectangle and settle in it.

The connectivity between spawning and nursery grounds varies between cold winter with negative NAO index (Figure 30A) and warm winter with positive NAO index (Figure 30B). First, the settlement success is lower during a cold winter (i.e. less links and less recruits on each link). A warm winter leads to more connectivity between the south and the north of the BoB. In south of the BoB, a cold winter favours connectivity along the cost of the Landes (7 on Figure 27) whereas connectivity from more offshore spawning areas is not represented (contrary to a warm winter; Figure 30B). In the north of the BoB, a cold winter results in lower connectivity and particularly no connectivity in the west of the Britanny (4 on Figure 27) and restricted connectivity between the BoB and the EC to the Iroise Sea (contrary to a warm year where there is connectivity between spawning areas in the BoB until nurseries in the north of the Britanny; Figure 30B). In the WEC, the main difference is that during a cold winter with negative NAO index, the connectivity is concentrated in the west of the UK (1 on Figure 27) whereas during a warm winter with positive NAO index, it is concentrated in the west of the Cotentin Peninsula (3 on Figure 27). In the EEC, a cold winter displays few links between spawning areas and nurseries. On the contrary, in 2014, spawning areas in the EEC are numerous and connected to nurseries up to the North Sea.

Removing spawning areas with a temperature below 9°C does not change the connectivity for the year 2014 and almost not the one in the BoB for the year 2010. On the contrary, it changes the connectivity in the EC for a cold year, particularly in the EEC where the connectivity disappears.

3.3. Intra- and inter-annual variability of the settlement success

The pattern of the inter-annual variability of the settlement success is the same in the BoB and the EC, excluding for year 2012, which presents a median of 0.30% in the BoB and of 0.19% in the EC (Figure 31).

Years 2008 and 2014 exhibit the best percentages of settlement success (median of 0.30 to 0.52%) while 2010 and 2013 have the lower ones (median of 0.04 to 0.12%). In both areas, outliers correspond to the scenarios with a size to reach of 0.9 cm before 90 or 100 days at 20 km from the coast.

The settlement success seems to be higher in the EC than in the BoB for each year. It was confirmed with a t-test that shows significant differences in the settlement success for each year between the two areas.

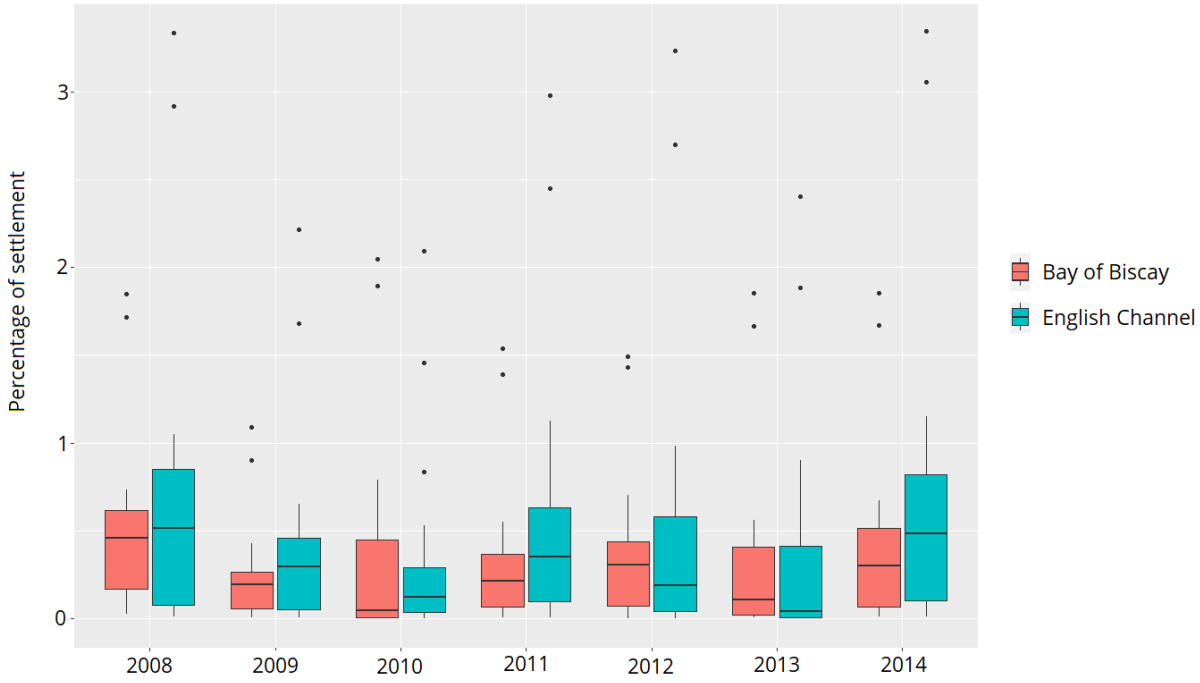

Figure 31. Average percentage of settlement (i.e. proportion of larvae born during one year that effectively settle) between all scenarios with larvae performing diel vertical migration for each year between 2008 and 2014 in the BoB and the EC.

It seems that the later the spawning occurs, the better the settlement in both areas (Figure 32). Particularly, in the EC, individuals born in January and February display very low percentages of settlement (median close to 0%).

This trend is not significant in the BoB but significant differences exist in the EC for the settlement success of individuals born in March or April, January or March, January or April and February or April. The outliers represent the scenarios with a size to reach of 0.9 cm before 80, 90 or 100 days at 20 km from the coast.

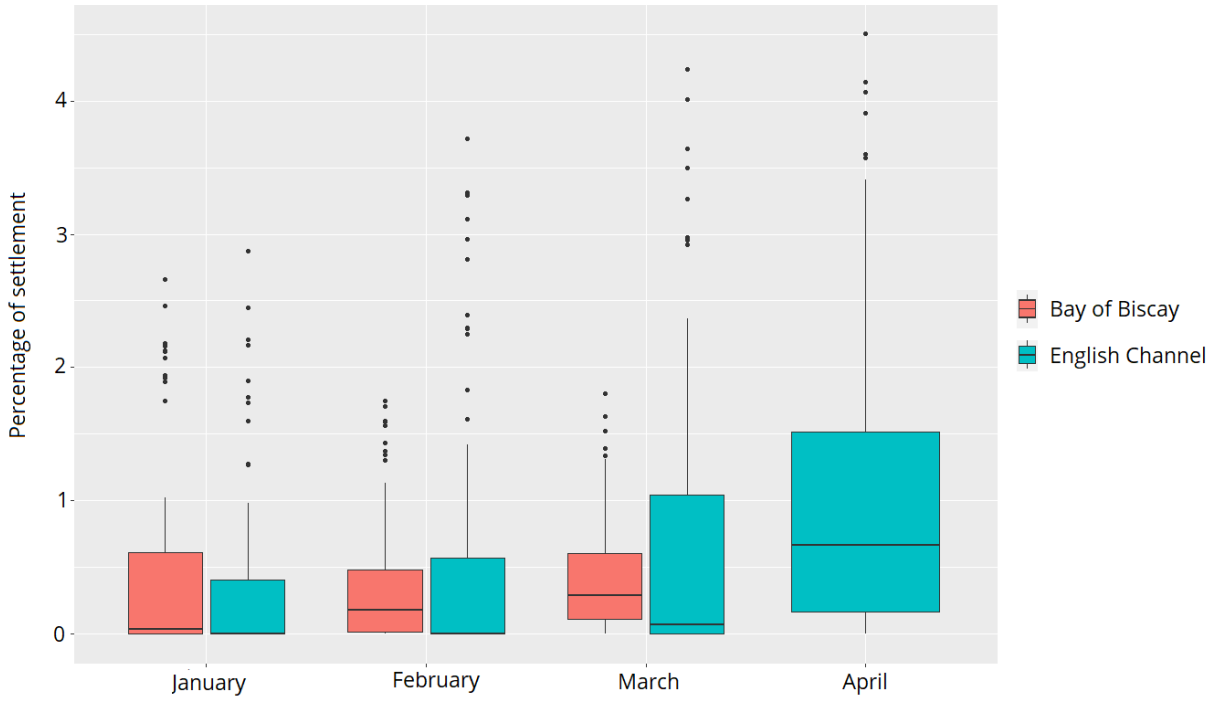

Figure 32. Average percentage of settlement (i.e. proportion of larvae born in a month that effectively settle) between all scenarios with larvae performing diel vertical migration for each month of the spawning season in the BoB (between January and March) and the EC (between January and April).

3.4. Efficiency's differences between coastal and offshore spawning areas

In both areas, the percentage of settlement decreases importantly with the increase of the size to reach (Figure 33). In the EC, for a size at settlement of 0.9 cm, offshore spawning areas show better percentage (e.g. for the scenario with a maximal drift duration of 100 days at a distance criterion from the coast of 20 km, the average percentage for coastal spawning areas is 2.4 and for offshore one is 3). When the size increases, coastal areas seem to be better (e.g. for the base-case scenario, the average settlement success of coastal spawning areas is 0.08% and for offshore one 0.05%). In the BoB, coastal spawning areas have always better percentages. Particularly for the scenarios with a size at settlement of 0.9 cm, coastal spawning areas can reach high settlement success (i.e. > 2% whereas offshore ones do not exceed 1.2%). When the size at settlement increases, percentages tend converge (e.g. for the base-case scenario, coastal spawning areas have an average percentage of 0.08 and offshore one of 0.05).

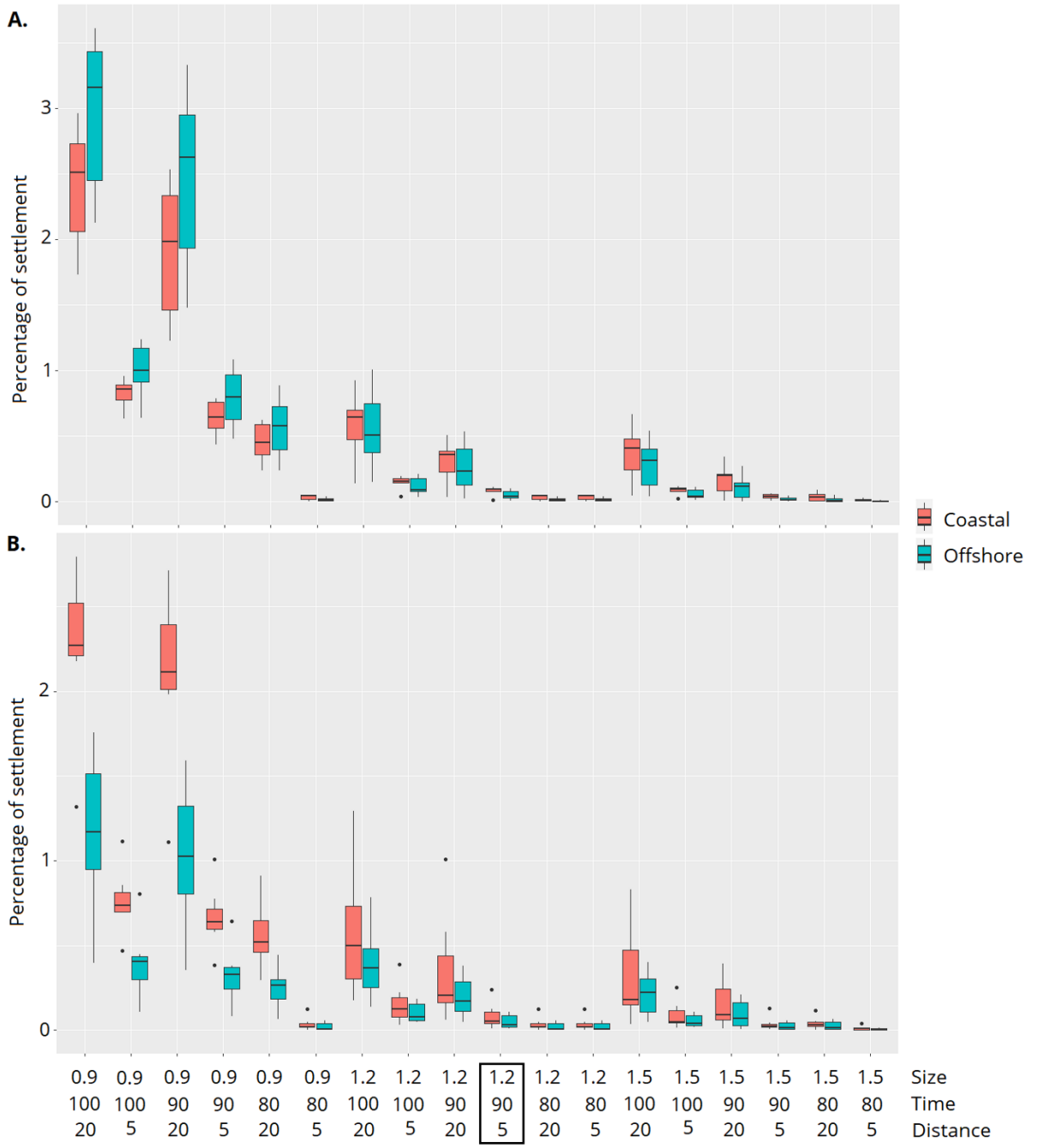

Figure 33. Percentage of settlement (i.e. proportion of larvae from a spawning area that effectively settle) for all scenarios with larvae performing diel vertical migration in the EC (A) and in the BoB (B) for coastal and offshore spawning areas. The rectangle indicates the base-case scenario.

4. Discussion

4.1. Validity of the model

Although the percentages of settlement are low under our simulations (i.e. mostly <1%), these values are not surprising for a marine species. Indeed, the pelagic phase is one of the most sensitive phase of fish lifecycle (e.g. Juanes, 2007). Besides, Le Pape & Bonhommeau (2015) estimated the survival rate of most marine species to one juvenile for 1000 eggs.

Like Beraud *et al*. (2018), that developed a larval drift model for European seabass in the EC, we showed that the vertical behaviour slightly affects the percentages of settlement in this area. Moreover, the relative importance of each spawning areas and nurseries highlighted in this study are in agreement with their previous results.

4.2. European seabass spawning areas and nurseries

Spawning areas with the best percentages of settlement are located in the WEC, the south of Britanny and the south of the BoB. Except the WEC, these are not the spawning areas identified as "recurring" by Dambrine *et al*. (2021). Indeed, these authors showed that the Cotentin Peninsula, the WEC and the plateau of Rochebonne were recurring spawning areas between years and during the whole spawning season. In addition, we showed that offshore spawning areas demonstrate lower percentages of settlement success although seabass favour an offshore migration for spawning (Pawson *et al*., 2007, de Pontual *et al*., 2019). It seems that seabass spawning areas of importance are not the one with the best settlement success. According to Dambrine *et al*. (2021), their distribution can neither be explained by the environmental variables they tested thus, the reproductive strategy of seabass is very intriguing. One hypothesis is that seabass migrate to target areas where eggs and larvae can be spread to distant nurseries. Indeed, with our model, it seems that the recurring spawning areas identified by Dambrine *et al*. (2021) correspond to spawning areas that spread recruits in the highest number of nurseries. Thus, the Rochebonne plateau supplies nurseries from the Gironde estuary to the Iroise Sea. The Western EC supplies nurseries of the northwest Brittany and the southwest of the UK and particularly the latter. The spawning areas of the north of the Cotentin peninsula supply local nurseries as well as the southeast of the UK coast.

In agreement with Beraud *et al*. (2018), we confirmed that in the EC most of the important nurseries are in the South of the UK. Nurseries along the French coast are scarce. In the BoB, French nurseries are larger, particularly in the south.

4.3. Temporal variability of the settlement

A significant seasonality in the settlement success has been highlighted during the spawning season in the EC. It is in agreement with Thompson & Harrop (1987), who showed an eastward gradient in the occurrence of seabass spawning areas in this area. Looking at the efficiency of spawning areas in the EC for each month of the spawning season (data not shown), this gradient is confirmed. Contrary to us, Thompson & Harrop (1987) considered the spawning season of seabass starting in February, which makes sense as with our model, individuals born in January have only limited chances to settle. Indeed, individuals born at the beginning of the year combine low temperatures and low level of food during their whole drift time, which does not favour their growth and decrease their potential to reach the imposed size at settlement.

We also highlighted inter-annual variability in the settlement success. According to ICES (2012), the seabass recruitment inter-annual variability is highly correlated to temperature. Our study confirms this assumption. Indeed, years showing the best settlement success are 2008 and 2014, which are the warmest winters in the EC and the BoB, respectively. On the contrary, year 2010 seems to be a bad year for seabass settlement success and corresponds to the coldest winter in the EC and the second coldest in the BoB. On the contrary, year 2010 seems to be a bad year for seabass settlement success with our model and corresponds to the coldest winter in the EC and the second coldest in the BoB. Beraud *et al*. (2018) also highlighted the importance of the wind direction in the settlement success. Looking at the North Atlantic Oscillation (NAO) index, we observed that winters of 2008, 2012 and 2014 are characterised by positive NAO index. This suppose a mild winter and an important north-eastward oceanic circulation that favour the settlement of larvae. On the contrary, the winter of 2010 and 2013 display negative NAO, which is characterised by cold winters and a weak eastward oceanic circulation that disfavour the settlement of ELS. As the inter-annual trend is the same between the EC and the BoB, it seems that the variability is mostly driven by these two large-scale forcing factors.

4.4. Connectivity between spawning and nursery areas

Generally, spawning areas are connected to their closest nurseries. Maybe currents in our study area favour retention. Moreover, the longer the migration, the greater the risk to be spread offshore. Whatever the year tested, few links exist between the WEC and the EEC. This is in agreement with the work of Robinet *et al*. (2020) who highlighted the Cotentin peninsula as a local barrier to gene flow. Connectivity between the BoB and the EC is scarce. Currents in our study area stop individuals from the EC to settle in the BoB. On the contrary, only high north-eastern currents (i.e. positive NAO) favour connectivity from the BoB to the north of Britanny in the WEC.

Important couples of spawning area and nursery could be the one that are highlighted during a cold and a warm winter. Thus, the cost of the Landes, the Rochebonne Plateau with the Iroise Sea, the WEC with the south of the UK or the Cotentin Peninsula and the EEC with the south-east of the UK or the Pas de Calais seem to be important.

4.5. Implications for seabass management

The most important nurseries of European seabass in the EC are in the South of the UK. As this country protects its estuaries, we could consider that main nurseries of the EC are well protected. In France, the north of the Cotentin peninsula and the Pas de Calais seem to be important nurseries that could then deserve particular attention.

Fishery ban is applied in February and March to protect the spawning areas of the EC (ICES, 2019). From our results, the timing of this ban could be extended until the end of April as eggs spawned at this time show good settlement success. Such management measures to protect spawning areas are not applied in the BoB except on the Rochebonne plateau, where pelagic pair trawlers cannot fish one every other winter. This measure could be applied every year from January to the end of March because this spawning area is recurring (Dambrine *et al*., 2021) and, according to our model, disseminate many recruits.

Moreover, this spawning area seems to be connected with areas located in the Northern stock, particularly the Iroise Sea. Even if the connectivity between the two stocks seems to be limited due to ELS dispersal, it needs to be investigated because some adults also migrate between the two stocks for reproduction (de Pontual *et al*., 2019). Thus, it raised questions about whether or not these stocks corresponded to two distinct populations. Studying genetic

connectivity could help understanding seabass' population(s) structure and improve the stock delineation for a better species management. Recent studies (Coscia & Mariani, 2011; Fritsch *et al*., 2007; Souche *et al*., 2015) highlighted non-significant genetic structure in the northern Atlantic, whereas Robinet *et al*. (2020) evidenced two barriers to gene flow (i.e. Galicia and Cotentin). These results suggest the need for a redefinition of the seabass stocks in the northern Atlantic in order to obtain the most precise stock assessment.

4.6. Further developments to improve the model

To validate their model and chose the best scenario, Beraud *et al*. (2018) used data of age 0 European seabass sampled in UK nurseries. Unfortunately, these data are not available in France, this would benefit to evaluate models' prediction and to better characterise the nurseries for this species.

Moreover, these authors choose a different vertical behaviour for feeding larvae than us, as it changes the settlement success in nurseries of the BoB, it should be characterised for seabass in the wild to improve our model. A scientific survey in winter dedicated to this species could be a good opportunity to investigate it together with bringing information on seabass eggs development, spawning period and locations of spawning areas.

Indeed, the reproduction of seabass is still few documented in the wild although we saw that removing spawning areas with a temperature below 9°C could significantly change the connectivity in the EEC during a cold winter. Thus, it would be important to characterise the thermal spawning window for seabass to improve the model. Thus, we could improve the timing of the spawning period in our model by, for example, using a peak of egg production depending on the water temperature to centred the spawning period (e.g. Lacroix *et al*., 2013).

Conclusion

We developed a larval drift model for European seabass in the BoB – EC area. It gives a first picture of the connectivity of seabass ELS in this area. Using seven years, we showed that the settlement success was mostly <1%, variable between months and years, better from coastal spawning areas and increased during mild winters. Our model focuses on seabass ELS, it could be combine to recent developments on seabass juveniles (Alp and Le Pichon, 2020) and adults (Walker *et al*., 2020) modelling to construct an IBM for seabass full lifecycle. This could be a powerful tool to test management strategies and improve seabass assessment.

Acknowledgements

This study was part of the Barfray project funded by the European Maritime and Fisheries Fund (EMFF- OSIRIS N°: PFEA 400017DM0720006), France Filière Pêche (FFP), the French Ministry of Agriculture and Food (MAF) and Ifremer. The findings and conclusions of the present paper are those of the authors.

Conflict of Interest Statement

The authors have no conflict of interest to declare.

Author Contribution Statement

CD, MW, MH and HdP conceived the research idea; CD ran data analyses and wrote the manuscript; MW, MH and HdP participated in discussions of the results and critically reviewed the manuscript.

Data Availability Statement

Research data are not shared.

Supplementary material

Table S7. Equations of the 'abj' model including the dynamics of the four state variables, the metabolic acceleration, the six energy fluxes (J/d) and the shape correction function. Brackets [] represent quantities per unit of structural volume and braces {} represent quantities per unit of structural surface area.

Reserve dynamics	$\frac{dE}{dt} = \acute{p}_A - \acute{p}_C$
Structural length dynamics	$\frac{dL}{dt} = \frac{\acute{p}_G}{3L^2[E_G]}$
Maturity level dynamics	$\frac{dE_H}{dt} = \acute{p}_R$ if $E_H < E_H^p$ else $\frac{dE_H}{dt} = 0$
Reproductive buffer dynamics	$\frac{dE_R}{dt} = \acute{p}_R$ if $E_H \geq E_H^p$ else $\frac{dE_H}{dt} = 0$
Metabolic acceleration	if $E_H < E_H^h$ $s_M = 1$ if $E_H^h \leq E_H < E_H^j$ $s_M = L/L_b$ if $E_H \geq E_H^j$ $s_M = L_j/L_b$
Assimilation flux	$\acute{p}_A = s_M\{\acute{p}_{Am}\}fL^2$ if $E_H \geq E_H^b$ else $\acute{p}_A = 0$
Mobilisation flux	$\acute{p}_C = \frac{E}{L^3}\frac{s_M\acute{v}[E_G]L^2 + [\acute{p}_M]L^3}{[E_G] + \frac{\kappa E}{L^3}}$
Somatic maintenance flux	$\acute{p}_M = [\acute{p}_M]L^3$
Growth flux	$\acute{p}_G = \kappa\acute{p}_C - \acute{p}_M$
Maturity maintenance flux	$\acute{p}_J = \acute{k}_J E_H$
Maturation or reproduction flux	$\acute{p}_R = (1-\kappa)\acute{p}_C - \acute{p}_J$
Shape correction function	$\delta_M(L) = \delta_{Mj} + (\delta_{Mb} - \delta_{Mj})\frac{L_j - L}{L_j - L_b}$

Table S8. Values of the 15 DEB parameters calibrated by Dambrine et al. *(2020). All rates are expressed at T_1 = 293.15 K (=20°C). Brackets [] indicate quantities per unit of structural volume and braces {} indicate quantities per unit of structural surface area.*

Symbol	Value	Unit	Definition
κ	0.478	-	Allocation fraction to soma
$\{\acute{p}_{Am}\}$	109.7 / 581.4 *	$J.cm^{-2}.d^{-1}$	Specific maximum assimilation rate
$\acute{v}$	0.023 / 0.122 *	$cm.d^{-1}$	Energy conductance
$[E_G]$	6678	$J.cm^{-3}$	Specific costs for structure
$[\acute{p}_M]$	18	$J.cm^{-3}.d^{-1}$	Volume-specific somatic maintenance rate
T_A	7002	K	Arrhenius temperature
E_H^h	0.047	J	Maturity threshold at hatching
E_H^b	0.306	J	Maturity threshold at birth
E_H^j	45.7	J	Maturity threshold at metamorphosis
E_H^p	2507273	J	Maturity threshold at puberty
δ_{Mb}	0.058	-	Shape coefficient for eggs and non-feeding larvae
δ_{Mj}	0.16	-	Shape coefficient for juveniles and adults
T_{AL}	38563	K	Arrhenius temperature at low boundary
T_{AH}	89833	K	Arrhenius temperature at high boundary
f	0.833	-	Scaled functional response for wild data
T_L	283.15 (Claireaux & Lagardère, 1999)	K	Critical lower boundary of thermal tolerance range
T_H	301.15 (Claireaux & Lagardère, 1999)	K	Critical upper boundary of thermal tolerance range
κ_R	0.95 (Kooijman, 2010)	-	Fraction of reproduction energy fixed in eggs
$\acute{k}_j$	0.002 (Marques *et al*., 2018)	d^{-1}	Maturity maintenance rate coefficient
ρ_V	23431 (Lika *et al*., 2011)	$J.g^{-1}$	Energy density for structure
ρ_E	23431 (Lika *et al*., 2011)	$J.g^{-1}$	Energy density for reserve
d_v	1 (Kooijman, 2010)	$g.cm^{-3}$	Specific density of wet structure
d_{vd}	0.2 (Kooijman, 2010)	$g.cm^{-3}$	Specific density of dry structure

DISCUSSION

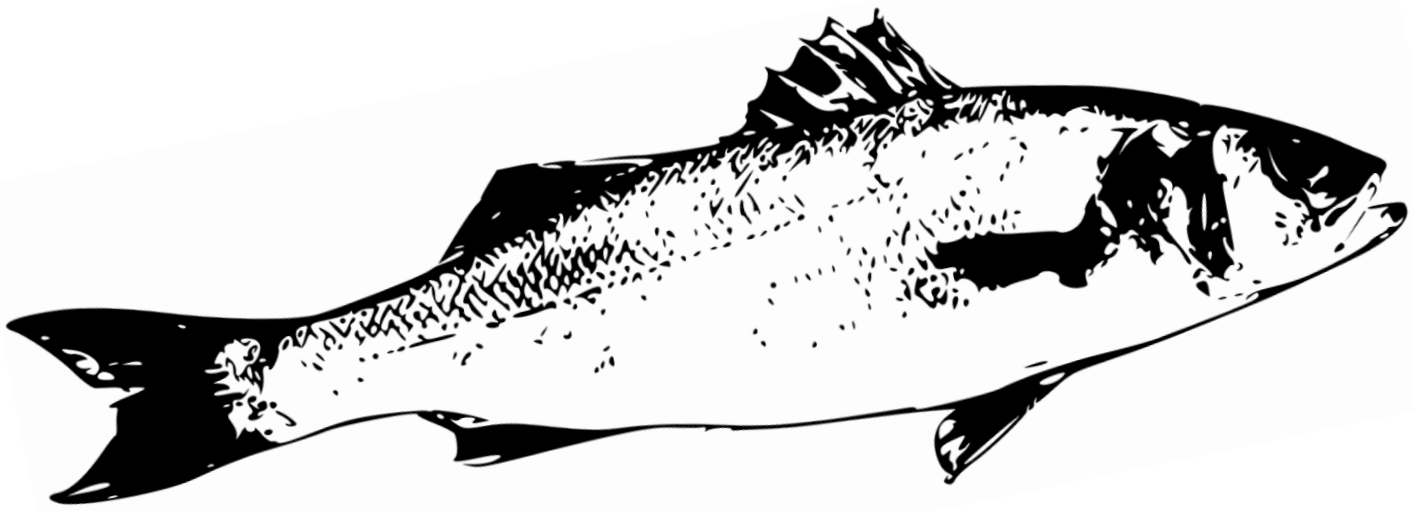

PRÉAMBULE

Les objectifs principaux de cette thèse étaient (i) l'étude de la connectivité entre les frayères et les nourriceries de bar européen et (ii) la caractérisation des principaux couples frayères – nourriceries contribuant le plus au maintien de la population en vue d'aider les gestionnaires dans leur choix de mesures de conservation et de gestion de l'espèce. Cette thèse fut également l'occasion d'étudier la connectivité liée aux premiers stades de vie entre les deux stocks de bar évalués annuellement par le CIEM (i.e. le stock Nord et le stock golfe de Gascogne). Le travail s'est organisé en trois grandes parties.

Tout d'abord, les frayères de bar, jusqu'alors connues de manière uniquement qualitative grâce aux connaissances des pêcheurs, ont été caractérisées quantitativement. À l'aide de données de pêche de bateaux géolocalisés (VMS), il a été possible de localiser, pour chaque mois de la période de reproduction, ainsi que pour chaque année étudiée (2008-2013), les frayères de bar sur la zone Manche – golfe de Gascogne. Une synthèse de ces informations a permis de faire ressortir les frayères les plus récurrentes, alors considérées comme les plus importantes pour l'espèce, et nécessitant le plus d'attention.

Ensuite, un modèle bioénergétique a été développé pour le bar atlantique sauvage. En couplant trois jeux de données sur des larves, des juvéniles et des adultes de souche atlantique élevés en aquaculture ou sauvages, un modèle suivant la théorie du Dynamic Energy Budget (DEB ; Kooijman, 2010) a été construit pour l'ensemble du cycle de vie de l'espèce. Sa validité sur les plus jeunes stades a été vérifiée grâce à un jeu de données indépendant de larves et juvéniles élevés en aquaculture à température variable. De plus, sa calibration a permis d'estimer la quantité de nourriture disponible pour les bars sur notre zone d'étude.

Enfin, un modèle de dérive larvaire simulant la croissance et la dispersion des jeunes stades de vie du bar européen a été développé en intégrant les résultats des deux premières parties. La caractérisation des frayères a permis des localisations réalistes pour les zones de ponte. Le modèle bioénergétique a quant à lui permis l'obtention de croissances et mortalités différentielles en fonction des conditions environnementales (i.e. température et nourriture) rencontrées par les individus durant leur dérive. L'estimation de la quantité de nourriture disponible pour le bar en Manche – golfe de Gascogne dans la deuxième partie a permis l'utilisation du zooplancton, issu d'un modèle biogéochimique, comme source de nourriture

pour les larves dans le modèle. Ainsi, la variation spatiale et temporelle de la ressource en nourriture a pu être prise en compte et induire des croissances et mortalités plus réalistes. En simulant, via ce modèle, la dispersion des jeunes stades de bar pour plusieurs années, dont certaines contrastées d'un point de vue thermique, et en multipliant les scenarii de dérive (i.e. en multipliant les zones de frayères et les dates de ponte, en étudiant 7 années dont certaines contrastées thermiquement, en testant divers scenarii de succès de colonisation des nourriceries), les frayères et nourriceries potentielles d'importance du bar européen ont pu être caractérisées. Par « zones potentielles d'importance », on entend des frayères dispersant de nombreuses larves qui colonisent effectivement des nourriceries, et des nourriceries qui accueillent de nombreuses larves, quel que soit le scenario envisagé. La connectivité entre ces habitats essentiels a ainsi pu être étudiée tout comme celle entre le stock golfe de Gascogne et le stock Nord. Ces précieuses informations, permettant de mieux appréhender le processus complexe de dérive, pourront ensuite être reprises pour guider les mesures de gestion du bar au niveau européen.

Dans cette partie, je reviendrai sur les connaissances acquises durant cette thèse sur les jeunes stades du bar européen ainsi que sur les habitats de ponte et de croissance des juvéniles. Je reviendrai également sur les objectifs et limites qui ont guidé ces travaux. Je terminerai avec une synthèse des implications de ces travaux en matière de gestion ainsi que par des perspectives pour approfondir ce travail et encore améliorer les connaissances sur la connectivité entre les frayères et les nourriceries de cette espèce.

1. Synthèse des connaissances acquises durant cette thèse

1.1. Adaptation du bar européen à une reproduction hivernale

Le bar est reconnu pour se reproduire en hiver (e.g. Fristch et al., 2007 ; Jennings & Pawson, 2007), l'analyse géostatistique des données de pêche a confirmé cette connaissance en affichant des seuils d'agrégation plus forts en hiver (chapitre 1). Une telle période pour se reproduire suppose des jeunes stades assez résistants puisque les conditions environnementales sont plus difficiles en hiver (faibles température et disponibilité en nourriture). Nous avons pu montrer que les jeunes stades de bar affichaient justement une grande résistance aux températures froides et à la privation de nourriture (chapitre 2).

Warlen & Burke (1990) expliquent que la reproduction hivernale est un avantage pour la dispersion des larves puisqu'elles vont rencontrer moins de prédateurs et de compétiteurs pour la nourriture à cette période et qu'une fois arrivées sur nourricerie au printemps, les températures augmentant, elles pourront grandir vite. De plus, au printemps, le zooplancton est abondant (Pingree & Garcia-Soto, 2014) assurant également une bonne croissance des larves. Nous avons pu montrer que cette disponibilité en nourriture sur nourricerie était essentielle pour la survie des jeunes stades de bar. En effet, au chapitre 2, il est apparu que les individus ayant rencontré des conditions de nourriture faibles pendant leurs premiers mois de vie étaient ensuite plus sensibles au jeûne. Il semblerait alors que le timing de reproduction du bar soit un compromis entre (i) une dérive à faible température limitant les besoins énergétiques, le nombre de prédateurs et de compétiteurs, (ii) l'accès à un minimum de nourriture durant la dérive pour assurer la survie et, (iii) une arrivée sur nourricerie permettant un développement à température et nourriture croissantes.

La reproduction en hiver suppose aussi l'exposition à des tempêtes qui sont nombreuses à cette période. Checkley *et al*. (1988) ont évalué leurs effets sur la reproduction et la dérive d'un poisson pélagique et suggéré une évolution pour venir se reproduire en hiver près des courants chauds (e.g. Gulf Stream) permettant un développement rapide et une dérive vers la côte des œufs et larves. Au chapitre 3, nous avons pu montrer que ces courant vers la côte (dans notre cas : vents d'ouest et circulation vers le nord) favorisaient en effet un meilleur succès de dérive. L'explication suggérée par ces auteurs peut donc potentiellement s'appliquer à notre cas d'étude.

1.2. Des frayères favorisant la colonisation de nombreuses nourriceries

Comme mentionné plus haut, Checkley *et al*. (1988) parlent « d'évolution », suggérant un processus mécaniste pour la fréquentation des frayères. Au chapitre 1, il a été difficile de trouver des variables environnementales expliquant la distribution des frayères du bar européen. Une explication possible serait justement un processus plus complexe tel que l'apprentissage (e.g. chez la morue : Rose *et al*., 1993) ou le homing (e.g. chez la plie : Hunter *et al*., 2003).

De tels processus expliqueraient également la persistance de la distribution spatiale des frayères identifiées dans ce même chapitre. Ainsi, trois zones de frayères sont apparues comme particulièrement intéressantes puisqu'elles ont été identifiées comme récurrentes entre années et persistantes durant toute la saison de reproduction : le plateau de Rochebonne dans le golfe de Gascogne, la Manche Ouest ainsi que le nord du Cotentin qui sépare la Manche Ouest de la Manche Est. Ces trois zones sont celles qui sont ressorties au chapitre 3 comme étant des frayères qui permettent la colonisation de nombreuses nourriceries, parfois même très éloignées. La stratégie reproductive du bar pourrait alors reposer sur la fréquentation de zones engendrant de bons succès de dérive et surtout, une colonisation de nombreuses nourriceries.

Au chapitre 1, un gradient temporel du sud du golfe de Gascogne jusqu'à la Manche Est a également pu être mis en évidence dans l'occurrence des frayères, la saison de reproduction du bar commençant plus tôt aux basses latitudes et s'y terminant également plus tôt. Ce gradient s'est également retrouvé dans le succès des dérives avec des mois de janvier et février très peu favorables au succès des dérives en Manche. Ainsi, l'analyse des données de pêcherie au chapitre 1 a peut-être mis en évidence des pré-agrégations de reproduction en Manche en janvier. La saison de reproduction du bar ne commençant alors qu'en février dans cette zone, comme considéré par Thompson & Harrop (1987).

1.3. La connectivité frayères – nourriceries sur notre zone d'étude

Il a pu être montré au chapitre 3 que les hivers doux favorisaient la colonisation des nourriceries. Les conditions environnementales moyennes de température et de nourriture engendrant le succès de la dérive via notre scenario de base sont 13.6 ± 0.6°C et 59 ± 2.7 $mgCm^{-3}$.

Les larves nées au sud du golfe de Gascogne colonisent principalement des nourriceries situées au sud tandis que celles nées au nord du golfe, des nourriceries au nord. En Manche, la

connectivité se fait principalement vers le nord-est, rarement vers l'ouest, les nourriceries du sud de l'Angleterre semblant être plus importantes que les françaises.

Les frayères de Manche Ouest alimentent particulièrement les nourriceries au sud-ouest de l'Angleterre, le nord Cotentin et les nourriceries du sud-est de l'Angleterre. Le plateau de Rochebonne alimente celles des Sables d'Olonne et de la mer d'Iroise.

Ainsi, une connectivité entre le stock « golfe de Gascogne » et le stock « Nord » a pu être mise en évidence. Il semble malgré tout que cette connectivité soit relativement limitée puisque la fréquence de cette connexion n'excède pas 4 ans sur les 7 années testées. Malgré tout, ces liens semblent pouvoir transporter de nombreuses larves puisque la connectivité entre le plateau de Rochebonne et la mer d'Iroise possède un des liens les plus fort du golfe de Gascogne avec une occurrence moyenne d'environ 40 larves.

2. Une tentative d'être le plus réaliste possible mais des améliorations possibles

2.1. Caractérisation des frayères du bar européen

Faute d'autres données disponibles, la caractérisation des frayères s'est appuyée sur des données de pêche et l'utilisation de telles données a inévitablement induit des biais dans la caractérisation des frayères et donc dans les conclusions que nous avons pu tirer de cette analyse. Des frayères ont pu être identifiées comme récurrentes simplement parce qu'elles sont fréquentées régulièrement par les pêcheurs qui savent que ces zones induisent de bons rendements. Au contraire, certaines frayères importantes ont pu ne pas être détectées ; soit parce que les bateaux qui y pêchent ne sont pas soumis à la VMS (car < à 12 m), soit parce que l'efficacité des engins qui les fréquentent est trop faible par rapport à celle des chalutiers pélagiques, soit parce que ces frayères se trouvent dans des zones où la pêche est interdite et ou bien des zones où les pêcheurs ne vont pas. On peut par exemple s'interroger sur le cas des frayères côtières qui, d'après les simulations de dérive larvaire, engendrent de meilleurs succès de colonisation des nourriceries mais qui n'ont pas été identifiées comme importantes à partir des données de pêche. Il serait pourtant intéressant de savoir dans quelle mesure elles sont fréquentées par rapport aux frayères du large afin de mieux appréhender la stratégie de reproduction de l'espèce. À dire d'expert, il semblerait que beaucoup d'entre elles aient disparues.

La caractérisation de ces frayères a permis la définition de zones de ponte pour le modèle de dérive larvaire plus « réalistes » qu'une disposition uniforme des œufs sur l'ensemble de la zone d'étude, ou dans les zones où la température est supérieure à un isotherme (Beraud *et al*., 2018). Cependant le choix a été fait de travailler sur des frayères potentielles, une frayère étant considérée comme telle si elle a été identifiée, au chapitre 1, au moins une fois pour un mois donné.

2.2. Caractérisation de la période de reproduction du bar européen

Face à des données parfois contradictoires dans la littérature sur la période de reproduction du bar, nous avons souhaité profiter de l'analyse géostatistique des données de pêche pour caractériser la période de reproduction du bar (i.e. recherche de seuils plus hauts en hiver témoignant de leur agrégation) et obtenir une méthode cohérente pour le reste de notre étude.

Ces seuils plus hauts en hiver ont été détectés et ont montré un gradient du sud vers le nord dans la fin de la période de reproduction mais pas dans son début. La période de reproduction semblait commencer plus tôt en Manche que dans le golfe de Gascogne (i.e. dès décembre). Comme cela ne paraissait pas cohérent avec la littérature (e.g. Vinagre *et al*., 2009), nous avons éliminé le mois de décembre sur la base d'une étude ancienne de l'indice gonado-somatique du bar en Manche (Pawson & Pickett, 1996). Par ailleurs, les résultats de dérive laissent penser qu'une naissance au mois de janvier, voire février, ne serait pas non plus propice puisque les succès de dérive associés sont très faibles. La littérature témoigne de pré-agrégations de reproduction chez le bar (Vázquez & Muñoz-Cueto, 2014). Il semble qu'en Manche nous ayons pu les détecter en décembre et janvier à partir des données de pêcherie.

2.3. Croissance et mortalité naturelle via un modèle bioénergétique

Un modèle bioénergétique a été développé pour simuler la croissance et la mortalité naturelle selon les conditions environnementales rencontrées par chaque individu dans le modèle de dérive larvaire. Il a permis également de définir des scenarii de succès de dérive dépendant de la taille des individus.

Lors du développement de ce modèle DEB, une attention particulière a été donnée à sa validation et ce, principalement pour les premiers stades : (i) la durée des stades de vie a été confrontée à la littérature tout comme (ii) la durée de survie à la privation de nourriture et (iii) un jeu de données indépendant sur des larves et juvéniles élevés en milieu contrôlé, à température variable, a été utilisé pour valider le modèle.

De plus, via la calibration de ce modèle bioénergétique, il a été possible d'estimer la disponibilité en nourriture pour un individu moyen au cours de l'ensemble de son cycle de vie. Nous avons ensuite pu utiliser ce résultat afin d'utiliser, dans le modèle de dérive, la quantité de zooplancton comme source de nourriture. Ceci a permis la prise en compte de la variabilité spatiale et temporelle de cette ressource. Mais, on peut se demander si la disponibilité en nourriture estimée sur l'ensemble du cycle de vie est fidèle à celle réellement rencontrée par les jeunes stades. De plus, la quantité de zooplancton utilisée dans le modèle de dérive provient d'un modèle biogéochimique à large échelle et on peut également questionner la validité de cette variable sur notre zone d'étude. Enfin, il n'a pas été pris en compte la sélectivité des larves sur le plancton (e.g. Gatti *et al*., 2016 pour l'anchois) ce qui pourrait faire l'objet d'une amélioration si les données étaient disponibles.

2.4. Un IBM assurant le comportement des jeunes stades de bar européen

Un modèle individu-centré assure un comportement différent pour chaque stade de vie considéré. Malheureusement, le comportement des jeunes stades de bar est mal connu en milieu naturel. Nous avons considéré les œufs et les larves vitellines comme flottants, restant à la surface (Pickett & Pawson, 1994) mais la densité des œufs n'était pas connue et a été considérée comme égale à celle de l'eau de surface. Les larves après ouverture de la bouche et les juvéniles (quand ce stade était atteint), pouvaient effectuer soit une migration nycthémérale soit rester dans la couche de surface. Malgré leur intérêt révélé par Beraud *et al*. (2018), les migrations tidales n'ont pas été prises en compte car ce processus est mal maîtrisé.

Au chapitre 3, nous avons observé que le comportement vertical des larves pouvait changer le succès de colonisation de certaines nourriceries dans le golfe de Gascogne (mais pas en Manche, confirmant les observations de Beraud *et al*., 2018). Ainsi, il serait important d'étudier ce comportement en milieu naturel afin d'améliorer les prédictions du modèle. Nous avons choisi de considérer pour notre scenario de base un comportement nycthéméral pour les larves qui se nourrissent puisqu'une étude en milieu aquacole a montré une réaction des celles-ci à la lumière (Schurmann *et al*., 1998) et que ce comportement est reconnu chez de nombreuses espèces de poissons démersales et pélagiques (e.g. Faillettaz, 2015; Stenevik *et al*., 2007). Pourtant, un autre choix a été fait par Beraud *et al*. (2018) qui ont considéré les larves comme restant en surface aboutissant à une colonisation plus massive des nourriceries, en meilleure adéquation avec leurs données de terrain.

3. Implications et perspectives

3.1. Pour de futurs travaux

Subsistent encore de nombreuses inconnues concernant la biologie du bar en milieu naturel : sa période de reproduction ainsi que la localisation de ses frayères sont encore mal cernées, le développement des œufs ou encore le comportement des larves durant la dérive n'ont, quant à eux, pas encore été étudiés. Il serait intéressant de mettre en place une campagne scientifique, en hiver, pour cette espèce, afin de répondre à ces questions qui sont essentielles pour comprendre sa dynamique spatio-temporelle et développer des modèles adéquats. De plus, il serait possible d'améliorer la caractérisation des frayères initiée durant cette thèse en effaçant les biais inhérents aux données de pêche. Pour cela, il conviendrait de standardiser les CPUEs à l'aide de modèles linéaires généralisés (e.g. Carruthers *et al*., 2011).

Dernièrement, un modèle individu-centré a été développé par Walker *et al*. (2020) afin de tester des mesures de gestion pour le stock Nord du bar européen. C'est un outil puissant qui vient en appui à l'évaluation annuelle de la ressource. Les résultats issus d'une campagne dédiée pourraient venir améliorer ce modèle et il pourrait également être intéressant de coupler cette approche à la nôtre pour mieux tenir compte de la biologie des individus. En effet, nous nous sommes ici focalisés sur la connectivité liée à la dispersion des œufs et larves mais il serait possible de modéliser l'ensemble du cycle de vie du bar d'autant que nous avons estimé la quantité de nourriture disponible pour les adultes sur notre zone d'étude (i.e. donnée complexe à modéliser puisque les bars sont opportunistes et se nourrissent de toute proie accessible). Ces auteurs ont proposé un modèle conceptuel de migration des individus. Des approches quantitatives telles que celles développées par Woillez *et al*. (2016) pour géolocaliser les bars à partir de données de marques électroniques pourraient venir en appui afin d'améliorer ce modèle. Il reste que la colonisation des nourriceries par les larves telle que nous l'avons modélisée pourrait être améliorée. En effet, les migrations tidales semblent importantes (Beraud *et al*., 2018). De plus, Alp & Le Pichon (2020) ont pu montrer la nécessité de la nage active dans le maintien de la connectivité au sein des estuaires or ce processus de déplacement n'a pas été pris en compte dans notre travail. De plus, l'habitat « nourricerie » mériterait d'être mieux caractérisé pour cette espèce.

Actuellement, des campagnes d'échantillonnage de juvéniles dans les principaux estuaires français sont mis en place pour obtenir des indices d'abondance. Les estuaires sont reconnus comme des zones propices à la croissance des juvéniles car ils assurent une nourriture en

quantité et de qualité ainsi qu'un abri contre les prédateurs (e.g. Vinagre & Cabral, 2008). Mais notre modèle montre que d'autres biotopes pourraient être échantillonnés (e.g. lagunes des Landes) car les courants semblent y amener de nombreuses larves. Malheureusement, les juvéniles d'âge 0 ne sont pas échantillonnés lors de ces campagnes ce qui ne permet pas de valider de façon directe les résultats de notre modèle. Néanmoins, s'il était possible de caractériser certaines nourriceries de bar le long de la façade française, ainsi qu'en Angleterre, il serait possible d'améliorer le modèle de dérive. En effet, une dérive serait considérée comme un succès si une larve rejoignait une de ces nourriceries et non si elle atteignait simplement une certaine distance à la côte.

Il faut souligner que le temps imparti pour réaliser ce travail n'a pas permis d'explorer pleinement le modèle de dérive larvaire développé. Des informations autres que celles liées à la connectivité pourraient en être tirées et renseigner sur le processus de dérive. Par exemple, il serait possible d'étudier statistiquement l'influence des facteurs environnementaux et des scenarii sur le succès de dérive (e.g. Huret *et al.*, 2010 ; Lacroix *et al.*, 2013). Par ailleurs, une comparaison entre les frayères potentielles et réalisées pourrait être menée afin de mieux comprendre pourquoi une frayère est fréquentée une année donnée (e.g. obtient-elle de bons succès de dérive ?). Un clustering sur la matrice de connectivité moyenne (e.g. Crochelet *et al.*, 2016) pourrait également renseigner d'une autre manière sur les zones d'importance, etc. Enfin, cette thèse s'inscrit dans un projet plus large qui entreprend d'étudier tous les habitats essentiels du bar européen. Particulièrement, des analyses complémentaires pourront compléter les résultats de cette thèse : l'hypothèse d'un processus de homing est étudiée via une analyse micro-chimique des otolithes de bars marqués et une étude pilote de marquage conventionnel d'adultes sur frayère a été réalisée visant à caractériser et quantifier les mouvements de dispersion des adultes vers les zones d'alimentation estivaules.

3.2. Pour la gestion de l'espèce

Depuis le début de la gestion européenne du bar, il est reconnu que sa dynamique spatio-temporelle est mal connue, pouvant compliquer sa gestion (ICES, 2012). Ce travail complémente les informations acquises par des campagnes de marquage de bars adultes (Pawson *et al.*, 2007 ; de Pontual *et al.*, 2019) en vue de mieux comprendre les habitats fréquentés par cette espèce partiellement migratrice ainsi que leur connectivité.

Le marquage a mis en évidence une fidélité des bars adultes à leurs habitats (i.e. zones de frayère et d'alimentation), ce qui renforce davantage l'importance de leur protection pour

préserver cette espèce. Au cours de cette thèse, trois zones de frayères ont été identifiées comme récurrentes (i.e. la Manche Ouest, le nord du Cotentin ainsi que le plateau de Rochebonne) et pourraient, dès lors, mériter une attention particulière. En Manche, la pêche sur frayères est déjà interdite entre le 1er février et le 31 mars (ICES, 2019). D'après mes travaux, cette mesure pourrait s'étendre jusqu'au 30 avril puisque les bars semblent toujours en reproduction en avril dans cette zone (e.g. Thompson & Harrop, 1987 ; Fritsch, 2005) et que ce mois de ponte est celui qui engendre les meilleurs succès de colonisation des nourriceries. De plus, il semble qu'il soit possible de détecter, en Manche, à partir des données de pêcherie, les pré-agrégations de reproduction des bars (Vázquez & Muñoz-Cueto, 2014) (i.e. en décembre et potentiellement janvier). Cela sous-entend que les bars se regroupent durant ces mois et qu'ils y sont pêchés en abondance, avant leur reproduction. Ceci peut participer à la diminution du stock reproducteur observée en Manche cette dernière décennie (ICES, 2019). Finalement, il conviendrait peut-être d'étendre les mesures de protection des frayères dès la pré-agrégation de Décembre. Cette fermeture pourrait ne concerner que quelques zones choisies à la lumière des résultats issus du chapitre 2 (i.e. en Manche Ouest et à la pointe nord du Cotentin). Dans le golfe de Gascogne, la pêche sur frayère n'est pas réglementée sauf sur le plateau de Rochebonne où, un an sur deux, les chalutiers pélagiques en bœuf ne peuvent pas pêcher (il existe néanmoins certaines dérogations). Vu l'importance de cette frayère, ainsi que sa connectivité avec le stock nord, cette mesure pourrait être renforcée et s'appliquer tous les ans et à tous les engins.

Comme mentionné plus haut, une connectivité entre le stock du golfe de Gascogne et le stock nord a pu être montrée lors de ce travail avec des individus nés dans le golfe de Gascogne (principalement sur le plateau de Rochebonne) pouvant coloniser des nourriceries de Bretagne nord (principalement en mer d'Iroise). À l'inverse, lors de ces simulations, aucun œuf pondu en Manche n'a colonisé de nourriceries dans le golfe. Ces résultats sont cohérents avec les données de marquage (de Pontual *et al.*, 2019) qui montrent également une connectivité entre les deux stocks avec certains individus marqués en Manche venant se reproduire dans le golfe (chemin de l'adulte inverse de celui des larves). Particulièrement, ces connexions entre zones géographiques différentes font s'interroger sur la structuration de la (des) population(s) atlantique(s). En terme de gestion, cette question est fondamentale puisque les différents stocks sont gérés de manière complètement indépendante. Or, de mauvais alignements entre stocks et populations peuvent mener à l'effondrement de certaines populations (e.g. Hilborn *et al.*, 2003 ; Neat *et al.*, 2014) et à une érosion de la diversité génétique dommageable pour l'espèce.

Il est d'autant plus important de bien délimiter les stocks de bar ou d'au moins prendre en compte leurs échanges puisque cette espèce présente une biomasse féconde en baisse depuis 2010 dans les deux stocks (ICES, 2012). Baisse qui est particulièrement inquiétante dans le stock « nord » (ICES, 2018). Pour tenter de mieux appréhender la structuration génétique du bar en atlantique des études ont été menées (Coscia & Mariani, 2011; Fritsch *et al*., 2007; Souche *et al*., 2015) mais n'ont pas pu montrer de structure significative dans cette zone. Plus récemment, Robinet *et al*. (2020) ont montré qu'il existe, dans les populations atlantiques un gradient latitudinal d'ascendance méditerranéenne sur l'ensemble du génome, avec deux barrières géographiques empêchant l'homogénéisation de ce gradient : le Cap Finistère en Galice et la façade ouest du Cotentin. Ces auteurs suggèrent alors de revoir la définition des stocks actuellement gérés par le CIEM. Selon eux, le stock « Nord » comprend un ensemble relativement hétérogène incluant la mer du Nord, la mer d'Irlande, le canal de Bristol, la mer Celtique et la Manche à l'exception des populations de la Manche ouest au nord de la Bretagne appartenant au stock « golfe de Gascogne ». Le stock « golfe de Gascogne » s'étendrait au sud du Golfe de Gascogne, incluant les côtes françaises au sud de la Gironde et les côtes nord de la péninsule Ibérique. Notre étude semble cohérente avec ces résultats. En effet, la connexion golfe de Gascogne – Manche Ouest a bien pu être démontrée tout comme la connexion Manche Ouest – mer Celtique. De plus, peu de connexions ont été révélées entre la Manche Ouest et la Manche Est.

4. Conclusion

Cette thèse a permis la construction d'un outil basé sur l'état actuel des connaissances pour modéliser la dérive des jeunes stades de bar en Atlantique nord-est. En attente d'améliorations grâce à une connaissance plus approfondie de certains processus via, par exemple, une campagne scientifique dédiée à cette espèce, cette thèse a déjà apporté des réponses concernant les habitats potentiels fréquentés par les bars adultes durant leur période de reproduction ainsi que par les larves lors de la colonisation des nourriceries. Plus particulièrement, la connectivité entre ces habitats potentiels a pu être approchée, donnant des pistes afin d'améliorer la gestion de cette espèce à haute valeur économique.

RÉFÉRENCES

Alliot, E., Pastoureaud, A., & Thebault, H. (1983). Influence de la température et de la salinité sur la croissance et la composition corporelle d'alevins de Dicentrarchus labrax. *Aquaculture, 31*(2-4), 181-194. https://doi.org/10.1016/0044-8486(83)90312-5

Alp, M., & Le Pichon, C. (2020). Getting from Sea to Nurseries: Considering Tidal Dynamics of Juvenile Habitat Distribution and Connectivity in a Highly Modified Estuarine Riverscape. *Ecosystems*, 1-19.

Andrews, J. M., Gurney, W. S., Heath, M. R., Gallego, A., O'Brien, C. M., Darby, C., & Tyldesley, G. (2006). Modelling the spatial demography of Atlantic cod (Gadus morhua) on the European continental shelf. *Canadian Journal of Fisheries and Aquatic Sciences, 63*(5), 1027-1048. https://doi.org/10.1139/f06-006

Artetxe-Arrate, I., Fraile, I., Crook, D. A., Zudaire, I., Arrizabalaga, H., Greig, A., & Murua, H. (2019). Otolith microchemistry: a useful tool for investigating stock structure of yellowfin tuna (Thunnus albacares) in the Indian Ocean. *Marine and Freshwater Research, 70*(12), 1708-1721. https://doi.org/10.1071/MF19067

Asch, R. G., & Checkley Jr, D. M. (2013). Dynamic height: a key variable for identifying the spawning habitat of small pelagic fishes. *Deep Sea Research Part I: Oceanographic Research Papers, 71*, 79-91. https://doi.org/10.1016/j.dsr.2012.08.006

Augustine, S., Gagnaire, B., Floriani, M., Adam-Guillermin, C., Kooijman, S.A.L.M. (2011). Developmental energetics of zebrafish, Danio rerio. Comparative Biochemistry and Physiology Part A: Molecular & Integrative Physiology 159, 275–283. https://doi.org/10.1016/j.cbpa.2011.03.016

Bäck, T., Schwefel, H.-P. (1993). An overview of Evolutionary Algorithms for Parameter Optimization. Evol. Comput. 1, 1–23. https://doi.org/10.1162/evco.1993.1.1.1

Bakka, H., Rue, H., Fuglstad, G. A., Riebler, A., Bolin, D., Illian, J., & Lindgren, F. (2018). Spatial modeling with R-INLA: A review. *Wiley Interdisciplinary Reviews: Computational Statistics*, *10*(6), e1443. https://doi.org/10.1002/wics.1443

Balon, E. K. (1990). Epigenesis of an epigeneticist: the development of some alternative concepts on the early ontogeny and evolution of fishes. *Guelph Ichthyology Reviews*, *1*.

Barbut, L., Groot Crego, C., Delerue-Ricard, S., Vandamme, S., Volckaert, F. A., & Lacroix, G. (2019). How larval traits of six flatfish species impact connectivity. *Limnology and Oceanography*, *64*(3), 1150-1171. https://doi.org/10.1002/lno.11104

Barnabé, G., Boulineau-Coatanea, F., Rene, F. (1976). Chronologie de la morphogenese chez le loup ou bar Dicentrarchus labrax (L.) (Pisces, Serranidae) obtenu par reproduction artificielle. Aquaculture 8, 351–363. https://doi.org/10.1016/0044-8486(76)90117-4

Barnabé, G. (1990). Rearing bass and gilthead bream. In: Barnabé, G. (Ed.), Aquaculture. Ellis Horwood, New York, pp.647–686.

Bartolino, V., Maiorano, L., & Colloca, F. (2011). A frequency distribution approach to hotspot identification. *Population Ecology*, *53*(2), 351-359. https://doi.org/10.1007/s10144-010-0229-2

Beck, M. W., Heck, K. L., Able, K. W., Childers, D. L., Eggleston, D. B., Gillanders, B. M., ... & Orth, R. J. (2001). The identification, conservation, and management of estuarine and marine nurseries for fish and invertebrates: a better understanding of the habitats that serve as nurseries for marine species and the factors that create site-specific variability in nursery quality will improve conservation and management of these areas. *Bioscience*, *51*(8), 633-641. https://doi.org/10.1641/0006-3568(2001)051[0633:TICAMO]2.0.CO;2

Bellido, J. M., Brown, A. M., Valavanis, V. D., Giráldez, A., Pierce, G. J., Iglesias, M., & Palialexis, A. (2008). Identifying essential fish habitat for small pelagic species in Spanish Mediterranean waters. In *Essential Fish Habitat Mapping in the Mediterranean* (pp. 171-184). Springer, Dordrecht.

Beraud, C., van der Molen, J., Armstrong, M., Hunter, E., Fonseca, L., & Hyder, K. (2018). The influence of oceanographic conditions and larval behaviour on settlement success—the European sea bass Dicentrarchus labrax (L.). *ICES Journal of Marine Science*, *75*(2), 455-470. https://doi.org/10.1093/icesjms/fsx195

Bernal, M., Stratoudakis, Y., Coombs, S., Angelico, M. M., De Lanzós, A. L., Porteiro, C. & Valdés, L. (2007). Sardine spawning off the European Atlantic coast: characterization of and spatio-temporal variability in spawning habitat. *Progress in Oceanography*, *74*(2-3), 210-227. https://doi.org/10.1016/j.pocean.2007.04.018

Bertignac, M. (1987). *L'exploitation du bar (Dicentrarchus labrax) dans le Morbras (Bretagne Sud)*. Ecole Nationale Supérieure Agronomique, Laboratoire de biologie halieutique.

Bláquez, M., Zanuy, S., Carillo, M., & Piferrer, F. (1998). Effects of rearing temperature on sex differentiation in the European sea bass (Dicentrarchus labrax L.). *Journal of experimental Zoology*, *281*(3), 207-216. https://doi.org/10.1002/(SICI)1097-010X(19980615)281:3<207::AID-JEZ6>3.0.CO;2-R

Bonhommeau, S., Le Pape, O., Gascuel, D., Blanke, B., Tréguier, A. M., Grima, N., ... & Rivot, E. (2009). Estimates of the mortality and the duration of the trans-Atlantic migration of European eel Anguilla anguilla leptocephali using a particle tracking model. *Journal of fish biology*, *74*(9), 1891-1914. https://doi.org/10.1111/j.1095-8649.2009.02298.x

Bopp, L., Monfray, P., Aumont, O., Dufresne, J. L., Le Treut, H., Madec, G., ... & Orr, J. C. (2001). Potential impact of climate change on marine export production. *Global Biogeochemical Cycles*, *15*(1), 81-99. https://doi.org/10.1029/1999GB001256

Bopp, L., Resplandy, L., Orr, J. C., Doney, S. C., Dunne, J. P., Gehlen, M. & Tjiputra, J. (2013). Multiple stressors of ocean ecosystems in the 21st century: projections with CMIP5 models. *Biogeosciences, 10*, 6225-6245. doi:10.5194/bg-10-6225-2013.

Bosley, K. M., Goethel, D. R., Berger, A. M., Deroba, J. J., Fenske, K. H., Hanselman, D. H., ... & Schueller, A. M. (2019). Overcoming challenges of harvest quota allocation in spatially structured populations. *Fisheries Research*, *220*, 105344. https://doi.org/10.1016/j.fishres.2019.105344

Bright, C. (1999). Invasive species: pathogens of globalization. *Foreign Policy*, 50-64.

Brodie, S., Hobday, A. J., Smith, J. A., Everett, J. D., Taylor, M. D., Gray, C. A., & Suthers, I. M. (2015). Modelling the oceanic habitats of two pelagic species using recreational fisheries data. *Fisheries Oceanography*, *24*(5), 463-477. https://doi.org/10.1111/fog.12122

Butenschon, M., Clark, J. R., Aldridge, J. N., Allen, J. I., Artioli, Y., Blackford, J. C., ... & Lessin, G. (2016). ERSEM 15.06: a generic model for marine biogeochemistry and the

ecosystem dynamics of the lower trophic levels. *Geoscientific Model Development*, *9*(4), 1293-1339. http://dx.doi.org/10.5194/gmd-9-1293-2016

Cadrin, S. X., & Secor, D. H. (2009). Accounting for spatial population structure in stock assessment: past, present, and future. In *The future of fisheries science in North America* (pp. 405-426). Springer, Dordrecht.

Cadrin, S. X., Kerr, L. A., & Mariani, S. (Eds.). (2013). *Stock identification methods: applications in fishery science*. Academic Press.

Carruthers, T. R., Ahrens, R. N., McAllister, M. K., & Walters, C. J. (2011). Integrating imputation and standardization of catch rate data in the calculation of relative abundance indices. *Fisheries Research*, *109*(1), 157-167. https://doi.org/10.1016/j.fishres.2011.01.033

Carson, H. S., Cook, G. S., López-Duarte, P. C., & Levin, L. A. (2011). Evaluating the importance of demographic connectivity in a marine metapopulation. *Ecology*, *92*(10), 1972-1984. https://doi.org/10.1890/11-0488.1

Chambers, R. C., & Trippel, E. A. (Eds.). (2012). *Early life history and recruitment in fish populations* (Vol. 21). Springer Science & Business Media.

Champalbert, G. (1971). Variations nycthémérales du plancton superficiel. II. Espéces non caractéristique de l'hyponeuston et hyponeuston nocturne. *Journal of Experimental Marine Biology and Ecology*, *6*(1), 55-70. https://doi.org/10.1016/0022-0981(71)90048-7

Checkley, D. M., Raman, S., Maillet, G. L., & Mason, K. M. (1988). Winter storm effects on the spawning and larval drift of a pelagic fish. *Nature*, *335*(6188), 346-348.

Claireaux, G., & Lagardère, J. P. (1999). Influence of temperature, oxygen and salinity on the metabolism of the European sea bass. *Journal of Sea Research*, *42*(2), 157-168. https://doi.org/10.1016/S1385-1101(99)00019-2

Colloca, F., Bartolino, V., Lasinio, G. J., Maiorano, L., Sartor, P., & Ardizzone, G. (2009). Identifying fish nurseries using density and persistence measures. *Marine Ecology Progress Series*, *381*, 287-296. https://doi.org/10.3354/meps07942

Compaire, J. C., Cabrera, R., Gómez-Cama, C., & Soriguer, M. C. (2016). Trophic relationships, feeding habits and seasonal dietary changes in an intertidal rockpool fish

assemblage in the Gulf of Cadiz (NE Atlantic). *Journal of Marine Systems*, *158*, 165-172. https://doi.org/10.1016/j.jmarsys.2016.02.006

Corrales, X., Coll, M., Tecchio, S., Bellido, J. M., Fernández, Á. M., & Palomera, I. (2015). Ecosystem structure and fishing impacts in the northwestern Mediterranean Sea using a food web model within a comparative approach. *Journal of Marine Systems*, *148*, 183-199. https://doi.org/10.1016/j.jmarsys.2015.03.006

Coscia & Mariani (2011). *Biological Journal of the Linnean Society*, *106*(2), 455-458. https://doi.org/10.1111/j.1095-8312.2012.01875.x

Coscia, I., Desmarais, E., Guinand, B., & Mariani, S. (2012). Phylogeography of European sea bass in the north-east Atlantic: a correction and reanalysis of the mitochondrial DNA data from

Cowen, R. K., Paris, C. B., & Srinivasan, A. (2006). Scaling of connectivity in marine populations. *Science*, *311*(5760), 522-527. doi: 10.1126/science.1122039

Cowen, R. K., Gawarkiewicz, G., Pineda, J., Thorrold, S. R., & Werner, F. E. (2007). Population connectivity in marine systems an overview. *Oceanography*, *20*(3), 14-21.

Cowen, R. K., & Sponaugle, S. (2009). Larval dispersal and marine population connectivity. https://doi.org/10.1146/annurev.marine.010908.163757

Cox, C. B., Moore, P. D., & Ladle, R. J. (2016). *Biogeography: an ecological and evolutionary approach*. John Wiley & Sons.

Crochelet, E., Roberts, J., Lagabrielle, E., Obura, D., Petit, M., & Chabanet, P. (2016). A model-based assessment of reef larvae dispersal in the Western Indian Ocean reveals regional connectivity patterns—Potential implications for conservation policies. *Regional Studies in Marine Science*, *7*, 159-167. https://doi.org/10.1016/j.rsma.2016.06.007

Crooks, K. R., M. Sanjayan (2006). Connectivity conservation: maintening connections for nature. Connectivity Conservation. K. R. Crooks and M. Sanjayan. New York, Cambridge University Press: 1-20.

Cury, P., & Roy, C. (1989). Optimal environmental window and pelagic fish recruitment success in upwelling areas. *Canadian Journal of Fisheries and Aquatic Sciences*, *46*(4), 670-680. https://doi.org/10.1139/f89-086

Dahlgren, C. P., & Eggleston, D. B. (2000). Ecological processes underlying ontogenetic habitat shifts in a coral reef fish. *Ecology*, *81*(8), 2227-2240. https://doi.org/10.1890/0012-9658(2000)081[2227:EPUOHS]2.0.CO;2

Dahlgren, C. P., Kellison, G. T., Adams, A. J., Gillanders, B. M., Kendall, M. S., Layman, C. A., ... & Serafy, J. E. (2006). Marine nurseries and effective juvenile habitats: concepts and applications. *Marine Ecology Progress Series*, *312*, 291-295. doi:10.3354/meps312291

Dambrine, C., Huret, M., Woillez, M., Pecquerie, L., Allal, F., Servili, A., & De Pontual, H. (2020). Contribution of a bioenergetics model to investigate the growth and survival of European seabass in the Bay of Biscay–English Channel area. *Ecological Modelling*, *423*, 109007. https://doi.org/10.1016/j.ecolmodel.2020.109007

Dambrine, C., Woillez, M., Huret, M., & De Pontual, H. (2021). Characterising Essential Fish Habitat using spatio-temporal analysis of fishery data: A case study of the European seabass spawning areas. *Fisheries Oceanography*. https://doi.org/10.1111/fog.12527

Dando, P. R., & Demir, N. (1985). On the spawning and nursery grounds of bass, Dicentrarchus labrax, in the Plymouth area. *Journal of the Marine Biological Association of the United Kingdom. Plymouth*, *65*(1), 159-168.

Darias, M. J., Zambonino-Infante, J. L., Hugot, K., Cahu, C. L., & Mazurais, D. (2008). Gene expression patterns during the larval development of European sea bass (Dicentrarchus labrax) by microarray analysis. *Marine Biotechnology*, *10*(4), 416-428.

Davis, S. J., Caldeira, K., & Matthews, H. D. (2010). Future CO2 emissions and climate change from existing energy infrastructure. *Science*, *329*(5997), 1330-1333. doi: 10.1126/science.1188566

Demanèche, S., Bégot, E., Gouello, A., Habasque, J., Merrien, C., Leblond, E., Berthou, P., Harscoat, V., Fritsch, M., Leneveu, C., & Laurans, M. (2010). Projet SACROIS "IFREMER/DPMA" - Rapport final. *Convention SACROIS 2008-2010.*

De Pontual, H., Lalire, M., Fablet, R., Laspougeas, C., Garren, F., Martin, S., & Woillez, M. (2019). New insights into behavioural ecology of European seabass off the West Coast of France: implications at local and population scales. *ICES Journal of Marine Science*, *76*(2), 501-515. https://doi.org/10.1093/icesjms/fsy086

Devauchelle, N., Coves, D. (1988). The characteristics of sea bass (Dicentrarchus labrax) eggs: description, biochemical composition and hatching performances. Aquatic Living Resources 1, 223–230. https://doi.org/10.1051/alr:1988022

Domeier, M. L. (2012). Revisiting Spawning Aggregations: Definitions and Challenges. In: Sadovy de Mitcheson Y., Colin P. (Eds), *Reef Fish Spawning Aggregations: Biology, Research and Management. Fish & Fisheries Series*, vol 35. Springer, Dordrecht

Doney, S. C., Ruckelshaus, M., Duffy, J. E., Barry, J. P., Chan, F., English, C. A., ... & Polovina, J. (2011). Climate change impacts on marine ecosystems. https://doi.org/10.1146/annurev-marine-041911-111611

Ellien, C., Thiebaut, É., Barnay, A. S., Dauvin, J. C., Gentil, F., & Salomon, J. C. (2000). The influence of variability in larval dispersal on the dynamics of a marine metapopulation in the eastern Channel. *Oceanologica Acta*, *23*(4), 423-442. https://doi.org/10.1016/S0399-1784(00)00136-5

Enberg, K., Dunlop, E.S., Jørgensen, C. (2008). Fish Growth, in: Encyclopedia of Ecology. Academic Press, Oxford, pp. 1564–1572.

EUMOFA. (2018). Le marché européen du poisson.

Faillettaz, R. (2015). *Estimation des capacités comportementales des larves de poissons et leurs implications pour la phase larvaire: un cas d'étude d'espèces démersales de Méditerranée Nord-Occidentale* (Doctoral dissertation).

FAO, 2016. FIRMS. http://firms.fao.org/firms/concepts/en

Forniés, M. A., Mañanós, E., Carrillo, M., Rocha, A., Laureau, S., Mylonas, C. C. & Zanuy, S. (2001). Spawning induction of individual European sea bass females (Dicentrarchus labrax) using different GnRHa-delivery systems. Aquaculture, 202(3-4), 221-234. https://doi.org/10.1016/S0044-8486(01)00773-6

Forward, R. B. (1988). Diel vertical migration: zooplankton photobiology and behaviour. *Oceanogr. Mar. Biol. Annu. Rev*, *26*(36), 1-393.

Fox, C. J., McCloghrie, P., Young, E. F., & Nash, R. D. M. (2006). The importance of individual behaviour for successful settlement of juvenile plaice (Pleuronectes platessa L.): a modelling

and field study in the eastern Irish Sea. *Fisheries Oceanography*, *15*(4), 301-313. https://doi.org/10.1111/j.1365-2419.2005.00396.x

Frisk, M. G., Jordaan, A., & Miller, T. J. (2014). Moving beyond the current paradigm in marine population connectivity: are adults the missing link?. *Fish and Fisheries*, *15*(2), 242-254. https://doi.org/10.1111/faf.12014

Fritsch, M. (2005). *Traits biologiques et exploitation du bar commun Dicentrarchus labrax (L.) dans les pêcheries françaises de la Manche et du golfe de Gascogne* (Doctoral dissertation, Université de Bretagne Occidentale).

Fritsch, M., Morizur, Y., Lambert, E., Bonhomme, F., and Guinand, B. (2007). Assessment of sea bass (Dicentrarchus labrax, L.) stock delimitation in the Bay of Biscay and the English Channel based on mark-recapture and genetic data. Fisheries Research, 83: 123–132. https://doi.org/10.1016/j.fishres.2006.09.002

Gallego A, North EW, Petitgas P (2007) Introduction: status and future of modelling physical-biological interactions during the early life of fishes. Mar Ecol Prog Ser 347:121-126. https://doi.org/10.3354/meps06972

Gascuel, D. (2019). Pour une révolution dans la mer de la surpêche à la résilience (pp. 544-p). Actes Sud.

Gatti, P., Cominassi, L., Duhamel, E., Grellier, P., Le Delliou, H., Le Mestre, S., ... & Huret, M. (2018). Bioenergetic condition of anchovy and sardine in the Bay of Biscay and English Channel. *Progress in Oceanography*, *166*, 129-138. https://doi.org/10.1016/j.pocean.2017.12.006

Gatti, P., Petitgas, P., Huret, M. (2017). Comparing biological traits of anchovy and sardine in the Bay of Biscay: A modelling approach with the Dynamic Energy Budget. Ecological Modelling 348, 93–109. https://doi.org/10.1016/j.ecolmodel.2016.12.018

Geisser, S. (1993). *Predictive Inference: an Introduction*. Chapman and Hall, London.

Griffin, D. R. (1953). Sensory physiology and the orientation of animals. *American Scientist*, *41*(2), 208-281.

Grimm, V., Reise, K., & Strasser, M. (2003). Marine metapopulations: a useful concept?. *Helgoland Marine Research*, *56*(4), 222-228.

Grimm, V., & Railsback, S. F. (2005). *Individual-based modeling and ecology* (Vol. 8). Princeton university press.

Gross, M. R. (1996). Alternative reproductive strategies and tactics: diversity within sexes. *Trends in Ecology & Evolution*, *11*(2), 92-98.

Hamdi, A., Vasquez, M. & Populus, J. (2010). Cartographie des habitats physiques EUNIS - Côtes de France. *Convention Ifremer/AAMP n° 09/12177764/FY*.

Hanski, I. (1999). *Metapopulation ecology*. Oxford University Press.

Harden Jones, F. R. (1968). *Fish migration*. Edward Arnold Ltd., London, 325p.

Harley, S. J., Myers, R. A., & Dunn, A. (2001). Is catch-per-unit-effort proportional to abundance?. *Canadian Journal of Fisheries and Aquatic Sciences*, *58*(9), 1760-1772. https://doi.org/10.1139/f01-112

Hedgecock, D., Barber, P. H., & Edmands, S. (2007). Genetic approaches to measuring connectivity. *Oceanography*, *20*(3), 70-79.

Heerah, K., Woillez, M., Fablet, R., Garren, F., Martin, S., & De Pontual, H. (2017). Coupling spectral analysis and hidden Markov models for the segmentation of behavioural patterns. *Movement ecology*, *5*(1), 1-15. https://doi.org/10.1186/s40462-017-0111-3

Hilborn, R., Quinn, T. P., Schindler, D. E., & Rogers, D. E. (2003). Biocomplexity and fisheries sustainability. *Proceedings of the National Academy of Sciences*, *100*(11), 6564-6568. https://doi.org/10.1073/pnas.1037274100

Hinrichsen, H. H., Dickey-Collas, M., Huret, M., Peck, M. A., & Vikebø, F. B. (2011). Evaluating the suitability of coupled biophysical models for fishery management. *ICES Journal of Marine Science*, *68*(7), 1478-1487. https://doi.org/10.1093/icesjms/fsr056

Hintzen, N. T., Bastardie, F., Beare, D., Piet, G. J., Ulrich, C., Deporte, N. & Degel, H. (2012). VMStools: Open-source software for the processing, analysis and visualisation of fisheries logbook and VMS data. *Fisheries Research*, *115*, 31-43. https://doi.org/10.1016/j.fishres.2011.11.007

Hjort, J. (1914). Fluctuations in the great fisheries of northern Europe viewed in the light of biological research. ICES.

Hoegh-Guldberg, O., & Bruno, J. F. (2010). The impact of climate change on the world's marine ecosystems. *Science*, *328*(5985), 1523-1528. doi: 10.1126/science.1189930

Holt, J. T., & James, I. D. (2001). An s coordinate density evolving model of the northwest European continental shelf: 1. Model description and density structure. *Journal of Geophysical Research: Oceans*, *106*(C7), 14015-14034. https://doi.org/10.1029/2000JC000304

Houde, E. D., & Hoyt, R. (1987). Fish early life dynamics and recruitment variability. *Trans. Am. Fish. Soc.*

Houde, E.D. (2008). Emerging from Hjort's shadow. *Journal of Northwest Atlantic Fishery Science*, *41*, 53-70.

Howald, S., Cominassi, L., Le Bayon, N., Claireaux, G., & Mark, F. C. (2019). Future ocean warming may prove beneficial for the northern population of European seabass, but ocean acidification does not. *bioRxiv*, 568428. doi: 10.1242/jeb.213017

Hunter, E., Metcalfe, J. D., & Reynolds, J. D. (2003). Migration route and spawning area fidelity by North Sea plaice. *Proceedings of the Royal Society of London. Series B: Biological Sciences*, *270*(1529), 2097-2103. https://doi.org/10.1098/rspb.2003.2473

Huret, M., Petitgas, P. & Woillez, M. (2010). Dispersal kernels and their drivers captured with a hydrodynamic model and spatial indices: a case study on anchovy (Engraulis encrasicolus) early life stages in the Bay of Biscay. Progress in Oceonography 87:6-17. https://doi.org/10.1016/j.pocean.2010.09.023

ICES. (2012). Report of the Working Group for the Celtic Seas Ecoregion (WGCSE), 9– 18 May 2012, Copenhagen, Denmark. *ICES CM 2012/ACOM:12.* 1715 pp.

ICES. (2015). Report of the Working Group for the Celtic Seas Ecoregion (WGCSE), 12– 21 May 2015, Copenhagen, Denmark. *ICES CM 2015/ACOM:12.* 1432 pp.

ICES. (2018). Report of the Working Group on Celtic Seas Ecoregion (WGCSE), 9–18 May 2018, Copenhagen, Denmark. ICES CM 2018/ACOM:13. 1887 pp.

ICES (2019). Working group for the Celtic seas ecoregion (WGCSE). *ICES Scientific Reports/Rapports scientifiques du CIEM.*, 1(29), 1078p. https://doi.org/10.17895/ices.pub.4982

Ihssen, P. E., Booke, H. E., Casselman, J. M., McGlade, J. M., Payne, N. R., & Utter, F. M. (1981). Stock identification: materials and methods. *Canadian journal of fisheries and aquatic sciences*, *38*(12), 1838-1855. https://doi.org/10.1139/f81-230

Islam, M. S., & Tanaka, M. (2005). Nutritional condition, starvation status and growth of early juvenile Japanese sea bass (Lateolabrax japonicus) related to prey distribution and feeding in the nursery ground. *Journal of Experimental Marine Biology and Ecology*, *323*(2), 172-183. https://doi.org/10.1016/j.jembe.2005.04.007

Jennings, S., & Pawson, M. G. (1991). The development of bass, Dicentrarchus labrax, eggs in relation to temperature. *Journal of the Marine Biological Association of the United Kingdom*, *71*(1), 107-116. https://doi.org/10.1017/S0025315400037425

Jennings, S., & Pawson, M. G. (1992). The origin and recruitment of bass, Dicentrarchus labrax, larvae to nursery areas. *Journal of the Marine Biological Association of the United Kingdom*, *72*(1), 199-212.

Jones, G. P. (1990). The importance of recruitment to the dynamics of a coral reef fish population. *Ecology*, *71*(5), 1691-1698. https://doi.org/10.2307/1937578

Jonsson, B., & Jonsson, N. (1993). Partial migration: niche shift versus sexual maturation in fishes. *Reviews in Fish Biology and Fisheries*, *3*(4), 348-365.

Juanes, F. (2007). Role of habitat in mediating mortality during the post-settlement transition phase of temperate marine fishes. *Journal of Fish Biology*, *70*(3), 661-677. https://doi.org/10.1111/j.1095-8649.2007.01394.x

Jusup, M., Klanjscek, T., Matsuda, H., Kooijman, S. (2011). A full lifecycle bioenergetic model for bluefin tuna. PLoS One 6, e21903. https://doi.org/10.1371/journal.pone.0021903

Kennedy, M., & Fitzmaurice, P. (1968). Occurrence of Eggs of Bass Dicentrarchus Labra X on the Southern Coasts of Ireland. *Journal of the Marine Biological Association of the United Kingdom*, *48*(3), 585-592. https://doi.org/10.1017/S0025315400019160

Kennedy, M., & Fitzmaurice, P. (1972). The biology of the bass, Dicentrarchus labrax, in Irish waters. *Journal of the Marine Biological Association of the United Kingdom*, *52*(3), 557-597. https://doi.org/10.1017/S0025315400021597

Kneib, T., Müller, J., & Hothorn, T. (2008). Spatial smoothing techniques for the assessment of habitat suitability. *Environmental and Ecological Statistics*, *15*(3), 343-364. https://doi.org/10.1007/s10651-008-0092-x

Kooijman, S. A. L. M. (2010). *Dynamic energy budget theory for metabolic organisation*. Cambridge university press.

Koutsikopoulos, C., Fortier, L., & Gagne, J. A. (1991). Cross-shelf dispersion of Dover sole (Solea solea) eggs and larvae in Biscay Bay and recruitment to inshore nurseries. *Journal of Plankton Research*, *13*(5), 923-945. https://doi.org/10.1093/plankt/13.5.923

Kutkuhn, J. H. (1981). Stock definition as a necessary basis for cooperative management of Great Lakes fish resources. *Canadian Journal of Fisheries and Aquatic Sciences*, *38*(12), 1476-1478. https://doi.org/10.1139/f81-199

Lacroix, G., Maes, G. E., Bolle, L. J., & Volckaert, F. A. (2013). Modelling dispersal dynamics of the early life stages of a marine flatfish (Solea solea L.). *Journal of Sea Research*, *84*, 13-25. https://doi.org/10.1016/j.seares.2012.07.010

Large, P. A., Diez, G., Drewery, J., Laurans, M., Pilling, G. M., Reid, D. G., & Vinnichenko, V. I. (2009). Spatial and temporal distribution of spawning aggregations of blue ling (*Molva dypterygia*) west and northwest of the British Isles. *ICES Journal of Marine Science*, *67*(3), 494-501. https://doi.org/10.1093/icesjms/fsp264

Lazure, P., & Dumas, F. (2008). An external–internal mode coupling for a 3D hydrodynamical model for applications at regional scale (MARS). *Advances in water resources*, *31*(2), 233-250. https://doi.org/10.1016/j.advwatres.2007.06.010

Le Corre, N., Pepin, P., Burmeister, A., Walkusz, W., Skanes, K., Wang, Z., ... & Snelgrove, P. V. (2020). Larval connectivity of Northern Shrimp (Pandalus borealis) in the northwest Atlantic. *Canadian Journal of Fisheries and Aquatic Sciences*, (ja). https://doi.org/10.1139/cjfas-2019-0454

Leis, J. M., Balma, P., Ricoux, R., & Galzin, R. (2012). Ontogeny of swimming ability in the European sea bass, Dicentrarchus labrax (L.)(Teleostei: Moronidae). *Marine Biology Research*, *8*(3), 265-272. https://doi.org/10.1080/17451000.2011.616898

Lelievre, S., Vaz, S., Martin, C. S., & Loots, C. (2014). Delineating recurrent fish spawning habitats in the North Sea. *Journal of Sea Research*, *91*, 1-14. https://doi.org/10.1016/j.seares.2014.03.008

Le Pape, O., & Bonhommeau, S. (2015). The food limitation hypothesis for juvenile marine fish. *Fish and Fisheries*, *16*(3), 373-398. https://doi.org/10.1111/faf.12063

Lévêque, C. (1995). L'habitat: être au bon endroit au bon moment?. *Bulletin Français de la Pêche et de la Pisciculture*, (337-338-339), 9-20.

Levin, L. A. (2006). Recent progress in understanding larval dispersal: new directions and digressions. *Integrative and comparative biology*, *46*(3), 282-297. https://doi.org/10.1093/icb/icj024

Lika, K., Kearney, M.R., Freitas, V., van der Veer, H.W., van der Meer, J., Wijsman, J.W.M., Pecquerie, L., Kooijman, S.A.L.M. (2011). The "covariation method" for estimating the parameters of the standard Dynamic Energy Budget model I: Philosophy and approach. Journal of Sea Research 66, 270–277. https://doi.org/10.1016/j.seares.2011.07.010

Lika, K., Kooijman, S.A.L.M., Papandroulakis, N. (2014). Metabolic acceleration in Mediterranean Perciformes. Journal of Sea Research 94, 37–46. https://doi.org/10.1016/j.seares.2013.12.012

Lindgren, F., Rue, H., & Lindström, J. (2011). An explicit link between Gaussian fields and Gaussian Markov random fields: the stochastic partial differential equation approach. *Journal of the Royal Statistical Society: Series B (Statistical Methodology)*, *73*(4), 423-498. https://doi.org/10.1111/j.1467-9868.2011.00777.x

Lowe-McConnell, R. H. (1985). The biology of the river systems with particular reference to the fishes. *The Niger and its neighbours–Environmental history and hydrology, human use and health hazards of the major West-African rivers. AA Balkema, Rotterdam/Boston*.

Magnuson-Stevens Fishery Act. (2007). Management Reauthorization Act of 2006. *Public Law 479*.

Marques, G. M., Augustine, S., Lika, K., Pecquerie, L., Domingos, T., & Kooijman, S. A. (2018). The AmP project: comparing species on the basis of dynamic energy budget

parameters. *PLoS computational biology*, *14*(5), e1006100. https://doi.org/10.1371/journal.pcbi.1006100

Martínez-Minaya, J., Cameletti, M., Conesa, D., & Pennino, M. G. (2018). Species distribution modeling: a statistical review with focus in spatio-temporal issues. *Stochastic environmental research and risk assessment*, *32*(11), 3227-3244. https://doi.org/10.1007/s00477-018-1548-7

Martinho, F., Dolbeth, M., Viegas, I., Teixeira, C.M., Cabral, H.N., Pardal, M.A., 2009. Environmental effects on the recruitment variability of nursery species. Estuarine, Coastal and Shelf Science 83, 460–468. https://doi.org/10.1016/j.ecss.2009.04.024

Masski, H. (1998). *Identification des frayères et étude des structures de population du turbot Psetta maxima L. Et du bar Dicentrachus labrax L. En Manche ouest et dans les zones avoisinantes* (Doctoral dissertation, Brest).

Matthews, S., & Brand, K. (2004). Africa invaded: the growing danger of invasive alien species. *Africa invaded: the growing danger of invasive alien species.*

Maunder, M. N., Sibert, J. R., Fonteneau, A., Hampton, J., Kleiber, P., & Harley, S. J. (2006). Interpreting catch per unit effort data to assess the status of individual stocks and communities. *Ices Journal of marine science*, *63*(8), 1373-1385. https://doi.org/10.1016/j.icesjms.2006.05.008

Mayer, I., Shackley, S.E., Witthames, P.R., 1990. Aspects of the reproductive biology of the bass, Dicentrarchus labrax L. II. Fecundity and pattern of oocyte development. J. Fish Biol. 141–148. https://doi.org/10.1111/j.1095-8649.1990.tb05590.x

Müller, C.L., Ofenbeck, G., Baumgartner, B., Schrader, B. and Sbalzarini, I.F., 2009. pCMALib: a parallel FORTRAN 90 library for the evolution strategy with covariance matrix adaptation. In *Proc. ACM Genetic and Evolutionary Computation Conference (GECCO'09),* Montreal, Canada. https://doi.org/10.1145/1569901.1570090

Munoz, F., Pennino, M. G., Conesa, D., López-Quílez, A., & Bellido, J. M. (2013). Estimation and prediction of the spatial occurrence of fish species using Bayesian latent Gaussian models. *Stochastic Environmental Research and Risk Assessment*, *27*(5), 1171-1180. https://doi.org/10.1007/s00477-012-0652-3

Neat, F. C., Bendall, V., Berx, B., Wright, P. J., Ó Cuaig, M., Townhill, B. & Righton, D. (2014). Movement of Atlantic cod around the British Isles: implications for finer scale stock management. *Journal of Applied Ecology*, *51*(6), 1564-1574. https://doi.org/10.1111/1365-2664.12343

Nelson, T. A., & Boots, B. (2008). Detecting spatial hot spots in landscape ecology. *Ecography*, *31*(5), 556-566. https://doi.org/10.1111/j.0906-7590.2008.05548.x

Northcote, T. G. (1978). Migratory strategies and production in freshwater fishes. *Ecology of freshwater fish production*, 326-359.

Olsen, E., Kaplan, I. C., Ainsworth, C., Fay, G., Gaichas, S., Gamble, R., ... & Johnson, K. F. (2018). Ocean futures under ocean acidification, marine protection, and changing fishing pressures explored using a worldwide suite of ecosystem models. *Frontiers in Marine Science*, *5*, 64. https://doi.org/10.3389/fmars.2018.00064

Paradinas, I., Conesa, D., Pennino, M. G., Muñoz, F., Fernández, A. M., López-Quílez, A., & Bellido, J. M. (2015). Bayesian spatio-temporal approach to identifying fish nurseries by validating persistence areas. *Marine Ecology Progress Series*, *528*, 245-255. https://doi.org/10.3354/meps11281

Paradinas, I., Marín, M., Grazia Pennino, M., López-Quílez, A., Conesa, D., Barreda, D., ... & Handling editor: Ernesto Jardim. (2016). Identifying the best fishing-suitable areas under the new European discard ban. *ICES Journal of Marine Science*, *73*(10), 2479-2487. https://doi.org/10.1093/icesjms/fsw114

Pawson, M. G., & Pickett, G. D. (1996). The annual pattern of condition and maturity in bass, Dicentrarchus labrax, in waters around England and Wales. *Journal of the Marine Biological Association of the United Kingdom*, *76*(1), 107-125. https://doi.org/10.1017/S0025315400029040

Pawson, M. (2000). The influence of temperature on the onset of first maturity in sea bass. Journal of Fish Biology 56, 319–327. https://doi.org/10.1006/jfbi.1999.1157

Pawson, M. G., Pickett, G. D., Leballeur, J., Brown, M., & Fritsch, M. (2007). Migrations, fishery interactions, and management units of sea bass (*Dicentrarchus labrax*) in Northwest Europe. *ICES Journal of Marine Science 64:* 332–345. https://doi.org/10.1093/icesjms/fsl035

Peck, Neuenfeldt, Essington, Trenkel, Takasuka, Gislason, Dickey-Collas, Andersen, Ravn-Jonsen, Vestergaard, Kvamsdal, Gårdmark, Link, Rice., 2014. Forage Fish Interactions: a symposium on "Creating the tools for ecosystem-based management of marine resources", *ICES Journal of Marine Science*, Volume 71, Issue 1, Pages 1–4, https://doi.org/10.1093/icesjms/fst174

Pecquerie, L., Petitgas, P., Kooijman, S.A.L.M. (2009). Modeling fish growth and reproduction in the context of the Dynamic Energy Budget theory to predict environmental impact on anchovy spawning duration. Journal of Sea Research 62, 93–105. https://doi.org/10.1016/j.seares.2009.06.002

Pecquerie, L., L. R. Johnson, S. A. L. M. Kooijman, and R. M. Nisbet. (2011). Analyzing variations in life-history traits of Pacific salmon in the context of Dynamic Energy Budget (DEB) theory. Journal of Sea Research 66:424-433.

Person-Le Ruyet, J., Mahé, K., Le Bayon, N., Le Delliou, H. (2004). Effects of temperature on growth and metabolism in a Mediterranean population of European sea bass, Dicentrarchus labrax. Aquaculture 237, 269–280. https://doi.org/10.1016/j.aquaculture.2004.04.021

Peterson, M. S. (2003). A conceptual view of environment-habitat-production linkages in tidal river estuaries. *Reviews in Fisheries science*, *11*(4), 291-313. https://doi.org/10.1080/10641260390255844

Pethybridge, H., Roos, D., Loizeau, V., Pecquerie, L., Bacher, C. (2013). Responses of European anchovy vital rates and population growth to environmental fluctuations: An individual-based modeling approach. Ecological Modelling 250, 370–383. https://doi.org/10.1016/j.ecolmodel.2012.11.017

Petitgas, P. (1998). Biomass-dependent dynamics of fish spatial distributions characterized by geostatistical aggregation curves. *ICES Journal of Marine Science*, *55*(3), 443–453. https://doi.org/10.1006/jmsc.1997.0345

Petitgas, P., Reid, D., Planque, B., Nogueira, E., O'Hea, B., & Cotano, U. (2006). The entrainment hypothesis: an explanation for the persistence and innovation in spawning migrations and life cycle spatial patterns. *ICES Document CM*.

Petitgas, P., Rijnsdorp, A. D., Dickey-Collas, M., Engelhard, G. H., Peck, M. A., Pinnegar, J. K., ... & Nash, R. D. (2013). Impacts of climate change on the complex life cycles of fish. *Fisheries Oceanography*, *22*(2), 121-139. https://doi.org/10.1111/fog.12010

Petitgas, P., Woillez, M., Doray, M., & Rivoirard, J. (2016). A geostatistical definition of hotspots for fish spatial distributions. *Mathematical Geosciences*, *48*(1), 65-77. https://doi.org/10.1007/s11004-015-9592-z

Pickett, G.D. & Pawson, M.G. (1994). Seabass: biology, exploitation, and conservation (1st ed). *Chapman & Hall, London ; New York.*

Pingree, R. D., & Garcia-Soto, C. (2014). Plankton blooms, ocean circulation and the European slope current: response to weather and climate in the Bay of Biscay and W English Channel (NE Atlantic). *Deep Sea Research Part II: Topical Studies in Oceanography*, *106*, 5-22. https://doi.org/10.1016/j.dsr2.2014.07.008

Planque, B., Loots, C., Petitgas, P., Lindstrøm, U. L. F., & Vaz, S. (2011). Understanding what controls the spatial distribution of fish populations using a multi-model approach. *Fisheries Oceanography*, *20*(1), 1-17. https://doi.org/10.1111/j.1365-2419.2010.00546.x

Pörtner, H. O. (2008). Ecosystem effects of ocean acidification in times of ocean warming: a physiologist's view. *Marine Ecology Progress Series*, *373*, 203-217. https://doi.org/10.3354/meps07768

Quere, N., Desmarais, E., Tsigenopoulos, C. S., Belkhir, K., Bonhomme, F., & Guinand, B. (2012). Gene flow at major transitional areas in sea bass (Dicentrarchus labrax) and the possible emergence of a hybrid swarm. *Ecology and Evolution*, *2*(12), 3061-3078. https://doi.org/10.1002/ece3.406

Regner, S., & Dulčić, J., 1994. Growth of sea bass, Dicentrarchus labrax, larval and juvenile stages and their otoliths under quasi-steady temperature conditions. *Marine biology*, *119*(2), 169-177.

Reynolds, W. J., Lancaster, J. E., & Pawson, M. G. (2003). Patterns of spawning and recruitment of sea bass to Bristol Channel nurseries in relation to the 1996 'Sea Empress' oil spill. *Journal of the Marine Biological Association of the United Kingdom*, *83*(5), 1163-1170.

Riis-Vestergaard, J. (2002). Energy density of marine pelagic fish eggs. Journal of Fish Biology, 60: 1511-1528. doi:10.1111/j.1095-8649.2002.tb02444.x

Rijnsdorp, A. D., Van Beek, F. A., Flatman, S., Millner, R. M., Riley, J. D., Giret, M., & De Clerck, R. (1992). Recruitment of sole stocks, Solea solea (L.), in the Northeast Atlantic. *Netherlands Journal of Sea Research*, *29*(1-3), 173-192. https://doi.org/10.1016/0077-7579(92)90018-A

Rijnsdorp, A. D., Peck, M. A., Engelhard, G. H., Möllmann, C., & Pinnegar, J. K. (2009). Resolving the effect of climate change on fish populations. *ICES journal of marine science*, *66*(7), 1570-1583. https://doi.org/10.1093/icesjms/fsp056

Robinet, T., Roussel, V., Cheze, K., & Gagnaire, P. A. (2020). Spatial gradients of introgressed ancestry reveal cryptic connectivity patterns in a high gene flow marine fish. *Molecular Ecology*. https://doi.org/10.1111/mec.15611

Rochette, S., Rivot, E., Morin, J., Mackinson, S., Riou, P., Le Pape, O., 2010. Effect of nursery habitat degradation on flatfish population: Application to Solea solea in the Eastern Channel (Western Europe). Proc. Seventh Int. Symp. Flatfish Ecol. Part I 64, 34–44. doi:10.1016/j.seares.2009.08.003

Rochette, S., Huret, M., Rivot, E., & Le Pape, O. (2012). Coupling hydrodynamic and individual-based models to simulate long-term larval supply to coastal nursery areas. *Fisheries Oceanography*, *21*(4), 229-242. https://doi.org/10.1111/j.1365-2419.2012.00621.x

Rose, G. A. (1993). Cod spawning on a migration highway in the north-west Atlantic. *Nature*, *366*(6454), 458-461.

Ross, O. N., & Sharples, J. (2004). Recipe for 1-D Lagrangian particle tracking models in space-varying diffusivity. *Limnology and Oceanography: Methods*, *2*(9), 289-302. https://doi.org/10.4319/lom.2004.2.289

Rue, H., Martino, S., & Chopin, N. (2009). Approximate Bayesian inference for latent Gaussian models by using integrated nested Laplace approximations. *Journal of the royal statistical society: Series b (statistical methodology)*, *71*(2), 319-392. https://doi.org/10.1111/j.1467-9868.2008.00700.x

Rue, H., Martino, S., Lindgren, F., Simpson, D., Riebler, A., & Krainski, E. T. (2014). INLA: Functions which allow to perform full Bayesian analysis of latent Gaussian models using Integrated Nested Laplace Approximaxion. *R package version 0.0-1404466487, URL http://www. R-INLA. org*.

Sale, P. F., Van Lavieren, H., Lagman, M. A., Atema, J., Butler, M., Fauvelot, C., ... & Steneck, R. (2010). Preserving reef connectivity: A handbook for marine protected area managers. Connectivity Working Group. *Coral Reef Targeted Research & Capacity Building for Management Program, UNU-INWEH*.

Sassa, C., Tsukamoto, Y., Nishiuchi, K., & Konishi, Y. (2008). Spawning ground and larval transport processes of jack mackerel Trachurus japonicus in the shelf-break region of the southern East China Sea. *Continental Shelf Research*, *28*(18), 2574-2583. https://doi.org/10.1016/j.csr.2008.08.002

Savina, M., Lacroix, G., & Ruddick, K. (2010). Modelling the transport of common sole larvae in the southern North Sea: influence of hydrodynamics and larval vertical movements. *Journal of Marine Systems*, *81*(1-2), 86-98. https://doi.org/10.1016/j.jmarsys.2009.12.008

Schurmann, H., Claireaux, G., & Chartois, H. (1998). Changes in vertical distribution of sea bass (Dicentrarchus labrax L.) during a hypoxic episode. In *Advances in invertebrates and fish telemetry* (pp. 207-213). Springer, Dordrecht.

Sentchev, A., & Korotenko, K. (2007). Modelling distribution of flounder larvae in the eastern English Channel: sensitivity to physical forcing and biological behaviour. *Marine Ecology Progress Series*, *347*, 233-245. https://doi.org/10.3354/meps06981

SHOM. (2015). MNT Bathymétrique de façade Atlantique. *SHOM (Projet Homonim).*

Sinclair, M. (1988). Marine populations: an essay on population regulation and speciation. *Books in recruitment fishery oceanography (USA).*

Souche, E. L., Hellemans, B., Babbucci, M., MacAoidh, E., Guinand, B., Bargelloni, L., ... & Volckaert, F. A. (2015). Range-wide population structure of European sea bass Dicentrarchus labrax. *Biological Journal of the Linnean Society*, *116*(1), 86-105. https://doi.org/10.1111/bij.12572

Stavrakidis-Zachou, O., Papandroulakis, N., Lika, K. (2018). A DEB model for European sea bass (Dicentrarchus labrax): Parameterisation and application in aquaculture. Journal of Sea Research. https://doi.org/10.1016/j.seares.2018.05.008

Stenevik, E. K., Sundby, S., & Cloete, R. (2007). Diel vertical migration of anchovy Engraulis encrasicolus larvae in the northern Benguela. *African Journal of Marine Science*, *29*(1), 127-136. https://doi.org/10.2989/AJMS.2007.29.1.12.77

Tanner, S. E., Reis-Santos, P., & Cabral, H. N. (2016). Otolith chemistry in stock delineation: a brief overview, current challenges and future prospects. *Fisheries Research*, *173*, 206-213. https://doi.org/10.1016/j.fishres.2015.07.019

Tétard, S., Feunteun, E., Bultel, E., Gadais, R., Bégout, M. L., Trancart, T., & Lasne, E. (2016). Poor oxic conditions in a large estuary reduce connectivity from marine to freshwater habitats of a diadromous fish. *Estuarine, Coastal and Shelf Science*, *169*, 216-226. https://doi.org/10.1016/j.ecss.2015.12.010

Thompson, B. M., & Harrop, R. T. (1987). The distribution and abundance of bass (Dicentrarchus labrax) eggs and larvae in the English Channel and southern North Sea. *Journal of the marine Biological Association of the United Kingdom*, *67*(2), 263-274. https://doi.org/10.1017/S0025315400026588

Tine, M., Kuhl, H., Gagnaire, P. A., Louro, B., Desmarais, E., Martins, R. S., ... & Dieterich, R. (2014). European sea bass genome and its variation provide insights into adaptation to euryhalinity and speciation. *Nature communications*, *5*(1), 1-10.

Vasconcelos, R. P., Eggleston, D. B., Le Pape, O., & Tulp, I. (2014). Patterns and processes of habitat-specific demographic variability in exploited marine species. *ICES Journal of Marine Science*, *71*(3), 638-647. https://doi.org/10.1093/icesjms/fst136

Vázquez, F. J. S., & Muñoz-Cueto, J. A. (Eds.). (2014). *Biology of European sea bass*. CRC press.

Vinagre, C., & Cabral, H. N. (2008). Prey consumption by the juvenile soles, Solea solea and Solea senegalensis, in the Tagus estuary, Portugal. *Estuarine, Coastal and Shelf Science*, *78*(1), 45-50. https://doi.org/10.1016/j.ecss.2007.11.009

Vinagre, C., Ferreira, T., Matos, L., Costa, M. J., & Cabral, H. N. (2009). Latitudinal gradients in growth and spawning of sea bass, Dicentrarchus labrax, and their relationship with temperature and photoperiod. *Estuarine, Coastal and Shelf Science*, *81*(3), 375-380. https://doi.org/10.1016/j.ecss.2008.11.015

Visser, A. W. (1997). Using random walk models to simulate the vertical distribution of particles in a turbulent water column. *Marine Ecology Progress Series*, *158*, 275-281. doi:10.3354/meps158275

Walker, N. D., Boyd, R., Watson, J., Kotz, M., Radford, Z., Readdy, L., ... & Hyder, K. (2020). A spatially explicit individual-based model to support management of commercial and recreational fisheries for European sea bass Dicentrarchus labrax. *Ecological Modelling*, *431*, 109179. https://doi.org/10.1016/j.ecolmodel.2020.109179

Walsh, M., Skogen, M. D., Reid, D., Svendsen, E., & MacMillan, J. A. (1996). The relationship between the location of western mackerel spawning, larval drift and recruit distributions: a modelling study. ICES.

Walter, J. F., Hoenig, J. M., & Christman, M. C. (2014). Reducing bias and filling in spatial gaps in fishery-dependent catch-per-unit-effort data by geostatistical prediction, I. Methodology and simulation. *North American Journal of Fisheries Management*, *34*(6), 1095-1107. https://doi.org/10.1080/02755947.2014.932865

Warlen, S.M., Burke, J.S. (1990). Immigration of Larvae of Fall/Winter Spawning Marine Fishes into a North Carolina Estuary. Estuaries 13, 453. https://doi.org/10.2307/1351789

Winberg, G. G., 1956. Rate of metabolism and food requirements of fish. *Fish. Res. Board Can., Transl. Ser., 194*, 1-253.

Woillez, M., Poulard, J. C., Rivoirard, J., Petitgas, P., & Bez, N. (2007). Indices for capturing spatial patterns and their evolution in time, with application to European hake (Merluccius merluccius) in the Bay of Biscay. *ICES Journal of Marine Science*, *64*(3), 537-550. https://doi.org/10.1093/icesjms/fsm025

Woillez, M., Fablet, R., Ngo, T. T., Lalire, M., Lazure, P., & De Pontual, H. (2016). A HMM-based model to geolocate pelagic fish from high-resolution individual temperature and depth

histories: European sea bass as a case study. *Ecological Modelling, 321*, 10-22. https://doi.org/10.1016/j.ecolmodel.2015.10.024

Ying, Y., Chen, Y., Lin, L., & Gao, T. (2011). Risks of ignoring fish population spatial structure in fisheries management. *Canadian Journal of Fisheries and Aquatic Sciences, 68*(12), 2101-2120. https://doi.org/10.1139/f2011-116

Acronymes

BARGEO : Base d'ARchivage et de la GEstion des Otolithes

CIEM : Conseil International pour l'Exploration de la Mer

CPUE : Capture Par Unité d'Effort

EUNIS : European Union Nature Information System

EVHOE : ÉValuation Halieutique de l'Ouest de l'Europe

FEAMP : Fonds Européen pour les Affaires Maritimes et la Pêche

HEE : Habitats Ecologiques Essentiels

Ifremer : Institut français de recherche pour l'exploitation de la mer

PFOM : Physiologie Fonctionnelle des Organismes Marins

SHOM : Service Hydrographique et Océanographique de la Marine

Acronyms

BoB: Bay of Biscay

CGFS: Channel GroundFish Survey

CMAES: Covariance Matrix Adaptation Evolution Strategy

CPO: Conditional Predictive Ordinate

CPUE: Catch Per Unit Effort

CRFD: Cumulative Relative Frequency Distribution

DEB: Dynamic Energy Budget

DIC: Deviance Information Criterion

EC: English Channel

EEC: Eastern English Channel

ELS: Early Life Stages

EUMOFA: EUropean Market Observatory for Fisheries and Aquaculture products

GAM: Generalized Additive Model

GLM: Generalized Linear Model

GRF: Gaussian Random Fields

IBM: Individual-Based Model

ICES: International Council for the Exploration of the Sea

INLA: Integrated Nested Laplace Approximation

LCPO: Logarithm of the Conditional Predictive Ordinate

MARBEC: MARine Biodiversity, Exploitation and Conservation

MARS: Model for Applications at Regional Scales

NAO: North Atlantic Oscillation

POLCOMS-ERSEM: Proudman Oceanographic Laboratory Coastal Ocean Modelling System-European Regional Seas Ecosystem Model

RMSE: Root Mean Square Error

SPDE: Stochastic Partial Differential Equation

SFG: Scope For Growth

SSB: Seabass Stock Biomass

TAC: Total Allowable Catches

VMS: Vessel Monitoring System

WAIC: Watanabe–Akaike information criterion

WEC: Western English Channel

Liste des figures

and then flattens), II. the variogram $\boldsymbol{\gamma_{i+1}(h)}$ is unstructured, III. the variogram ratio $\frac{\boldsymbol{\gamma_{i\times(i+1)}(h)}}{\boldsymbol{\gamma_i(h)}}$ is flat (i.e. $\mathbf{A_{i+1}}$is positioned randomly within $\mathbf{A_i}$) and IV. the variogram of the residuals of the regression between $\mathbf{1_{A_{i+1}}(x)}$ and $\mathbf{1_{A_i}(x)}$ is unstructured.

Figure 9. Monthly average maps of seabass spawning areas, from the geostatistical analysis, in the Bay of Biscay during the period 2008-2013: A. January, B. February and C. March. A probability of presence between 0 and 0.33 suggests that the area was rarely favourable every year. In contrast, a probability of presence between 0.66 and 1 indicates that the area was identified as a spawning area for several years. Values in between suggest that the area was occasionally favourable.

Figure 10. Monthly average maps of seabass spawning areas, from the geostatistical analysis, in the English Channel during the period 2008-2013: A. January, B. February, C. March and D. April. A probability of presence between 0 and 0.33 suggests that the area was rarely favourable every year. In contrast, a probability of presence between 0.66 and 1 indicates that the area was identified as a spawning area for several years. Values in between suggest that the area was occasionally favourable.

Figure 11. Predicted maps of probabilities for the presence of seabass spawning areas in January 2008 for the English Channel (A&B) and the Bay of Biscay (C&D) with the best spatio-temporal model compared to the maps of observed seabass spawning areas.

Figure 12. Predicted probabilities of presence of seabass spawning areas vs. observed seabass spawning areas with the best spatio-temporal model for A. the English Channel and B. the Bay of Biscay.

Figure 13. Predicted probabilities of presence with the best model in the English Channel under A. mixed layer depth, B. surface current velocities, C. mean salinity of the water column and D. mean temperature of the water column. For A. and B., each boxplot corresponds to an interval of 5 m for the mixed layer depth and 0.01 $m.s^{-1}$ for current velocities. The rectangles go from the first to the third quartiles and are cut by a horizontal line, which represents the median. The whiskers lead to the outliers, which are represented by dots. For C. and D., dotted lines represent the 25% and 95% quantiles.

Figure 14. Predicted probabilities of presence with the best model in the Bay of Biscay under A. bathymetry, B. mixed layer depth and C. mean temperature of the water column. For A. and B., each boxplot corresponds to an interval of 15 m for the bathymetry and 5 m for the mixed

layer depth. The rectangles go from the first to the third quartiles and are cut by a horizontal line, which represents the median. The whiskers lead to the outliers, which are represented by dots. For C., dotted lines represent the 25% and 95% quantiles.

Figure 15. Schematic representation of the standard DEB model applied to European seabass. Arrows represent energy fluxes (J/d, Table 1). Table 1 records the dynamics of the state variables E, V, E_H and E_R.

Figure 16. Temperature climatology reconstructed from tagged seabass, and used for the "wild" dataset during calibration (see Methods).

Figure 17. Temperatures experienced by young seabass in the experiment of Allal et al. (unpublished) and used to validate our DEB model with an independent dataset.

Figure 18. Model fitted to the three "length-at-age" datasets: A) 0-250 days, B) 0-1,600 days and C) 0-8,200 days. Dots represent mean observations with their standard deviation (not used for calibration). Lines represent model predictions for the aquaculture experiment at 20°C (red), the aquaculture experiment at 15°C (orange), and the "wild" dataset (blue).

Figure 19. Model fitted to the three" weight-at-age" datasets: A) 0-250 days, B) 0-1,600 days and C) 0-8,200 days. Dots represent mean observations with their standard deviation (not used for calibration). Lines represent the model predictions for the aquaculture experiment at 20°C (red), the aquaculture experiment at 15°C (orange), and the "wild" dataset (blue).

Figure 20. Plot of observed weight values with their standard deviation error bars (y-axis) vs. predicted weight values (x-axis) compared to the 1:1 line for the 0-110 days time period: A) experiment at 15°C and B) experiment at 20°C.

Figure 21. Validation of our model (line) using an independent dataset (dots with their standard deviation) for A) length and B) weight. Individuals were fed ad libitum and raised at temperatures shown on Fig.17.

Figure 22. Experiment 1: Starvation survival time of seabass larvae (in days) relative to the spawning month (x-axis) and the month at which starvation starts (directly at mouth opening, or 1, 2 or 3 months after mouth opening) (y-axis). The feeding level corresponds to f = 0.833 (estimated from the calibration procedure) and the temperature follows Fig.16.

Figure 23. Experiment 2: Starvation survival time of seabass larvae when food deprivation begins at recruitment size (L = 1.2 cm) according to experimental temperature and feeding history: f=1 (dots) and f=0.2 (triangles).

Figure 24. Experiment 3: Mean sizes and standard deviations for 30 individuals with different $\{\dot{p}_{Am}\}$ according to experimental temperatures and feeding history: f=1(dots) and f=0.2 (triangles). The dotted line represents the target size of 1.2 cm.

Figure 25. Experiment 3: Distribution of individuals according to their specific maximum assimilation rate. A) initial population; B) and C) individuals that would have reached at least 1.2 cm-long on day 110 and either fed at f = 0.2 and raised at 20°C (B) or fed and raised using the environmental conditions experienced by the wild dataset (i.e. calibrated f and T as shown in Fig.16)(C).

Figure 26. Scheme of the modelling approach: a hydrodynamic model (MARS) simulates the temperature and currents whereas a biogeochemical model (POLCOMS-ERSEM) provides the food availability; a bioenergetics model (DEB) controls the growth, the mortality and transitions between stages (i.e. depending on threshold of maturity $E_H^{h,b,j}$); two vertical behaviour were tested: in both cases, eggs and yolk larvae remain in the surface whereas first-feeding larvae and juveniles can either perform a diel migration or remain in the surface.

Figure 27. Location of the spawning areas for January (A), February (B), March (C) and April (D) from Dambrine et al. (2021). ICES rectangles and the main locations used in the results are also provided. 1. United Kingdom (UK), 2. Pas de Calais, 3. Cotentin, 4. Britanny, 5. Loire Estuary, 6. Charente Estuary, 7. Landes, 8. Spain, 9. Sables d'Olonne, 10. Gironde Estuary, 11. Jersey/Guernesey, 12. Iroise Sea, 13. Rochebonne Plateau.

Figure 28. Percentage of larval settlement from seabass spawning areas at the scale of ICES rectangles for simulations with A) larvae performing diel vertical migration and B) larvae remaining at surface. The colour of each rectangle represents the number of individuals that effectively settled divided by the total number of individuals. The value is averaged over all simulations (Table 12). Ellipse represents the area in the EC for which the percentage differs slightly.

Figure 29. Percentage of larval settlement on seabass nurseries at the scale of ICES rectangles for A) larvae performing diel vertical migration and B) larvae remaining at surface. The colour

of each rectangle represents the number of individuals that settle in a nursery divided by the total number of individual and weighted by the surface of the nursery in the ICES rectangle. The value is averaged over all simulations. Blue arrows represent nurseries with lower percentage of settlement whereas red one represent areas with better percentage of settlement.

Figure 30. Diagrams of connectivity using the base-case scenario for years 2010 (A; cold winter with negative NAO index) and 2014 (B; warm winter with positive NAO index); blue squares represent the spawning areas; black circles represent the nurseries; black lines represent the links between a spawning area and a nursery, their size are proportional to the number of individuals that perform that link; red circles represent self-recruitment, their size are proportional to the number of individuals that was born in an ICES rectangle and settle in it.

Figure 31. Average percentage of settlement (i.e. proportion of larvae born during one year that effectively settle) between all scenarios with larvae performing diel vertical migration for each year between 2008 and 2014 in the BoB and the EC.

Figure 32. Average percentage of settlement (i.e. proportion of larvae born in a month that effectively settle) between all scenarios with larvae performing diel vertical migration for each month of the spawning season in the BoB (between January and March) and the EC (between January and April).

Figure 33. Percentage of settlement (i.e. proportion of larvae from a spawning area that effectively settle) for all scenarios with larvae performing diel vertical migration in the EC (A) and in the BoB (B) for coastal and offshore spawning areas. The rectangle indicates the base-case scenario.

Figure S1. Yearly gear composition in the study area (No. of fishing events). GNS: set gillnets, GTR: trammel nets, OTB: bottom otter, OTM: midwater otter, OTT: otter twin trawls, PS: purse seines, PTB: bottom pair trawls, PTM: midwater pair trawls, and SDN: Danish seines.

Figure S2. Fishery distribution (No. of fishing events per square of three nautical miles) throughout the time series in the English Channel.

Figure S3. Fishery distribution (No. of fishing events per square of three nautical miles) throughout the time series in the Bay of Biscay.

Figure S4. Predicted maps of the probability of presence of seabass spawning areas for each spawning month of the time series (2008-2013) in the English Channel with the best spatio-temporal model.

Figure S5. Predicted maps of the probability of presence of seabass spawning areas for each spawning month of the time series (2008-2013) in the Bay of Biscay with the best spatio-temporal model.

Figure S6. Posterior distribution in the English Channel of A. the spatial effect nominal range (km), B. the spatial effect nominal variance, C. the temporal effect (for months of the spawning period) and D. the temporal effect variance. Note that the scale is different on each figure. For C., dotted lines represent the 25 and 95% quantiles.

Figure S7. Posterior distribution in the Bay of Biscay of A. the spatial effect nominal range (km), B. the spatial effect nominal variance, C. the temporal effect (for months of the spawning period) and D. the temporal effect variance. Note that the scale is different on each figure. For C., dotted lines represent the 25 and 95% quantiles.

Figure S8. Posterior A. mean and B. standard deviation of the spatial effect in the English Channel.

Figure S9. Posterior A. mean and B. standard deviation of the spatial effect in the Bay of Biscay.

Figure S10. Fit using the DEB model of Stavrakidis-Zachou et al. (2018) (black line) at f=0.71 and T reconstructed from tagged seabass, to our length-at-age dataset for wild seabass (red dots with their standard deviation error bars).

Liste des tables

Table 11. Quantities derived from the calibrated ‘abj’ DEB model (f=0.833) and values from the literature used for comparison and validation.

Table 12. Comparison of lengths and ages at hatch, birth, metamorphosis and puberty, as predicted using the parameters of this study (wild seabass), with those of farmed seabass (Stavrakidis-Zachou et al., 2018).

Table 13. Scenarios of settlement success ran from 2008 to 2014. There were three modalities of size to reach and maximal drift time and two modalities of distance from the coast and vertical behaviour for a total of 252 simulations.

Table S1. The EUNIS habitats cluster in seven along the French coast.

Table S2. The EUNIS habitats cluster in four along the French coast.

Table S3. Monthly hotspot cut-offs between 2008 and 2014 for the English Channel area and corresponding four variograms indicating if they are structured (“1”) or not (“0”).

Table S4. Monthly hotspot cut-offs between 2008 and 2016 for the Bay of Biscay area and corresponding four vraiograms indicating if they are structured (“1”) or not (“0”).

Table S5. Summary of the models tested for the English Channel. Bathy: bathymetry, Chl: surface chlorophyll-a, Mld: mixed layer depth, mean S: mean salinity of the water column, mean T: mean temperature of the water column, and UoVoS: surface current velocities. The subscripts lin and rw1 indicate whether the variable was tested as a linear predictor or following a random walk 1 model. * indicates the best model.

Table S6. Summary of the models tested for the Bay of Biscay. Mean T: mean temperature of the water column, UoVoS: surface current velocities, Mld: mixed layer depth, and Hab4:bottom grain size. The subscripts lin and rw1 indicate whether the variable was tested as a linear predictor or following a random walk 1 model. * indicates the best model.

Table S7. Equations of the ‘abj’ model including the dynamics of the four state variables, the metabolic acceleration, the six energy fluxes (J/d) and the shape correction function. Brackets [] represent quantities per unit of structural volume and braces {} represent quantities per unit of structural surface area.

Table S8. Values of the 15 DEB parameters calibrated by Dambrine et al. (2020). All rates are expressed at T_1 = 293.15 K (=20°C). Brackets [] indicate quantities per unit of structural volume and braces {} indicate quantities per unit of structural surface area.

DOCTORAT SCIENCES BRETAGNE DE LA MER LOIRE ET DU LITTORAL

UBO Université de Bretagne Occidentale

Titre : Caractérisation et connectivité des Habitats Ecologiques Essentiels des stades adulte et juvénile du bar européen

Mots clés : Frayères, Nourriceries, Dynamique spatio-temporelle, *Dicentrarchus labrax*

Résumé : Les Habitats Ecologiques Essentiels des poissons sont le siège d'au moins un stade de leur cycle de vie. Pouvant être distants, le maintien de leur connectivité est essentiel pour le bouclage du cycle de vie et le maintien des populations. Cette thèse s'est intéressée à la connectivité entre les frayères et les nourriceries du bar européen. Ses principales frayères ont été caractérisées via une approche de géostatistiques non linéaires appliquée à des données de pêche hautement résolues. Un modèle bayésien spatio-temporel a montré qu'elles s'expliquent principalement par une structure spatio-temporelle stable, plutôt que par des facteurs hydro-climatiques. Un modèle bioénergétique (DEB) sur l'ensemble du cycle de vie a été développé et validé sur les premiers stades. Il a montré que les larves et juvéniles sont résistants aux faibles températures et au manque de nourriture expérimentés durant leurs premiers mois de vie du fait d'une ponte hivernale. La connectivité frayères — nourriceries a été analysée via un modèle individu-centré incluant ce modèle DEB et couplé à un modèle hydrodynamique. Par le biais de scénarii de complexité croissante, les frayères et nourriceries potentielles les plus importantes pour l'espèce ont été identifiées. En moyenne, le succès des dérives est plus élevé en Manche que dans le golfe de Gascogne. Les frayères récurrentes du large permettent la colonisation de nombreuses nourriceries, alors que les frayères côtières fournissent en quantité les nourriceries les plus proches. Une connectivité entre les frayères du nord du golfe de Gascogne et les nourriceries de Manche ouest existe mais est peu récurrente, sauf entre le plateau de Rochebonne et la mer d'Iroise. Ces résultats ont pour vocation d'aider les gestionnaires dans leurs choix de mesures pour cette espèce à haute valeur économique.

Title: Characterisation and connectivity between the Essential Fish Habitats of adults and juveniles European seabass

Keywords: Spawning areas, Nurseries, Spatio-temporal dynamic, *Dicentrarchus labrax*

Abstract: Essential Fish Habitats host, at least, one stage of their life cycle. As they can be distant, maintaining their connectivity is essential for the closure of fish life cycle and populations' sustainability. This thesis focused on the connectivity between spawning areas and nurseries of European seabass. Its main spawning areas have been characterised using a non-linear geostatistical approach applied to highly resolved fishery data. A Bayesian spatio-temporal model showed that they are mainly explained by a stable spatio-temporal structure, rather than by hydro-climatic factors. A bioenergetics model (DEB) over the entire life cycle of seabass was developed and validated for the early life stages. It showed that larvae and juveniles are resistant to low temperatures and food deprivation experienced during their first months of life due to a spawning in winter. The spawning areas — nurseries' connectivity was analysed via an individual-based model including the DEB model previously developed and coupled to a hydrodynamic model. Through scenarios of increasing complexity, the potential most important spawning areas and nurseries for the species were identified. On average, the drift success is higher in the English Channel than in the Bay of Biscay. Recurrent offshore spawning areas allow the colonisation of numerous nurseries, while coastal one supply in quantity the closest nurseries. Connectivity between spawning areas in the northern Bay of Biscay and nurseries in the Western English Channel exists but is not recurrent, except between the Rochebonne plateau and the Iroise Sea. These results are intended to help managers in their measures' choices for this species of high economical value.